

RELIABILITY-BASED OPTIMIZATION OF RIVER BRIDGES USING ARTIFICIAL
INTELLIGENCE TECHNIQUES

A THESIS SUBMITTED TO
THE GRADUATE SCHOOL OF NATURAL AND APPLIED SCIENCES
OF
MIDDLE EAST TECHNICAL UNIVERSITY

BY

KAMİL HAKAN TURAN

IN PARTIAL FULFILLMENT OF THE REQUIREMENTS
FOR
THE DEGREE OF DOCTOR OF PHILOSOPHY
IN
CIVIL ENGINEERING

FEBRUARY 2011

Approval of the thesis:

**RELIABILITY-BASED OPTIMIZATION OF RIVER BRIDGES USING
ARTIFICIAL INTELLIGENCE TECHNIQUES**

submitted by **KAMİL HAKAN TURAN** in partial fulfillment of the requirements for
the degree of **Doctor of Philosophy in Civil Engineering Department, Middle
East Technical University** by,

Prof. Dr. Canan Özgen
Dean, Graduate School of **Natural and Applied Sciences** _____

Prof. Dr. Güney Özcebe
Head of Department, **Civil Engineering** _____

Prof. Dr. A. Melih Yanmaz
Supervisor, **Civil Engineering Dept., METU** _____

Examining Committee Members:

Assoc. Prof. Dr. Nuri Merzi
Civil Engineering Dept., METU _____

Prof. Dr. A. Melih Yanmaz
Civil Engineering Dept., METU _____

Prof. Dr. Osman N. Özdemir
Civil Engineering Dept., Gazi University _____

Asst. Prof. Dr. Alp Caner
Civil Engineering Dept., METU _____

Asst. Prof. Dr. Şahnaz Tiğrek
Civil Engineering Dept., METU _____

Date: 04 / 02 / 2011

I hereby declare that all information in this document has been obtained and presented in accordance with academic rules and ethical conduct. I also declare that, as required by these rules and conduct, I have fully cited and referenced all material and results that are not original to this work.

Name, Last name : Kamil Hakan Turan

Signature :

ABSTRACT

RELIABILTY-BASED OPTIMIZATION OF RIVER BRIDGES USING ARTIFICIAL INTELLIGENCE TECHNIQUES

Turan, Kamil Hakan
Ph.D., Department of Civil Engineering
Supervisor: Prof. Dr. A. Melih Yanmaz

February 2011, 200 pages

Proper bridge design is based on consideration of structural, hydraulic, and geotechnical conformities at an optimum level. The objective of this study is to develop an optimization-based methodology to select appropriate dimensions for components of a river bridge such that the aforementioned design aspects can be satisfied jointly. The structural and geotechnical design parts uses a statistically-based technique, artificial neural network (ANN) models. Therefore, relevant data of many bridge projects were collected and analyzed from different aspects to put them into a matrix form. ANN architectures are used in the objective function of the optimization problem, which is modeled using Genetic Algorithms with penalty functions as constraint handling method. Bridge scouring reliability comprises one of the constraints, which is performed using Monte-Carlo Simulation technique. All these mechanisms are assembled in a software framework, named as AIROB. Finally, an application built on AIROB is presented to assess the outputs of the software by focusing on the evaluations of hydraulic – structure interactions.

Keywords: Bridge, optimization, artificial intelligence, reliability, AIROB.

ÖZ

AKARSU KÖPRÜLERİNİN YAPAY ZEKA TEKNİKLERİNİ KULLANARAK GÜVENİLİRLİK TEMELLİ OPTİMİZASYONU

Turan, Kamil Hakan
Doktora, İnşaat Mühendisliği Bölümü
Tez Yöneticisi : Prof. Dr. A. Melih Yanmaz

Şubat 2011, 200 sayfa

Kabul edilebilir bir köprü tasarımı yapısal, hidrolik ve geoteknik uygunlukların optimum seviyede değerlendirilmesi üzerine oluşturulur. Bu çalışmanın amacı, yukarıda belirtilmiş tasarım kriterlerini bütünlük olarak sağlayacak bir akarsu köprüsünün yapı elemanlarının uygun boyutlarının seçimi için optimizasyon temelli bir metodoloji geliştirilmesidir. Yapısal ve geoteknik tasarım kısımları istatistiksel temelli bir teknik olan, yapay sinir ağları (YSA) modellerini kullanmaktadır. Bu nedenle, ilgili birçok köprü projesi toplanmış ve değişik açılardan analiz edilerek bir matris formuna sokulmuştur. YSA mimarileri, kısıtların denetlenmesi amacıyla ceza fonksiyonlarını kullanarak Genetik Algoritmalar tekniği ile modellenen optimizasyon probleminin amaç fonksiyonunda kullanılmaktadır. Kısıtlardan birini oluşturan köprü oylama güvenilirliği, Monte-Carlo benzeşimi yöntemi ile gerçekleştirilmiştir. Tüm bu mekanizmalar, AIROB ismi verilen bir yazılım çatısında birleştirilmiştir. En son olarak, yazılım sonuçlarının hidrolik – yapı etkileşiminin incelenmesine odaklanılarak değerlendirilmesi amacıyla AIROB üzerinde geliştirilen bir uygulama sunulmuştur.

Anahtar Kelimeler: Köprü, optimizasyon, yapay zeka, güvenilirlik, AIROB.

To my grandfather, Kamil Turan

ACKNOWLEDGEMENTS

This study is composed of long-term efforts contributed by many academicians specialized in various fields of study. In this context, the author would like to express his deepest gratitude and sincere thanks to his advisor Prof. Dr. A. Melih Yanmaz for his continuous guidance, recommendations, patience, and his both academic and psychological support throughout the course of this study. I am very grateful for working with him in this academic study.

I would like to thank Asst. Prof Dr. Alp Caner for his supply of statistical data about bridge projects and invaluable guidance about the structural modeling of the bridges.

Special thanks are extended to Assoc. Prof. Dr. Nuri Merzi and also Prof. Dr. O. Nuri Özdemir for their special guidance about the artificial intelligence techniques, especially in optimization.

I would like to thank to my family members, for their psychological support and encouragements during the period of this study. Their support for all long-term studies I have been involved is so important for me. In this manner, I would like to express a distinct thanks to my father, Oğuz Turan for his sustained support and encouragement for the course of this study, and for tolerating my lack of efforts about the jobs in our company.

All my remaining big-family members; my grandmothers, my aunts, my cousins deserve thanks for their understanding and forgiving me for all the postponed get-togethers with them.

Finally, I would like to give my thanks to my beloved wife, Gökçen for her support during this long period.

TABLE OF CONTENTS

ABSTRACT	iv
ÖZ	v
ACKNOWLEDGEMENTS	vii
TABLE OF CONTENTS	viii
LIST OF TABLES	xi
LIST OF FIGURES	xiii
LIST OF SYMBOLS	xvii
CHAPTER	
1. INTRODUCTION	1
1.1. Statement of the Problem	1
1.2. Objective of the Study	2
2. FLOW THROUGH BRIDGES	5
2.1. General	5
2.2. Flow Through Bridges	7
2.2.1. Flow Types Through Bridges	9
2.2.1.1. Low Flow Conditions	10
2.2.1.2. High Flow Conditions	13
2.3. Water Surface Profile Computations through Bridges	13
2.3.1. The Energy Approach	13
2.3.2. The Momentum Approach	16
2.3.3. The Yarnell Equation	19
3. BRIDGE SCOURING	21
3.1. General	21
3.2. The Mechanism of Scouring	22
3.2.1. Contraction Scour	24
3.2.2. Local Scour Around Piers and Abutments	25

4. AN OVERVIEW OF APPLIED ARTIFICIAL INTELLIGENCE	
TECHNIQUES	31
4.1. Introduction	31
4.2. Artificial Intelligence	33
4.3. Artificial Neural Networks	34
4.3.1. Network of Artificial Neurons as ANN	38
4.3.2. ANN Architectures	39
4.3.3. Feed-Forward Artificial Neural Networks	40
4.3.4. Learning (Training) in Feed-forward ANNs	43
4.3.4.1. Back-propagation Algorithm	44
4.3.5. Modeling Feed-forward ANNs	46
4.3.6. Testing of the ANN Performance	47
4.3.7. Benefits of Using ANNs	48
4.4. Optimization Techniques	49
4.4.1. Characteristics of Genetic Algorithms (GA)	52
4.4.1.1. Discretization and Encoding the Decision Variables ...	54
4.4.1.2. Generating the Initial Population	55
4.4.1.3. Selection Operation	56
4.4.1.4. Crossover Operation.....	57
4.4.1.5. Mutation Operation	58
4.4.1.6. Regeneration	59
4.4.1.7. Stopping Criteria	59
5. DEVELOPMENT OF THE DESIGN FRAMEWORK	60
5.1. General	60
5.2. Brief Description of Bridge Design Stages	61
5.3. Description of the Design Framework	63
5.3.1. Structural and Geotechnical Design of Bridges.....	64
5.3.2. Hydraulic – Structure Interaction in Bridge Engineering	66
5.3.3. Definition of the Optimization Problem	68
5.4. Guidelines for the Structural Design of Bridge	69
5.5. Design of Bridge Structural Components by Feed-forward Artificial Neural Networks	72
5.5.1. Modeling of the Artificial Neural Network Architectures	75
5.6. Bridge Hydraulics Computations	84

5.6.1. Reliability Analysis.....	85
5.7. Formulation of the Optimization Problem.....	90
5.7.1. Selection of the Optimization Technique	93
5.7.1.1. Dynamic Programming Approach.....	93
5.7.1.2. Characteristics of the Optimization Problem in terms of GA	95
5.7.1.2.1. Examination of Search Space	96
5.7.1.2.2. Handling of the Constraints of the Optimization Problem	98
5.8. Programmatic Details of AIROB.....	98
5.8.1. Algorithmic Description of AIROB	100
6. APPLICATION	105
6.1. Application Problem	105
6.2. Examination of Bridge Hydraulic Computations	114
6.3. Examination of Genetic Algorithm Results	118
6.3.1. Sensitivity Analysis of Genetic Algorithm Parameters	125
6.3.2. Sensitivity Analysis of Penalty Function Coefficients	129
6.4. Examination of Reliability Calculations	130
7. DISCUSSION, CONCLUSION and RECOMMENDATIONS	132
REFERENCES	137
APPENDICES.....	143
A. BRIDGE DATABASE.....	143
B. SAMPLE COST CALCULATIONS.....	154
C. COMPARISON OF GENETIC ALGORITHMS AND DYNAMIC PROGRAMMING OPTIMIZATION TECHNIQUES	177
D. USER-MANUAL FOR AIROB	187
CIRRICULUM VITAE.....	200

LIST OF TABLES

TABLES

Table 2.1. Subcritical flow contraction and expansion loss coefficients (USACE, 1998)	15
Table 2.2. Typical drag coefficients for various pier shapes (USACE, 1998)	18
Table 2.3. Yarnell's pier shape coefficients, K_p (USACE, 1998)	20
Table 3.1. k_1 , exponent in Laursen's model (USACE, 1998)	23
Table 3.2. Correction factor, K_1 , for pier nose shape (USACE, 1998)	28
Table 3.3. Correction factor, K_3 , for bed condition (USACE, 1998)	29
Table 3.4. Correction factor for abutment shape (USACE, 1998)	30
Table 5.1. Characteristic information about the bridge design database	73
Table 5.2. Characteristic information of the databases for bridge components ..	74
Table 5.3. Characteristic information for the final ANN models.....	80
Table 5.4. Statistical properties of the parameters in reliability calculations	89
Table 6.1. The optimum span arrangements for each case (Reliability-based constraints)	109
Table 6.2. Basic dimensions of the structural components of the optimized bridge for reliability-based constraints ($N_s=3$)	109
Table 6.3. The optimum span arrangements for each case (Deterministic constraints)	113
Table 6.4. Hydraulic information for the cross-section 0	114
Table 6.5. Hydraulic information for the cross-section 1	115
Table 6.6. Hydraulic information for the cross-section 2	115
Table 6.7. Hydraulic information for the cross-section 3	116
Table 6.8. Hydraulic information about conservation of energy calculations ...	116
Table 6.9. Hydraulic information about conservation of momentum calculations	117
Table 6.10. Initial GA population of the application problem (For $N_s=3$ and reliability-based constraints)	119
Table 6.11. GA population after the first generation (for $N_s=3$ and reliability-based constraints)	120

Table 6.12. Final population at the end of the generations	124
Table A.1. Summarized information of the bridges in the database	143
Table A.2. Summarized information of abutments in the database	147
Table A.3. Summarized information of piers in the database	149
Table A.4. Summarized Information of superstructures in the database	151
Table B.1. Sample input table for cost calculation of abutments	154
Table B.2. Sample details table for cost calculation of abutments	157
Table B.3. Sample results table for cost calculation of abutments	161
Table B.4. Sample input table for cost calculation of piers	163
Table B.5. Sample details table for cost calculation of piers	165
Table B.6. Sample results table for cost calculation of piers	168
Table B.7. Sample input table for cost calculation of superstructure	170
Table B.8. Sample details table for cost calculation of superstructure	172
Table B.9. Sample results table for cost calculation of superstructure	175
Table C.1. Summarized comparison table for GA versus dynamic programming	178
Table C.2. Comparison table for the results of GA and dynamic programming approach for the case study	180
Table C.3. The tabular results of stage-0 for the case study in dynamic programming approach	181
Table C.4. The tabular results of stage-1 for the case study in dynamic programming approach	182
Table C.5. The tabular results of stage-2 for the case study in dynamic programming approach	184
Table C.6. Completed form of the dynamic programming result	185

LIST OF FIGURES

FIGURES

Figure 2.1. Typical flow pattern through a bridge (Adapted from USACE, 1998)	7
Figure 2.2. Typical water surface profile through a bridge (Adapted from Yanmaz (2002-a))	10
Figure 2.3. Water surface profiles for low flow conditions (Subcritical regime) (Yanmaz, 2002-a)	11
Figure 2.4. Water surface profiles for low flow conditions (Supercritical regime) (Yanmaz, 2002-a)	12
Figure 2.5. Flow profile through bridge opening for the momentum approach ...	16
Figure 3.1. Variation of scour depth with time and velocity (Yanmaz, 2002-a) ...	23
Figure 3.2. Formation of vortex systems around a bridge pier (Yanmaz, 2002-a)	26
Figure 4.1. Typical biological neuron in a human brain (Adapted from Heaton (2008))	35
Figure 4.2. Artificial neuron as a mathematical tool (Russell and Norvig, 2003)..	36
Figure 4.3. Logsigmoid activation function (Demuth and Beale, 2002)	38
Figure 4.4. Basic types of ANN architectures (Adapted from Heaton (2008))	40
Figure 4.5. Black-box model representation of feed-forward ANN Architecture..	42
Figure 4.6. Variation of errors throughout the training and testing phases (Adapted from Demuth and Beale (2002))	47
Figure 4.7. General classification of optimization techniques (Adapted from Dianati and Song (2002))	50
Figure 4.8. General flowchart of GA (Adapted from Weise (2009))	53
Figure 4.9. Representation of a decision variable in GA (Haupt, 2004)	54
Figure 4.10. Schematic views of typical crossover operators (Haupt, 2004)	57
Figure 4.11. Schematic description of a typical mutation operator (Haupt, 2004)	58
Figure 5.1. Typical cross-section for a river bridge	68
Figure 5.2. Descriptive sketch for the connection nodes	70

Figure 5.3. Influence of column aspect ratio on the ductility of columns designed to the Caltrans confinement requirements (Adapted from ATC-32-1 (1999))	71
Figure 5.4. Schematic representation of selected parameters in ANN model for the design of abutments	75
Figure 5.5. Schematic representation of selected parameters in ANN model for the design of piers	76
Figure 5.6. Schematic representation of selected parameters in ANN model for the design of superstructure	76
Figure 5.7. Schematic representation of selected parameters in ANN model for the cost of abutments	77
Figure 5.8. Schematic representation of selected parameters in ANN model for the cost of piers	78
Figure 5.9. Schematic representation of selected parameters in ANN model for the cost of superstructure	78
Figure 5.10. Variation of MSE values with respect to the amount of nodes in the hidden layer (For abutment design model)	80
Figure 5.11. Variation of MSE values with respect to the amount of nodes in the hidden layer (For abutment cost model)	81
Figure 5.12. Variation of MSE values with respect to the amount of nodes in the hidden layer (For pier design model)	81
Figure 5.13. Variation of MSE values with respect to the amount of nodes in the hidden layer (For pier cost model)	82
Figure 5.14. Variation of MSE Values with respect to the amount of nodes in the hidden layer (For superstructure design model)	82
Figure 5.15. Variation of MSE values with respect to the amount of nodes in the hidden layer (for superstructure cost model)	83
Figure 5.16. Graphical Description of Inverse Transform Sampling Procedure ..	88
Figure 5.17. Descriptive sketch illustrating the dynamic programming formulation of the river bridge optimization problem	95
Figure 5.18. Variation of search space according to the number of spans (Size of search space axis is in logarithmic scale)	97
Figure 5.19. General flowchart of AIROB	101

Figure 6.1. River cross-section details at bridge opening for the application problem (Not to scale)	105
Figure 6.2. Plan view of the river reach at bridge opening for the application problem (Not to scale)	106
Figure 6.3. Variation of total cost of the bridge according to the number of spans	110
Figure 6.4. Velocity distribution across the bridge cross-section for the optimum alternative (in scale) (Footings not to scale)	112
Figure 6.5. Water surface profile through the bridge for the application problem	117
Figure 6.6. Chromosome structure depicting decision variables	121
Figure 6.7. Variation of average and maximum fitness values at each generation	123
Figure 6.8. The effect of the crossover rate on the optimization results	125
Figure 6.9. The effect of the mutation rate on the optimization results	126
Figure 6.10. The effect of the population size on the optimization results	126
Figure 6.11. The effect of the crossover type size on the optimization results..	127
Figure 6.12. Variation of failure probability of abutment footings with respect to the footing depth	130
Figure 6.13. Variation of failure probability of pier footings with respect to the footing depth	131
Figure B.1. Schematics for abutments	162
Figure B.2. Schematics for piers	169
Figure B.3. Schematics for superstructures	172
Figure C.1. River cross-section details at bridge opening for the case study (Not to scale)	176
Figure D.1. General layout of AIROB graphical user interface	187
Figure D.2. Opening an AIROB file	189
Figure D.3. ANN input tab-page	190
Figure D.4. Structural–geotechnical input tab-page	191
Figure D.5. Input data for bridge cross-section	192
Figure D.6. Graphical view of bridge cross-section	193
Figure D.7. Input data for the downstream cross-section	193
Figure D.8. Graphical view of the downstream cross-section	194

Figure D.9. Input data for the upstream cross-section	194
Figure D.10. Graphical view of the upstream cross-section	195
Figure D.11. Optimization engine related Input tab-page	196
Figure D.12. Calculation settings tab-page	197
Figure D.13. Computational process related tab-page	198
Figure D.14. Computational process information	198
Figure D.15. Dynamic optimization graphs	199
Figure D.16. Saving the results into file	199

LIST OF SYMBOLS

SYMBOLS

a : activation function in ANN model.

A_1 : flow area at cross section just downstream of bridge.

A_m : flow area in motion.

A_{p2} : obstructed area of the piers and abutments at Section (2).

A_t : total flow area.

$\overline{A_{2-1}}$: average flow area between just downstream and just upstream of bridge.

ANN_a : artificial neural network model for abutments.

ANN_p : artificial neural network model for piers.

ANN_{ss} : artificial neural network model for superstructure.

b : number of encoding bits.

b_a : wall thickness of abutments.

b_s : pier wall thickness.

b_{CL} : net bridge opening width at the centerline cross-section of bridge.

B_a : footing width of abutments.

B_s : pier footing width.

C : cost function.

C_e : expansion coefficient for channel transitions.

C_t : transition head loss coefficient.

C_c : contraction coefficient ratio for channel transitions.

C_D : drag coefficient for piers.

C_V : limiting value of a constraint.

$Cost_{add}$: additional excavation costs.

$Cost_{min}$: cost of the optimal decision to be taken for stage_n in dynamic programming.

d_f : depth of footing.

$d_{f_{min}}$: the optimal depth of footing to be taken for stage_n in dynamic programming.

d_{fa} : depth of footing for abutments.

d_{famax} : maximum depth of footing for abutments.

d_{famin} : minimum depth of footing for abutments.

d_{fp} : depth of footing for piers.
 d_{fpmax} : maximum depth of footing for piers.
 d_{fpmin} : minimum depth of footing for piers.
 d_g : depth of girder of superstructure.
 d_s : depth of scour.
 d_{sa} : depth of scour around abutments.
 d_{sc} : contraction scour.
 d_{se} : equilibrium depth of scour.
 d_{sp} : depth of scour around piers.
 del_g : girder spacing for superstructure
 D : hydraulic depth.
 D_{50} : median size of bed material.
 D_m : diameter of the smallest non-transportable particle size at the contracted section.
 e : error term.
 E : width of bridge.
 E_1 : energy head at the upstream of bridge before choking.
 E_1' : increased energy head at the upstream of bridge after choking.
 EL_{bridge} : lower chord elevation of bridge deck.
 EL_{min} : minimum bed elevation at a cross section
 EL_w : water surface elevation
 f_d : the cost of the current stage's selected state in dynamic programming.
 F : fitness functions of the optimization problem.
 F_{d_n} : the total cost of the bridge up total the current Stage $_n$.
 F_{ds} : total hydraulic force on cross-section 1 (just downstream of bridge).
 F_f : friction force between successive cross sections
 F_r : Froude number
 F_{sp} : specific force
 F_{us} : total hydraulic force on cross-section 2 (just upstream of bridge).
 F_{CDF} cumulative distribution function.
 F_D : drag force on piers.
 F_R : resistance force to flow.
 g_i : inequality constraints of optimization problem.
 Gen_{max} : maximum number of generation in GA search.

Δh_{2-1} : water surface difference between just upstream and just downstream of bridge.

h_{ce} : head loss due to transition loss between cross sections.

h_i : equality constraints of optimization problem.

H_a : height of abutment.

H_{fa} : foundation height for abutments

H_{fp} : foundation height for piers.

H_p : height of pier.

HL_{ce} : contraction / expansion loss between cross-sections.

HL_f : friction loss between cross-sections.

HL_e : total energy loss between cross-sections.

I_i : input to the neuron

k_1 : exponent for mode of bed material transport

K : conveyance of a cross section

K_1 : scour depth correction factor due to pier shape.

K_{1a} is the correction factor for the shape of abutments

K_2 : scour depth correction factor due to flow angle of attack.

K_{2a} is the correction factor for angle of attack of flow with abutment

K_3 : scour depth correction factor due to armoring effect.

K_4 : scour depth correction factor due to bed condition.

K_p : Yarnell's pier shape coefficient

L : distance between Sections (1) and (2),

L^* : average length of the obstruction created by left and right abutments

L_a is the wetted embankment (abutment) length perpendicular to the flow

L_c : flow contraction length at bridge upstream.

L_e : flow expansion length at bridge downstream.

L_{em} : width of embankment.

L_p : pier length.

L_t : total bridge length.

L_w : sidewall length of abutment.

n_c : Manning's roughness coefficient at the main channel.

n_{Mann} : Manning's roughness coefficient.

n_{ob} : Manning's roughness coefficient at the overbank section.

N_c : total number of constraints.
 N_{dfa} : number of discretization points for abutment.
 N_{dfp} : number of discretization points for piers.
 N_{pop} : population Size for GA.
 N_s number of spans of a bridge.
 N_{spi} : number of discretization points for span lengths.
 M_{select} : Selection Method for GA.
 O : objective function of the optimization problem.
perc: violation percentage of a constraint.
 P : wetted perimeter.
 P_c is the total penalty cost amount.
 P_f : probability of failure.
 P_{f_max} : maximum allowed failure probability for probabilistic constraints.
 P_r : probability function.
 Q : flow discharge
 Q_{si} : the rates of sediment transport into the control volume.
 Q_{so} : the rates of sediment transport out of the control volume.
 r_i : violation amount of each constraint.
 R : hydraulic radius
 R_{cross} : crossover rate for GA.
 R_{mut} : mutation rate for GA.
 R_L : Reliability (survival probability) of the system.
 S : the size of the search space for a certain number of spans
 S_f : friction slope at specified cross section
 \overline{S}_f : average friction slope at specified cross section.
 S_o : river bed slope.
 S_p : girder span length.
 S_{p_tot} : total span length passed up to the current Stage_n.
 S_{pimax} : maximum span length.
 S_{pimin} : minimum span length.
 S_{type} : soil type.
 St_r : amount of steel per m³ of concrete volume
 $SPTN_{ave}$: average value of standard penetration test number for foundation soils.
 t : time.

T: top width of the water surface at a cross-section.

Typ_{cross} : crossover type for GA.

u: average flow velocity at specified cross section.

u_0 : velocity of the approach flow.

u_c : critical flow velocity for beginning sediment motion at the river bed.

u_{ds} : average flow velocity at the downstream of bridge.

u_R : random number generated by uniform distribution.

u_{us} : average flow velocity at the upstream of bridge.

UC_e : unit cost of excavation for foundations.

V: volume of the control element at the alluvial bed.

V^* : the shear velocity in the main channel or floodplain at the approach section.

W_3 : bottom width of the main channel or floodplain at the approach section.

W_{CL} : width of channel cross section at the centerline of bridge.

W_x : weight of control volume along the bed slope.

$WANN_{ca}$: weight vector for abutment ANN cost model.

$WANN_{cp}$: : weight vector for pier ANN cost model.

$WANN_{css}$: weight vector for superstructure ANN cost model

$WANN_{da}$: weight vector for abutment ANN design model.

$WANN_{dp}$: : weight vector for pier ANN design model.

$WANN_{dss}$: weight vector for superstructure ANN design model.

x_R : random variable.

X_b : decimal value of a decision variable in binary format.

X_d : the decision (span length) to be taken for the current $Stage_n$ in dynamic programming.

X_{d_min} : the optimal decision (span length) to be taken for the $Stage_n$ in dynamic programming.

X_i : decision variables of optimization problem.

X_{max} : upper bound of the interval of a decision variable.

X_{min} : lower bound of the interval of a decision variable.

y: maximum water depth at a cross section.

y_0 : average flow depth in the contracted section before scour,

y_1 : water depth at the upstream of the bridge before choking.

y_1' : water depth at the upstream of the bridge after choking.

y_{2c} : critical water depth at the bridge opening before choking.

y'_{2c} : critical water depth at the bridge opening when the critical contraction ratio is reached.

y''_{2c} : critical water depth at the bridge opening beyond the critical contraction ratio.

y_3 : average flow depth in the main channel or floodplain at the approach section

y_{CL} : average depth of scour in the contracted section,

α : energy correction coefficient at a cross section.

α_c : obstructed area of the piers divided by the total unobstructed area at cross-section 1.

α_e : the energy correction coefficient at the most upstream section.

β : momentum correction coefficient at a cross section.

δ_i : the penalty coefficient for each violation amount.

γ : specific weight of water.

φ : diameter of pile

μ : ductility of bridge.

θ : angle of attack of the flow with respect to the pier axis.

θ_a : angle of inclination of the abutment axis with the approach flow axis.

θ_b : threshold value in an artificial neuron.

ρ : the water density.

Ω : coefficient of variation.

Ω_R the coefficient of variation of the reliability value.

Γ : contraction ratio for successive cross sections

Γ_c : critical contraction ratio for successive cross sections

∇ : Gradient operator.

ε : level of accuracy.

ε_L : the energy loss coefficient between sections CL and 0.

ω : indicates the fall velocity of bed material

ABBREVIATIONS

AASHTO: American Association of State Highway and Transportation Officials.
AI: artificial intelligence
AIROB: artificial intelligent framework for reliability based optimization of bridges.
ANN: artificial neural networks
CDL: critical energy depth level.
CFD: cumulative density function.
CPU :central processing unit.
CSI: Computers and Structures Inc.
D/S :downstream.
EGL: energy grade line.
EQ : earthquake.
FHWA: Federal Highway Administration.
FIB: Fédération Internationale de la Précontrainte.
GA: genetic algorithms.
GUI: graphical user interface.
LRFD: Load and resistance factor design.
MSE: mean squared error.
NI: no information
PDF: probability density functions
SPTN: Standard penetration test number.
U/S : upstream.
USACE: United States Army Corps of Engineers

CHAPTER 1

INTRODUCTION

1.1 Statement of the Problem

Bridges are one of the integral components of transportation systems, failures of which would result in loss of lives and properties as well as socio-economic inconveniences in close environment. Requirement of safe and functional systems led to evolution of a separate field in civil engineering, i.e. bridge engineering, which is specifically focused on analysis and design of various types of bridges. Being isolated elements, bridges, especially those crossing wide rivers or estuaries, are subject to more external effects than those structures bounded by different buildings. For this reason, wide-spread evaluation of various aspects from view points of different disciplines is needed. As a result, development of specifications concerning applications of universal context based on sophisticated analyses, experience, and intuition is of importance. Elaborate guidelines, such as specifications of AASHTO (1998), give necessary information to be collected and used in design applications of bridges.

Bridge design is in fact not a straight-forward task. It requires effective collaboration of a group of engineers who are experts of various fields in civil engineering profession. Although handling the central part of the design is the main concern of structural engineers, transportation, construction, and geotechnical engineers also undertake the analysis and design of relevant components of a bridge. In case of a bridge crossing a wide river, a hydraulic engineer takes an important role to check the system safety and conformity from

view point of hydraulics. Therefore, bridge hydraulics should be considered as an essential step in the design of river bridges.

Bridge design can be categorized according to the structural model to be selected at the initial stages of the design process. Various types of bridge structural models exist, such as conventional concrete bridges, pre-stressed concrete girder bridges, suspension bridges, arch bridges, cable-supported bridges, truss bridges, etc. Each of them has its own characteristics; therefore a bridge structural model is selected according to the site conditions, design requirements and economical considerations. This leads to difficulty in standardization of bridge designs. Because of this reason, a typical design usually focuses on a specific type of a structural model. Bridge design is, therefore, a complicated task due to the requirement of inter-disciplinary communications and inherent difficulties in the design. So a preliminary design is an important phase in the whole process since subsequent proportioning is based on it. A poor preliminary design may lead to uneconomical solution. Therefore, a rational approach needs to be developed to offset possible deficiencies that may be encountered in preliminary design by using contemporary tools.

1.2 Objective of the Study

In literature, there have been some attempts to automate the bridge analysis and design. However, most of these studies focus on the analysis phase rather than the design. There exists some computer software, which are capable of making extensive and detailed finite element analysis. However, they are mostly applicable for general-purpose and are considered more suitable for final analysis and design. Another deficiency in these packages is that they are usually specialized for only one aspect of design, such as structural design rather than assembling the other required design fragments, such as hydraulic and geotechnical designs in a single framework. Some studies regarding the unification of structural design with hydraulic design for bridge projects can be found in literature, such as Yanmaz and Bulut (2001). The optimization aspects

of bridge engineering have also been studied academically (Aguilar et al., 1973, and Hassanain and Loov, 2003), but these are usually for a particular structural component of the bridge rather than encompassing the bridge as a whole system. In the light of this gap, this study proposes a methodology for the optimum design of bridges crossing rivers. In this study, a desk-top methodology for the optimum preliminary design of river bridges is proposed. Due to the inherent difficulty to cover up all types of structural configurations, this methodology is built on a particular structural type. To this end, pre-stressed concrete bridges, which are widely used throughout the world, are selected. They are applicable to small and medium span lengths, i.e. approximately 10 to 40 m. The design is supplemented with a reliability-based assessment of bridge scouring.

The proposed desk-top methodology was put into practice by developing a software framework, named AIROB for the optimum design of such bridges crossing rivers. AIROB consists of wide range of numerical software libraries, almost all of which are coded throughout the course of this study in order to set up a computing basement to serve for optimization of river bridges. AIROB is complemented by developing a user friendly graphical interface in order to enhance the usability of the framework.

This thesis is composed of the following chapters: Chapter 1 presents the general information about the scope and objective of the study. In Chapter 2 and Chapter 3, the essential information about the flow through bridges and bridge scouring is introduced, respectively, which are the fundamental theoretical information on which the framework is established. An overview of applied artificial intelligence techniques utilized by the framework is presented in Chapter 4. The procedure followed during the development of the framework, which is the central part of the study, is given in Chapter 5. Chapter 6 introduces an application for the usage of the framework. Finally, the discussion, conclusions and the recommendations for further studies are presented in Chapter 7. Appendix A presents the tabular form of the statistical database on which some key parts of the framework are founded; while the sample computation tables about the records in the database are given in Appendix B. Additionally, comparison of genetic algorithms and dynamic

programming, which are the optimization techniques applied in the development of AIROB is explained in Appendix C. The thesis is concluded by a user-manual for the graphical user interface of AIROB, which is described in Appendix D.

CHAPTER 2

FLOW THROUGH BRIDGES

2.1 General

Bridges crossing rivers are one of the most commonly designed structures in civil engineering projects. Therefore, the hydraulics of flow through bridges deserves an elaborate analysis in the overall design process. In this context, starting from approximately the mid of the twentieth century, many studies have been carried out regarding various aspects of bridge hydraulics. To this end, water surface profiles computations in close vicinity to bridge openings, mechanics of sediment-laden flow through bridges leading to scouring, soil-structure-hydraulic interaction, and scour countermeasures were studied extensively. The majority of the earlier studies were supplemented by laboratory experiments. Relevant field data are usually scarce and of poor quality because of difficulties in collecting data during high flows. General scour and contraction scour may also be important depending on the general regime and degree of constriction at the bridge site. The aforementioned hydraulic aspects should be examined and their effects on bridge foundation safety should be addressed quantitatively such that necessary remedial actions can be taken in the final design stage. High level of hydraulic information has been gathered throughout the earlier researches based on these aspects. Some design specifications and guidelines regarding universal applicability were built up according to the state of the art of the research, such as ASSHTO (1998), Richardson and Davis (2001), Lagasse et al. (2001).

Structural and hydraulic interaction is the major issue of bridge hydraulics. For example, for low flows, the river flow is only in contact with the piers, abutments

and their footings. In case of high flows, however, the bridge may be subject to pressure-type flow or may be fully submerged such that the geometrical properties and dimensions of the girders and slab come into picture. Furthermore, extensive scouring may lead to appearance of caissons or piles at the foundation level and flow-foundation interaction may alter. That is why all possible structure-hydraulic-geotechnic interactions and configurations should be identified in the design phase to generate safe solutions under the worst possible scenario. This condition increases the complexity of bridge hydraulics analysis. The uncertainties arising from different sources of relevant parameters involved in the aforementioned interactions are another problem. Unless treated realistically and incorporated into the design tools, high level of uncertainties may lead to unpredictable risks. Therefore, probability-based approaches have been developed in order to consider the effects of these uncertainties. There is a growing tendency to use reliability-based analyses since they are superior to conventional methodologies in view of handling uncertainties and random nature of design parameters. The reliability analysis focused on various failure modes using proper techniques, such as fault tree analysis (Johnson, 1998 and 1999) provides valuable information on the safety level of a bridge. Therefore, the degree of repairing and maintenance is determined based on the existing situation of the bridge concerned.

Since bridge hydraulics is closely associated with river engineering, various topics of river engineering can also be included within the scope of bridge hydraulics, such as detailed analysis of turbulent boundary layers, unsteady flow effects through bridges, sediment transportation through the bridge opening, etc. The computational framework developed in this study considers only the basic principles of steady flow computation through bridges and probabilistic treatment of bridge scouring. That is why following subsections are devoted to the description of the fundamentals of flow through bridges.

2.2 Flow Through Bridges

A bridge is composed of a superstructure and substructure. Superstructure consists of bridge slab and girders, whereas substructure refers to piers, abutments, and their foundation system. In general, abutments and a set of piers are those parts of the bridge, which form obstacle to the river flow. Therefore, the interference of these structural components with the flow alters the nature of the stream flow and cause changes in the water surface profile of the river in the vicinity of the bridge site. According to the criterion of USACE (1998), the typical flow patterns through a bridge are categorized into three zones as contraction zone, flow in the bridge opening, and expansion zone (See Figure 2.1). In the direction of the flow, the undisturbed upstream flow is constricted by the bridge. The flow passes through the bridge piers and abutments, which resist to the flow and then the flow expansion takes place along the downstream direction and finally flow reaches up to the undisturbed downstream river flow.

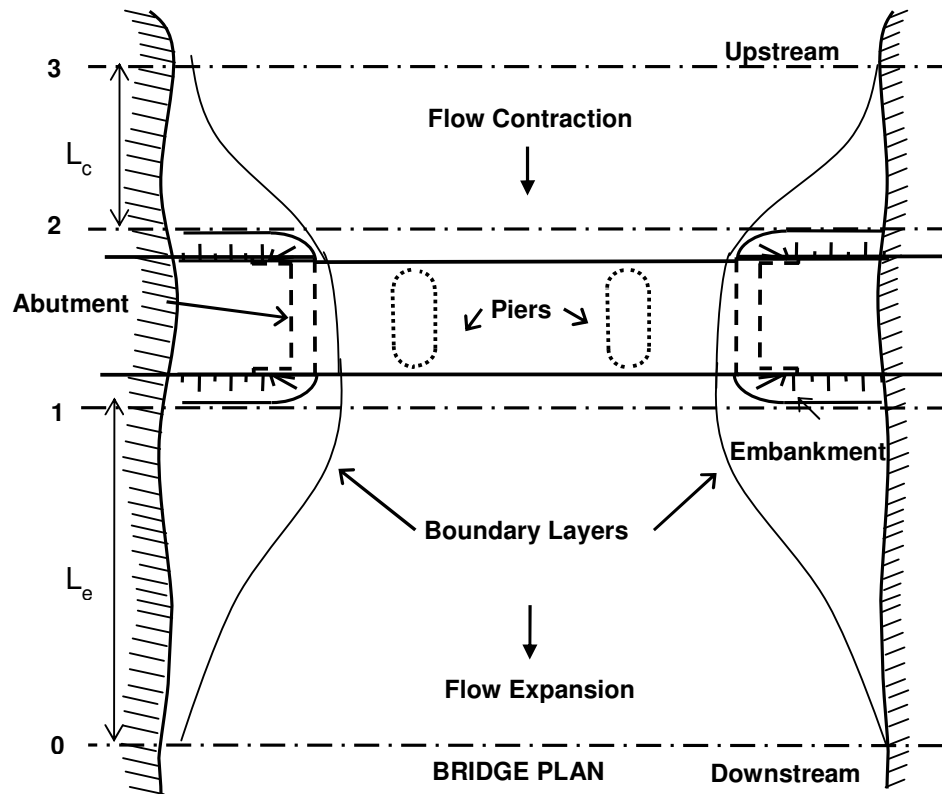


Figure 2.1. Typical flow pattern through a bridge (Adapted from USACE, 1998).

This description of flow pattern imposes at least four cross-section locations through the bridge site in order to perform a water surface profile calculation. These cross-sections are taken at the locations where the flow transitions starts and ends within this flow pattern. The explanations of these cross-sections are given from the downstream to the upstream (Figure 2.1) as follows:

- Cross-section 0: This is the most downstream cross-section, where the effect of flow expansion diminishes. From this location on, the downstream flow is governed by the geometric and flow characteristics of the downstream reach for which flow conditions are not affected by the bridge.
- Cross-section 1: This cross-section is taken at immediately downstream of the bridge. It is commonly taken at the downstream toe of the road embankment (USACE, 1998).
- Cross-section 2: It is located just upstream of the bridge. Similar to that of cross-section 1, it is commonly taken at the upstream toe of the road embankment (USACE, 1998).
- Cross-section 3: It is the end location where the approach flow is not influenced by the constriction effect of the flow.

The aforementioned cross-section locations represent the locations where the local changes occur in the flow pattern. That is why cross-sections should be taken at these locations in order to describe the flow pattern adequately. The expansion and contraction lengths need to be determined to initiate flow computations. The following expressions are proposed by USACE (1998):

$$L_c = -298 + 257 \left(\frac{F_{rc1}}{F_{rc0}} \right) + 0.918L^* + 0.00479Q \quad (2.1)$$

$$L_c = 263 + 38.8 \left(\frac{F_{rc1}}{F_{rc0}} \right) + 257 \left(\frac{Q_{ob}}{Q} \right)^2 - 58.7 \left(\frac{n_{ob}}{n_c} \right)^{0.5} + 0.161L^* \quad (2.2)$$

where L_e and L_c are expansion and contraction lengths (ft), respectively, F_{rc1} and F_{rc0} are Froude numbers at sections 1 and 0 in Figure 2.1, L^* is the average length of the obstruction created by left and right abutments (ft), Q is total discharge in the river (cfs), Q_{ob} is discharge conveyed by two overbanks at section 3 (cfs), and n_{ob} and n_c are Manning's roughness coefficients at the overbank section and main channel, respectively. In this analysis, the flow separation due to contraction and expansion effects are assumed to follow linear paths in which ineffective flow areas generate. An ineffective flow area is a region where no flow contribution occurs, i.e. the flow does not exist, but the water ponds (USACE, 1998). With this description, the flow is assumed to be one dimensional.

2.2.1 Flow Types Through Bridges

Determination of water surface profiles in close vicinity to bridges is of importance in checking possibility of choking, submergence, and formation of a hydraulic jump. Possibility of such adverse effects should be examined so that the hydraulic interference of the overall structural configuration can be modified to a tolerable form in view of bridge safety. Different flow profiles through bridge openings occur under various hydraulic conditions. The flow profiles are classified according to the corresponding hydraulic characteristics. Bridges located on plain rivers are mostly subject to subcritical flow regime, in which the flow is controlled by downstream section. An M_1 profile develops upstream of a bridge due to its constriction effect with the maximum stage at section 3. When the flow enters the contraction zone it accelerates and the flow depth tends to decrease to its minimum value at the bridge opening. Converging velocity vectors in front of the bridge may pronounce the turbulence level and create eddies. In the expansion zone, the flow decelerates with the accompanied increase in stage until section 0, where the flow reaches almost its uniform characteristics as shown in Figure 2.2. Several possibilities of flow conditions under subcritical and supercritical flows at bridge openings are presented in Figures 2.3 and 2.4 respectively. Further explanation to these possibilities is provided in Section 2.2.1.1.

In general terms, the flow conditions at a bridge site are mainly classified as “Low Flow” and “High Flow” depending on whether or not the flow interferes with the lower chord of the superstructure. The characteristics of low and high flow conditions are described in the following subsections.

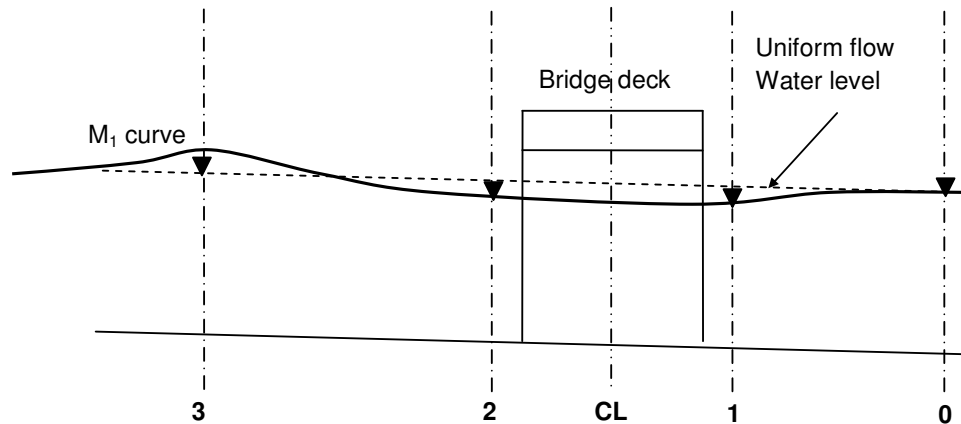


Figure 2.2. Typical water surface profile through a bridge (Adapted from Yanmaz (2002-a)).

2.2.1.1 Low Flow Conditions

Low flow conditions occur when flow takes place freely through the bridge opening without contact with the lower chord of the slab. According to the flow regime throughout the profile in the reach, low flow conditions are categorized as class A, B, or C flows having the following characteristics. In Class A flow, the flow is always subcritical throughout the bridge opening. Class B flow occurs when the flow throughout the opening is either subcritical or supercritical with the critical depth in the bridge constriction. When the flow throughout the bridge is completely in supercritical regime, this type of flow is said to be Class C flow. The water surface profiles for each class in subcritical and supercritical flow regimes are presented in Figures 2.3 and 2.4, respectively. In these figures, EGL and CDL stand for the energy grade line and critical depth line, respectively. It should be noted that the section numbers are not identical to those in Figure 2.2. When the

net flow area through the bridge opening is relatively large, type A flow occurs for subcritical flow conditions as shown in Figure 2.3.a. For the same discharge as that of part a, the maximum allowable contraction for no upstream choking occurs when the flow depth at the bridge opening is equal to the critical depth, y_{2c} . Further contraction beyond the maximum allowable value would lead to upstream choking associated with increase in the specific energy at the approach section (1) and flow depth. Therefore, the new values tend to E_1' and y_1' . Pronounced acceleration at the bridge opening would force the flow to intersect the critical depth line. Hence an M_3 profile develops with an accompanying hydraulic jump at the close downstream of the bridge opening. This case should be inhibited by providing sufficient span length between neighboring piers since hydraulic jump generates severe rollers, which may be accompanied with the vortex systems generated around piers. This action causes severe scouring problems.

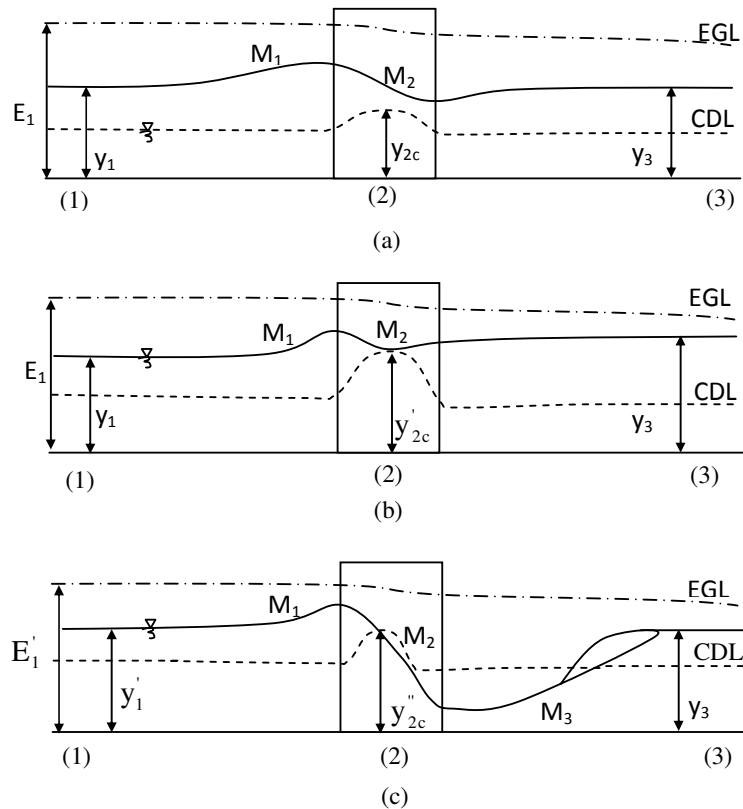


Figure 2.3. Water surface profiles for low flow conditions (Subcritical regime) (Yanmaz, 2002-a).

To inhibit upstream choking, the contraction ratio, $\Gamma = b_{CL} / b_0$, where b_{CL} and b_0 are the channel widths at sections CL and 0 shown in Figure 2.2, respectively, should be greater than a critical contraction ratio, Γ_c , which is given by Yanmaz (2002-a)

$$\Gamma_c = \sqrt{\frac{27\varepsilon_L^3 F_{r0}^2}{(2 + F_{r0}^2)^3}} \quad (2.3)$$

where, ε_L is the energy loss coefficient between sections CL and 0, and F_{r0} is the Froude number at section 0 (see Figure 2.2). Similar discussions are also valid for supercritical conditions. The only difference between the subcritical case is that a highly contracted bridge opening would lead to generation of a hydraulic jump at the upstream part of the bridge as shown in Figure 2.4.c.

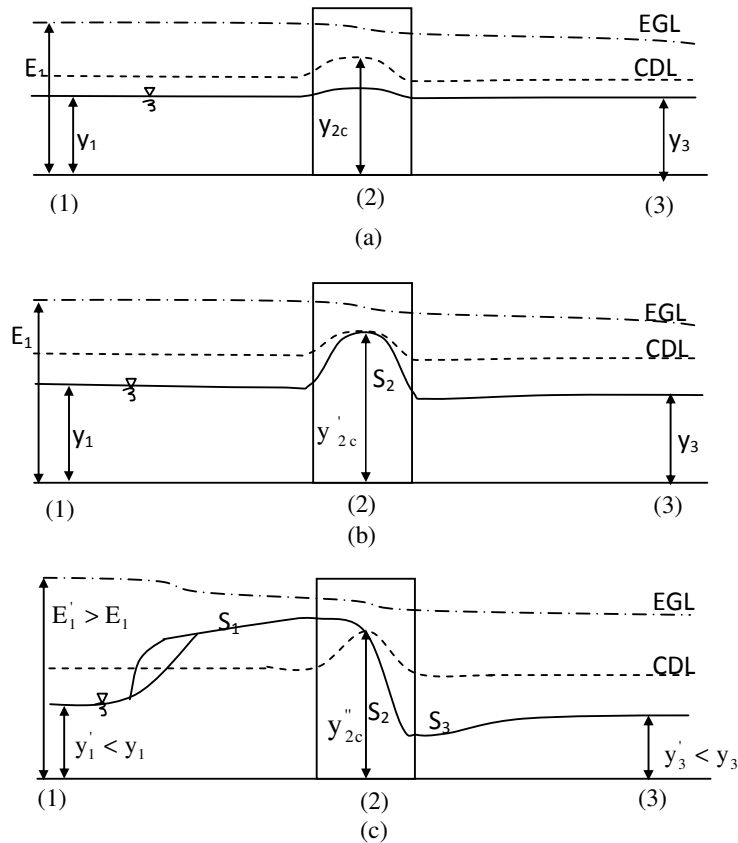


Figure 2.4. Water surface profiles for low flow conditions (Supercritical regime) (Yanmaz, 2002-a).

2.2.1.2 High Flow Conditions

High flow conditions may prevail during a severe flood. When the bridge contraction area is not large enough to transmit the flood discharge freely or when the flood is extremely large even for a tolerably large contraction, the water surface elevation gets contact with the lower chord elevation of the bridge deck. In this case, the full flow is generated through the opening, which is referred to as a pressurized type of flow. Further increase in water level leads to overtopping of the slab by the flow. In this case, hydraulic conditions dictate combination of weir and pressurized flows. Pressure type flow is extremely hazardous since developed uplift force would threaten the bridge safety. Hydraulics of pressure and weir flows is not given in this text.

2.3 Water Surface Profile Computations through Bridges

Flow profiles through bridges can be obtained using the governing conservation laws of hydraulics. To this end, energy and momentum conservation approaches can be applied with some simplifications such that one dimensional modeling is applicable for most bridges, except those having wide and irregular floodplains and curvatures. Analytical solutions are then available using either of these approaches (French, 1987). Some empirical methods have also been developed based on the field surveys. However, they are relatively simple and assumed to be applicable to the cases having similar characteristics with those of the calibration data. That is why empirical approaches are not cited in this thesis. This study deals with Class A type low flows. Therefore, modeling principles of such flows will be presented in detail.

2.3.1 The Energy Approach

The energy approach is based on application of the Standard Step Method, which is commonly applicable for determining one dimensional water surface profiles in rivers. Most of the hydraulics softwares, such as HEC-RAS (USACE, 1998) use

this approach for one dimensional hydraulic computations. It is an iterative numerical method which is built on the conservation of energy principle between two consecutive cross-sections as well as use of the conservation of mass principle through the cross-sections. The details of the standard step method can be found in most text books e.g. French (1987). The software HEC-RAS is capable of determining water surface profiles through rivers including some intermediary boundary conditions, such as bridges and culverts for subcritical, supercritical, and mixed flow regimes (USACE, 1998). Thus, some important hydraulic phenomena, such as hydraulic jump locations can be captured by this procedure.

The precision of the energy approach is closely linked to proper description of the local losses, which occur throughout the bridge opening, i.e. contraction and expansion losses. The total hydraulic loss between two successive cross-sections is the summation of frictional loss and the minor headlosses. The friction loss can be simply computed by multiplying the average friction slope between these sections with the horizontal distance between them. However, the computation of minor losses is sensitive to the selection of an appropriate transitional local loss coefficient, C_t , which reflects the headloss amount caused by the expansion or contraction of the flow. Therefore, the characteristics of the transition i.e. abrupt or gradual should also be considered. The minor loss due to transition, h_{ce} is calculated as a function of velocity head differences between the upstream and the downstream cross-sections as follows:

$$h_{ce} = C_t \left| \frac{u_{us}^2}{2g} - \frac{u_{ds}^2}{2g} \right| \quad (2.4)$$

where, u_{us} and u_{ds} are the average flow velocities at the upstream and downstream of the cross-section, respectively. The transitional headloss coefficient, C_t is equal to either contraction coefficient, C_c or expansion coefficient, C_e , depending on whether the flow is expanding or contracting, respectively.

Table 2.1 shows the typical contraction and expansion coefficients that can be selected for preliminary analysis.

Table 2.1. Subcritical flow contraction and expansion loss coefficients (USACE, 1998)

Type of transition	Contraction C_c	Expansion C_e
No transitional loss	0.0	0.0
Gradual transition	0.1	0.3
Typical bridge sections	0.3	0.5
Abrupt transitions	0.6	0.8

A single-step computation using energy approach is based on the application of the energy equation between Sections (1) and (3) as shown in Figure 2.1 to result in Chow (1959)

$$Q = C_d A_1 \sqrt{2g \left((y_3 - y_1) + \alpha_e \frac{u_3^2}{2g} - \left(L_c \left(\frac{Q^2}{K_1 K_3} \right) + L \left(\frac{Q^2}{K_1^2} \right) \right) \right)} \quad (2.5)$$

where C_d is a discharge coefficient which reflects the effects of flow conditions and geometric characteristics of the bridge opening, A_1 is the flow area just downstream of the bridge as shown in Figure 2.1, α_e is the energy correction coefficient at the most upstream section i.e. Section (3), and K_1 and K_3 are conveyances at sections 1 and 3, respectively. A set of charts have been generated by Matthai (1976) for determining C_d coefficient and its modification according to various types of flow conditions and bridge opening geometries. Several applications of the energy approach are illustrated by Yanmaz (2002-a). The computer program WSPRO (FHWWA, 1998) developed by the United States Federal Highway Administration (FHWA) is based on application of Equation (2.5).

2.3.2 The Momentum Approach

The momentum approach is based on application of the momentum balance through the bridge opening. The uniform flow depth corresponding to the design discharge can be determined at section (0) shown in Figure 2.1 using a proper equation, such as Manning's equation. The flow depth at section (1) is then determined using the momentum equation between sections (0) and (1). Afterwards, the momentum equation is applied between the cross-sections (2) and (1). The definition sketch for the conservation of momentum is shown in Figure 2.5.

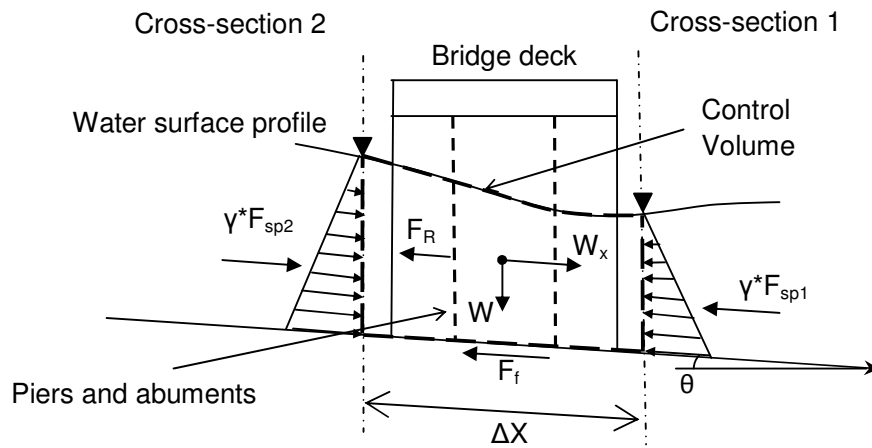


Figure 2.5. Flow profile through bridge opening for the momentum approach.

The conservation of momentum between sections (1) and (2) is written with reference to Figure 2.5 as follows:

$$\gamma(F_{sp2} - F_{sp1}) = F_f - W_x + F_R \quad (2.6)$$

where;

γ : specific weight of water,

F_{sp1} : specific force at Section (1),

F_{sp2} : specific force at Section (2),

F_f : friction force between Sections (1) and (2),

W_x : weigh component of water column in the control volume along the flow direction

F_R : resistance force against flow which is equal to the total drag force on the piers and abutments (obstacles)

The specific forces, F_{sp} at the cross-sections, the friction force, F_f , the flow resistance force, F_R , and the weight component of the control volume along the flow direction, W_x are calculated by the following equations:

$$F_{sp} = A_t \bar{Y} + \beta \frac{Q^2}{gA_m} \quad (2.7)$$

$$F_f = \gamma \overline{A_{2-1}} \overline{LS_f} \quad (2.8)$$

$$W_x = \gamma \overline{A_{2-1}} \overline{LS_o} \quad (2.9)$$

$$F_R = \gamma C_D \frac{u_2^2}{2g} A_{p2} \quad (2.10)$$

where;

A_t : total flow area including ineffective flow areas,

A_m : effective flow area,

\bar{Y} : depth from the water surface to centroid of the total flow area,

β : momentum correction coefficient,

$\overline{A_{2-1}}$: average flow area between Sections (1) and (2),

L : distance between Sections (1) and (2),

$\overline{S_f}$: average friction slope between Sections (1) and (2),

- S_0 : slope of the river bed,
- u_2 : flow velocity at Section (2),
- A_{p2} : obstructed area of the piers and abutments at Section (2),
- C_D : drag coefficient.

The momentum balance method requires determination of the drag coefficient C_D . Drag force accounts for the effect of force induced by flow according to the degree of obstruction presented to the flow, the separation of the flow, and wake formation at the rear face of the obstacle. Therefore, it mainly depends on the geometrical properties of the object and the Reynolds number. For fully developed turbulent flow conditions, the effect of the Reynolds number can be ignored. Typical values of C_D with respect to various pier shapes are given in Table 2.2.

Table 2.2. Typical drag coefficients for various pier shapes (USACE, 1998).

Pier Shape	Drag Coefficient C_D
Circular pier	1.20
Elongated piers with semi-circular ends	1.33
Elliptical piers with 2:1 length to width ratio	0.60
Elliptical piers with 4:1 length to width ratio	0.32
Elliptical piers with 8:1 length to width ratio	0.29
Square nose piers	2.00
Triangular nose with 30° angle	1.00
Triangular nose with 60° angle	1.39
Triangular nose with 90° angle	1.60
Triangular nose with 120° angle	1.72

Equation (2.6) is solved by a trial and error procedure. For the subcritical flow condition, with the know water surface elevation at Section (1), a suitable value is assumed for the water surface elevation at Section (2) and the values of the

associated variables involved in Equations (2.7), (2.8), (2.9) and (2.10) are calculated to check if Equation (2.6) is satisfied. This iterative scheme is repeated until the desired precision is achieved. In the computational procedure, the weight component in the direction of flow, W_x , is conventionally neglected since the bed slope is relatively small for plain rivers.

2.3.3 The Yarnell Equation

Yarnell (1934) developed an empirical equation that is used to predict the change in water surface elevation between Sections (1) and (2) defined in Figure 2.1. The equation is based on 2600 laboratory experiments. This equation is of practical significance since it deals with the shape and size of piers, the approach angle of the flow with the pier axis, and the Froude number. That is why it is still in use in bridge hydraulics applications for preliminary purposes. However, it should be kept in mind that Yarnell's equation is mainly dependent on pier and flow characteristics but not sensitive to geometrical properties of the bridge opening including abutments. Therefore, it may give realistic values for the cases in which the energy losses are mainly associated with the piers. The equation is as follows (USACE, 1998):

$$\frac{\Delta h_{2-1}}{y_1} = K_p F_{r1}^2 (K_p + 5F_{r1}^2 - 0.6) (\alpha_c + 15\alpha_c^2) \quad (2.11)$$

where;

Δh_{2-1} : drop in water surface elevations from section 2 to 1,

K_p : Yarnell's pier shape coefficient (See Table 2.3),

F_{r1} : Froude number Section (1),

α_c : Obstructed area of the piers divided by the total unobstructed area at Section (1)

Table 2.3. Yarnell's pier shape coefficients, K_p (USACE, 1998).

Pier Shape	K_p
Semi-circular nose and tail	0.90
Twin-cylinder piers with connecting diaphragm	0.95
Twin-cylinder piers without diaphragm	1.05
90° triangular nose and tail	1.05
Square nose and tail	1.25
Ten pile trestle bent	2.50

This chapter is intended to introduce basic hydraulic computations for the flow over fixed boundaries through bridge openings. An overview of bridge scouring concepts will be introduced in Chapter 3.

CHAPTER 3

BRIDGE SCOURING

3.1 General

Many river bridges fail because of excessive scouring at infrastructural elements during heavy floods. Understanding the overall scouring mechanism is of importance in order to develop realistic methods for determining safe depth of burial of bridge footings. However, the problem is in fact relatively complicated because of the combined effects of general, localized and local scours leading to a three-dimensional riverbed degradation at piers and abutments, and some human-induced interference, such as channel mining upstream of a bridge site (Yanmaz and Çicekdağ, 2000). Most of the parameters characterizing this phenomenon are of probabilistic nature. For the sake of practical simplicity, the aforementioned scouring processes are treated as independent events.

Bridge design should be based on joint consideration of hydraulic and structural interactions. Lack of such evaluations may lead to generation of considerable backwatering, increased scouring potential at infrastructural elements or accelerated flow conditions associated with a hydraulic jump and debris accumulation at the bridge opening (Yanmaz and Kürkçüoğlu, 2000). Simplified deterministic approaches are incapable of modeling the true behavior of the flow conditions and hence introduce considerable uncertainty in hydraulic design. To handle this problem, conventional design approaches consider high safety margins for the depth of footings of piers and abutments, which increases the total cost of the structure. There are plenty of research studies investigating several aspects of the scouring mechanism. In this thesis, a brief information will

be given for the scouring mechanism and the most commonly used scour equations will be presented.

3.2 The Mechanism of Scouring

Alluvial river beds composed of loose non-cohesive material is susceptible to scouring whenever the rate of sediment transport is accelerated due to the contraction of the flow area, such as natural contractions along the river alignment and at bridge openings as well as generation of vortex systems around piers and abutments. The scouring mechanism can be explained with reference to the sediment continuity equation (Yanmaz, 2002-a):

$$\frac{dV}{dt} = Q_{so} - Q_{si} \quad (3.1)$$

in which V is volume of the control element at the alluvial bed, t is time, Q_{si} and Q_{so} are the rates of sediment transport into and out of the control volume, respectively. A localized contraction, such as a bridge opening, causes an increase in the local sediment transport capacity because of flow acceleration. Since the upstream sediment transport rate is smaller than that of the contracted section, Q_{so} becomes greater than Q_{si} in the control volume. As can also be observed from Equation (3.1), this will lead to bed lowering with respect to time. This phenomenon is termed as scouring.

The general scour is related to the bed and flow regime of the river, which occurs irrespective of the presence of any hydraulic structure, such as a bridge. It may take place over a very long time scale of the order of greater than lifetime of bridge. Due to its slow processing, the general scour is of minor importance in assessing total scouring of a bridge. Therefore, in practice, mainly localized (contraction) and local scours are considered for estimating the maximum scour at bridge sites. This study also deals with this approach and the computational algorithm will not consider general scouring.

There are two types of scour at loose boundaries. Clear water scour occurs when the inertia of the flow is relatively low such that the bed shear stress is not capable of initiating sediment motion at the bed. This type of scour normally occurs in floodplains, in main channels having low flow rates, and downstream of dam outlets, where reservoir captures almost all incoming sediment. Live-bed scour occurs when there is active-bed load transportation at the upstream. The sediment-laden flow interferes with the erosive action in the scour hole developed around a pier or abutment. Scour evolution is dependent on the sediment transport capacity of the approach flow and the flow characteristics in the scour hole. The characteristics of flow in the scour hole are influenced by the flow intensity and geometric characteristics of pier or abutment and the scour hole. Live-bed scour depth, d_s increases rapidly with time and then fluctuates about an equilibrium scour depth, d_{se} . Figure 3.1 shows the scour development around a bridge pier against time, t , and velocity, u , in which u_c is the mean threshold velocity. Temporal variation of live-bed scour shows fluctuations due to continuous changes of the bed resistance in turbulent flow and random sediment supply into the scour hole,

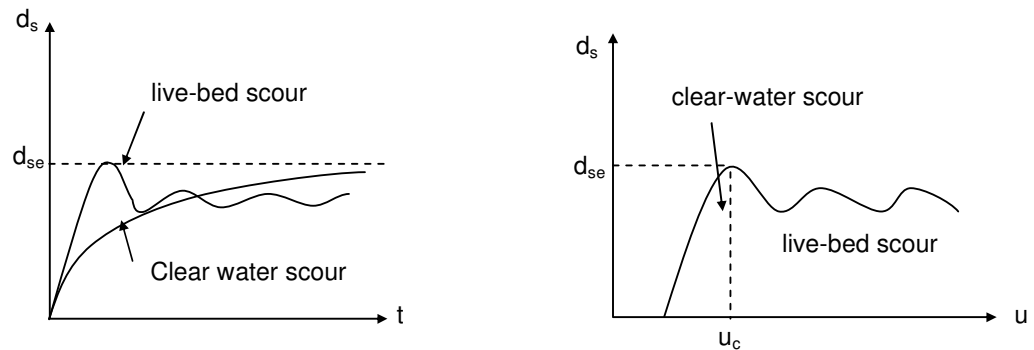


Figure 3.1. Variation of scour depth with time and velocity (Yanmaz, 2002-a).

3.2.1 Contraction Scour

Contraction or localized scour occurs when the flow area of the river is constricted either naturally or a man-made barrier, such as a bridge. The modified version of Laursen's live-bed scour equation is given as (USACE, 1998):

$$y_{CL} = y_3 \left(\frac{Q_{CL}}{Q_3} \right)^{6/7} \left(\frac{W_3}{W_{CL}} \right)^{k_1} \quad (3.2)$$

$$d_{sc} = y_{CL} - y_0 \quad (3.3)$$

where, y_0 : average flow depth in the contracted section before scour,

y_{CL} : average depth of scour in the contracted section,

d_{sc} : depth of contraction scour,

y_3 : average flow depth in the main channel or floodplain at the approach section i.e. Section 3 in Figure 2.1,

Q_{CL} : sediment laden discharge in the main channel or floodplain at the contracted section,

Q_3 : sediment laden flow in the main channel or floodplain at the approach section,

W_{CL} : net bottom width of the main channel or floodplain at the contracted section, which is approximated as the top width of the active flow area for an irregular cross-section.

W_3 : bottom width of the main channel or floodplain at the approach section, which is approximated as the top width of the active flow area for an irregular cross-section.

k_1 : exponent for mode of bed material transport, which can be selected from Table 3.1.

Table 3.1. k_1 , exponent in Laursen's model (USACE, 1998).

V^* / ω	k_1	Mode of bed material transport
< 0.50	0.59	Mostly contact bed material discharge
0.50 to 2.0	0.64	Some suspended bed material discharge
> 2.0	0.69	Mostly suspended bed material discharge

In Table 3.1, ω , indicates the fall velocity of bed material based on median size of bed material, D_{50} and V^* denotes the shear velocity in the main channel or floodplain at the approach section, which is computed from

$$V^* = \sqrt{gy_3 S_{f3}} \quad (3.4)$$

where, S_{f3} : slope of the energy grade line at the approach cross-section,

USACE (1998) recommends the following equation for contraction scour under clear water conditions:

$$y_{CL} = \left[\frac{Q_{CL}^2}{40D_m^{2/3} W_{CL}^2} \right]^{3/7} \quad (3.5)$$

where, D_m is the diameter of the smallest non-transportable particle size at the contracted section, which may be taken as $1.25D_{50}$. Thus, the depth of scour, d_{sc} can be calculated from Equation (3.3).

3.2.2 Local Scour Around Piers and Abutments

The scouring mechanism around bridge piers and abutments are similar except that flow around a pier is symmetrical, whereas an abutment is fixed to the side at one face. Therefore, the scouring action will only be described for piers in detail.

When a pier is placed in a flow section, water surface elevation at its upstream face increases due to an abrupt decrease of velocity. A stagnation pressure plane occurs at the upstream face of the bridge. The amount of increase of upstream water level depends on the velocity of the approach flow, u_0 , and geometric characteristics of the bridge pier. In case of a strong pressure increase at the upstream face of a pier, a three-dimensional turbulent boundary layer separates. Since the velocity u_0 decreases from the free surface downwards, the stagnation pressure, $\rho u_0^2 / 2$, ρ being the water density, also decrease from the surface downwards. Therefore, this produces a downward pressure gradient, and hence a downward velocity component. This velocity component interferes with the approach flow and creates the so-called horse-shoe vortices at the bed level as shown in Figure 3.2. The downflow erodes the bed and the eroded materials are carried by the horse-shoe vortices. The strength or material carrying ability of these vortices depends on the flow Reynolds number and the geometry of the bridge pier. The use of pointed nosed piers decreases the strength of horseshoe vortices. However, their construction is difficult. That is why rounded-nosed rectangular piers or a group of cylindrical piers are frequently used in practice.

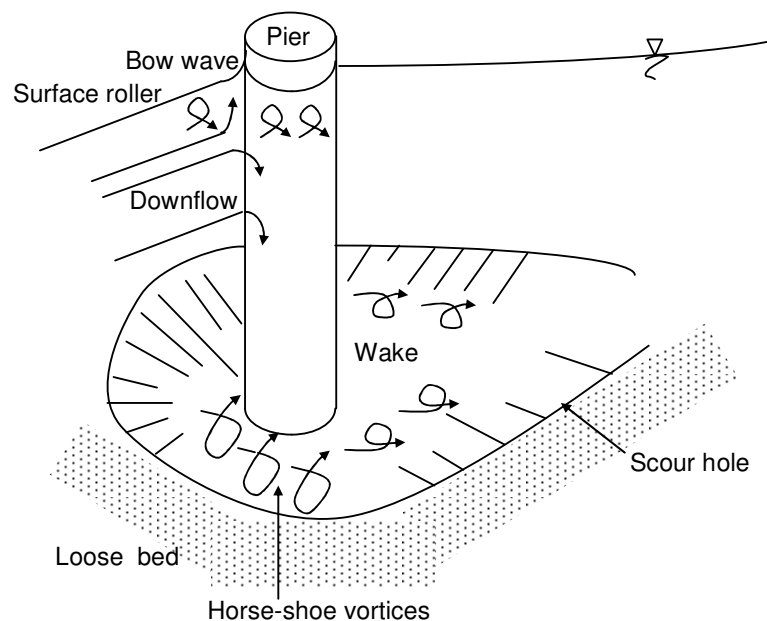


Figure 3.2. Formation of vortex systems around a bridge pier (Yanmaz, 2002-a).

Wake vortices develop at the rear side of the pier as a result of shear stress gradients in the separated negative-pressure zone around the bridge pier (see Figure 3.2). Eroded particles from the bed by the wake vortices are transported to the downstream in relation to the flow intensity and the geometric characteristics of the pier. As the wake region behind the pier may extend far downstream from the pier, the eroded particles are carried by wake vortices to the downstream until the effects of these vortices diminish. The horseshoe vortices are stronger than wake vortices. Therefore, the maximum scour depths are normally observed at the upstream side of the pier.

Yanmaz (2002-a) presents the following functional relationship for a given shape of single bridge pier scouring

$$\frac{d_s}{b} = f\left(\frac{y}{b}, F_r, \sigma_g, \frac{b}{D_{50}}, \frac{ut}{D_{50}}\right) \quad (3.6)$$

in which, d_s is depth of scour, b is pier size perpendicular to the flow direction, F_r is Froude number, σ_g is geometric standard deviation of particle size distribution, u is mean approach flow velocity, and t is time. Equation (3.6) is valid under the conditions of fully developed turbulent flow over non-cohesive bed in a wide and straight river flow approaching with zero angle of inclination to the pier axis. The effects of governing variables presented in Equation (3.6) are not discussed in this text. The most widely used design equations are presented in the following. The HEC-18 procedure uses the so-called Colorado State University (CSU) equation (Richardson and Davis, 2001) for the computation of depth of pier scour under both clear water and live-bed conditions. Maximum depth of scour, d_s , can be determined from

$$d_s = 2.0K_1K_2K_3K_4b^{0.65}y_2^{0.35}F_{r2}^{0.43} \quad (3.7)$$

where, K_1 : correction factor for pier nose shape,
 K_2 : correction factor for angle of attack of flow,
 K_3 : correction factor for bed condition,
 K_4 : correction factor for armoring of bed material,
 y_2 : flow depth just upstream of the pier, taken by the flow distribution calculations at Section (2) in Figure 2.1,
 F_{r2} : Froude number just upstream of the pier, taken by the flow distribution calculations at Section (2) in Figure 2.1.

In case of the round nosed piers aligned with the flow direction, the maximum depth of scour is limited to $d_s \leq 2.4b$ for $F_{r2} \leq 0.8$ and $d_s \leq 3.0b$ for $F_{r2} > 0.8$. The correction factors adjust the scour depth value according to several circumstances. The application of these correction factors is summarized as follows:

- K_1 : the correction factor for the pier nose shape (Table 3.2).

Table 3.2. Correction factor, K_1 , for pier nose shape (USACE, 1998).

Shape of Pier Nose	K_1
Square Nose	1.1
Round Nose	1.0
Circular Cylinder	1.0
Group of Cylinders	1.0
Sharp Nose (triangular)	0.9

- K_2 : the correction factor for angle attack of the flow is calculated by the following equation:

$$K_2 = \left(\cos \theta + \frac{L}{b} \sin \theta \right)^{0.65} \quad (3.8)$$

where, L: length of the pier along the flow,
 θ : angle of attack of the flow with respect to the pier axis.

- **K₃**: the correction factor for the bed condition is selected from Table 3.3.

Table 3.3. Correction factor, K₃, for bed condition (USACE, 1998).

Bed Condition	Dune Height (ft)	K ₃
Clear Water Scour	N/A	1.1
Plane Bed and Antidune Flow	N/A	1.1
Small Dunes	10 > H ≥ 2	1.1
Medium Dunes	30 > H ≥ 10	1.1 to 1.2
Large Dunes	H ≥ 30	1.3

K₄: the correction factor accounts for the effect of armoring of bed material. The computational procedure is provided in USACE (1998).

For the computation of the abutment scour, d_{sa} , the procedure used in HEC-18 (FHWA, 2001) methodology will be followed in this study. If $(L_a/y_3 > 25)$, where L_a is the wetted embankment (abutment) length perpendicular to the flow and y_3 is the depth of flow at the approach section, the HIRE equation is used (USACE, 1998):

$$d_s = 4y_2 \left(\frac{K_{1a}}{0.55} \right) K_{2a} F_{r2}^{0.33} \quad (3.9)$$

where, y_2 and F_{r2} are the depth of flow and Froude number, respectively, taken at the aforementioned Section (2), K_{1a} is the correction factor for the shape of abutments (see Table 3.4), K_{2a} is the correction factor for angle of attack of flow with abutment, which can be computed from $(\theta_a/90)^{0.13}$ (USACE, 1998). Herein θ_a is the angle of inclination of the abutment axis with the approach flow axis.

Table 3.4. Correction factor for abutment shape (USACE, 1998).

Shape of Abutment	K_{1a}
Vertical-wall Abutment	1.0
Vertical-wall Abutment with wingwalls	0.82
Spill through Abutment	0.55

If $(L_a / y_3 \leq 25)$, Froehlich's equation is suggested (USACE, 1998).

$$d_s = 2.27K_{1a}K_{2a}(L_a)^{0.43}y_3^{0.57}F_{r3}^{0.61} + y_3 \quad (3.10)$$

where, y_3 and F_{r3} are the depth of flow and Froude number on the floodplain, respectively, taken at the approach section.

The total scour depth around the piers and abutments are calculated by simply adding the contraction scour values to the corresponding local scour values. The rest of the bridge opening is affected by only the contraction scour. The top width of the local scour hole at a pier is approximated as $2.0d_s$ to each side of the pier (USACE, 1998).

CHAPTER 4

AN OVERVIEW OF APPLIED ARTIFICIAL INTELLIGENCE TECHNIQUES

4.1 Introduction

The optimization of river bridges have been implemented within the scope of two fundamental artificial intelligence techniques, each of which is responsible for different purpose in the overall flowchart of the developed methodology. The computational complexities of these underlying methods in the developed framework require comprehensive examination of various artificial intelligence techniques to be exploited in the scope of the study. Among these AI techniques, artificial neural networks are the basis of estimating the basic design dimensions of bridge components, their corresponding costs, and the total cost of the bridge as whole. This is the statistical-based part of the study on which the remaining optimization procedures are built.

The major rationale behind the utilization of ANN approach in this study is to avoid cumbersome conventional structural design procedures. This is required because, the overburden of the conventional design methods adversely affect the performance of the optimization engine of the framework due to the requirement of excessive computational effort for CPU of the computer. On the other hand, after modeling ANNs, the computational efficiency significantly increases due to very lightweight CPU performance requirement for ANN processing. Another reason for selecting ANNs as the structural design tool for the framework is their capability of capturing inherent practical design requirements since they are built on real design projects.

For the optimization part, the selection of the appropriate technique requires more in-depth analysis. There are various optimization techniques in the literature, each having its own advantages and disadvantages. This study is relied on a heuristic based optimization approach, Genetic Algorithms (GA), of which the details are presented in the following sections of this chapter. There are basically two major justifications of selecting GA as the nonlinear form of the objective function of the optimization problem and the dimension of the search space. Since the cost of the bridge is to be minimized, the objective function of this study relies on ANN models, which have highly nonlinear forms. Therefore, conventional calculus-based optimization approaches are inadequate for this study. Another restriction is the computational effort needed for single execution of calculating the objective function, which is handled by ANNs in cooperation with reliability based bridge hydraulic calculations. Among these procedures, reliability based hydraulic calculations are not economical in terms of computational effort, so that the number of executions is another important parameter for selection of the appropriate optimization technique. Classical trial and error based procedures built upon searching without any intelligent guidance greatly increases the computational time required to obtain the solution. For this reason, the computational burden of reliability-based hydraulic computations along with the corresponding size of the search space in this optimization study is not so suitable for performing a brute force technique. This circumstances guide the study to select a heuristic based technique, in which search is performed by an intelligent supervision. Among various heuristic based techniques, GA is decided to be the major optimization method for this study because of its robust, widespread, justified usage among various studies in engineering design problems.

In the light of the above discussion, two major topics of AI, ANN and GA are explained along with their overall position in AI studies.

4.2 Artificial Intelligence

Artificial intelligence (AI) has a very broad meaning; therefore its brief definition encircling all its associated research fields is quite difficult. The common implication of the term is accepted to be the study and the design of intelligent agents which is a system that can perceive its environment and that maximize its possibility of success according to the extracted information from observations (Russell and Norvig, 2003). Regarding this definition, it is highly expected that AI researches are comprised of technically detailed studies which can be easily detached into subfields, each of which can be considered as a separate field of study. The extensiveness of the area introduces some difficulties to assemble these subfields under a global framework. For this reason, each AI research has been carried out within its own contextual mathematical grounds among which there is not a direct communication. Consequently, an AI research is usually recalled by the associated mathematical foundation rather than using a generic term such as “artificial intelligence”.

Throughout the history of AI, subfields have matured around particular institutions, the work of individual researchers, the solution of specific problems, and differences in the viewpoint to the solution of some particular AI problems and the differences between the tools applied (Wikipedia, 2011-a). A common AI classification is done according to the following aspects:

- problems that AI studies are concerned with,
- approaches or paradigms that AI researches are based on, and
- the employed mathematical tools.

Therefore, an AI research falls into the following principal problems; reasoning, knowledge, planning, learning, communication, perception, and the ability to move and manipulate objects (Wikipedia, 2011-a). The main paradigms in the AI researches can be stated as cybernetics and brain simulation, symbolic approaches, sub-symbolic approaches, and statistical-based approaches. It is also possible to integrate different solution paradigms into a framework which is commonly done in order to produce flexible solutions to the complicated

problems. AI researches also hosted various mathematical models and tools throughout its history. The notable ones are search and optimization techniques, logic, probabilistic methods for uncertain reasoning, classifiers and statistical learning methods, neural networks, and programming languages.

From the view point of civil engineering, the categorization can be narrowed such that the main objectives of an AI-based study is done in order to accomplish subsequent purposes, such as advanced estimation and regression analyses, function approximation, expert systems, decision support systems, case-based reasoning systems, optimization, etc. In civil engineering, two fundamental AI topics; artificial neural networks and optimization are very popular among researchers. That is why many adaptations of these problems into certain civil engineering problems have been performed. This study makes use of these two common AI techniques in an assembled form so that the interaction between these two different fields of AI can also be shown to work satisfactorily. Therefore, it is highly promising to examine the outcomes of this study from a generic AI point of view, in addition to its particular assessment within the civil engineering researches.

Since AI is a very wide-ranging area such that its boundaries cannot be drawn explicitly, all the topics within the context of AI will not be described in detail. For this purpose, this chapter deals with the concepts of AI involved specifically in this study. These are artificial neural networks and optimization techniques, specifically Genetic Algorithms.

4.3 Artificial Neural Networks

Artificial neural networks (ANN) are one of the fundamentals mathematical models in AI computing. They are inspired by neural networks in human brain. Although the first attempts in simulating neural networks go back to 1940's, the attractiveness of them rise at 1980's by the studies of Hopfield (1982) as the development of nonlinear neural network models. Kohonen (1982) and Anderson (1983) extended the studies further by the development of neural network models

based on unsupervised learning. As the development of back-propagation learning algorithm for feed-forward ANNs emerges by Rumelhart et. al. (1986), a popularity of ANNs surged up at various disciplines. As a result, the great capacity of human brain in recognizing patterns in natural world encouraged AI researchers to simulate this capability in computing world. Thus, ANNs are developed as a mathematical tool for the usage in practical computational problems. Figure 4.1 represents a typical neuron connection within the brain.

The basic idea underlying ANN is to develop a mathematical model such that the input signals to a neuron is fired as output from the neuron to the adjacent connected neurons if the level of input signals reaches a threshold value. This mechanism is reflected to a mathematical model called as “artificial neuron” (see Figure 4.2). An artificial neuron is the founding component of ANN models so that an ANN mathematical model is simply comprised of a number of interconnected artificial neurons.

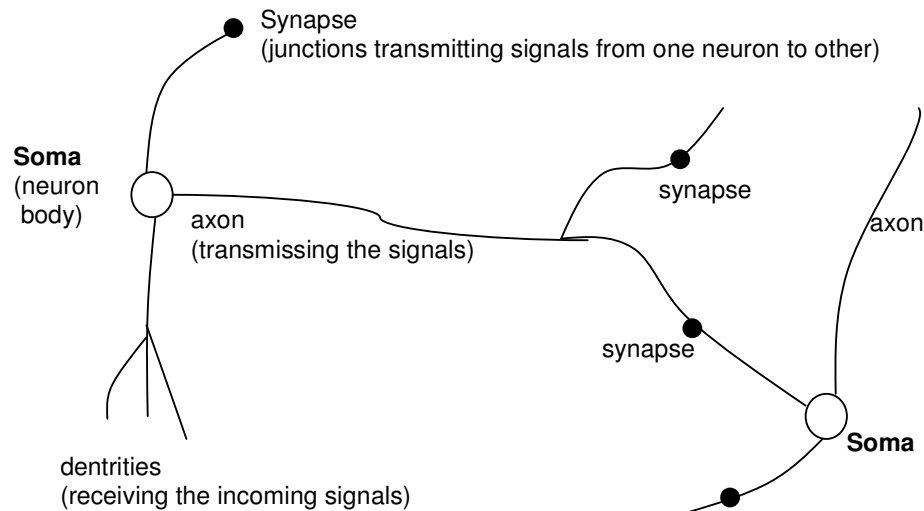


Figure 4.1. Typical biological neuron in a human brain (Adapted from Heaton (2008)).

The mathematical representation of an artificial neuron can be drawn with reference to schematics in Figure 4.2 as follows:

$$a = \left(\sum_{j=1}^N w_j I_j \right) + \theta_b \quad (4.1)$$

in which, each input to the neuron is denoted by I_i , while each connection from input to the neuron is assigned a weight, represented as w_i . Threshold value in artificial neuron is represented as θ_b and the activation of the neuron is shown as a . Threshold value, θ_b in artificial neuron model is usually assigned a positive value so as to refer to it as “bias” in ANN terminology.

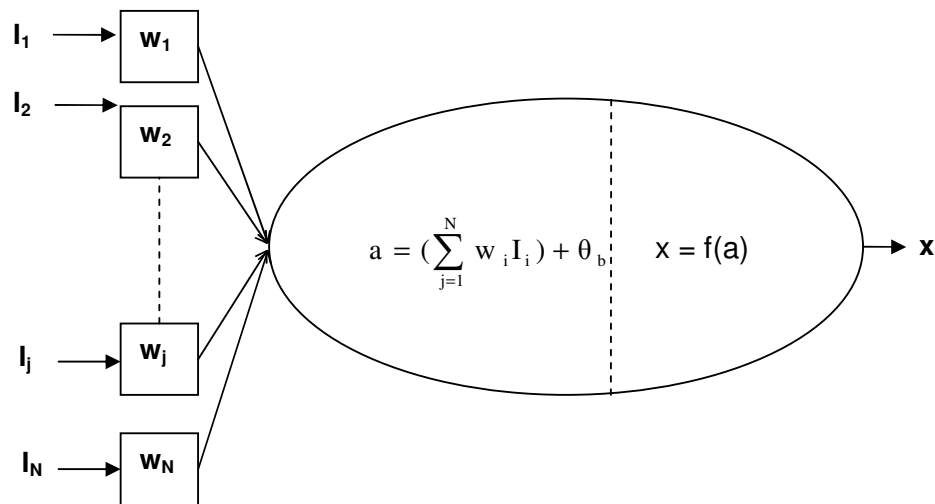


Figure 4.2. Artificial neuron as a mathematical tool (Russell and Norvig, 2003).

The output value of an artificial neuron is a function of activation value, a . This function is called as activation function or transformation function which forms the real behavior of an artificial neuron. The activation functions can be selected

among various functions as presented in Figure 4.3. Although, it is possible to use a linear activation function, almost all of ANN models use a nonlinear activation function in order to use ANNs for the solution of complicated problems. Thus ANN models are regarded as highly nonlinear mathematical models. This nonlinear behavior gives great power to ANN models in order to solve a wide range of complicated problems efficiently, while conventional techniques have deficiencies for the solutions. As a result of this discussion, the output of an artificial neuron, x can be represented by Equation (4.2) along with some classic activation functions (Russell and Norvig, 2003):

$$x = (a) = Ka \tag{4.2}$$

$$x = (a) = \left\langle \begin{array}{l|l} 0 & a \leq 0 \\ 1 & 0 < a \end{array} \right\rangle \tag{4.3}$$

$$x = (a) = \left\langle \begin{array}{l|l} 0 & a \leq 0 \\ \frac{a}{K} & 0 < a \leq K \\ K & K < a \\ 1 & \end{array} \right\rangle \tag{4.4}$$

$$x = f(a) = \frac{1}{1 + e^{-Ka}} \tag{4.5}$$

where; K is the constant of equations. Among typical activation functions, Equation (4.3) is called threshold function, whereas Equations (4.4) and (4.5) are called as Ramp and Logsigmoid functions, respectively. Logsigmoid function is a

frequently used nonlinear activation function within ANN studies. The activation functions are bounded by some interval such that whatever the activation value is, the output, x is limited by an interval. For Logsigmoid activation function, this boundary is $[0, 1]$ (see Figure 4.3).

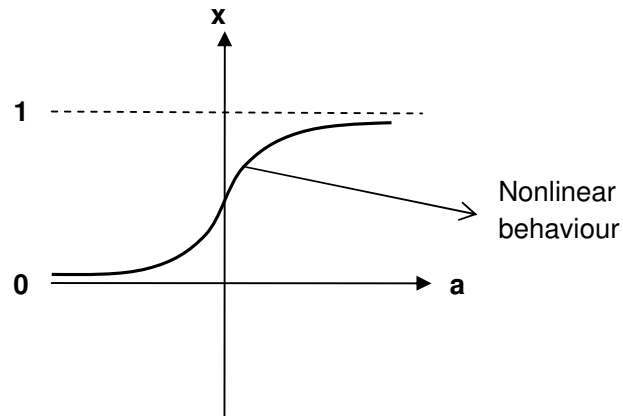


Figure 4.3. Logsigmoid activation function (Demuth and Beale, 2002).

4.3.1 Network of Artificial Neurons as ANN

An artificial neural network is composed of interconnected artificial neurons in order to form a network of neurons. In this case, there are several artificial neurons in the system such that the system is capable of performing high level of nonlinear achievement. In practice, any non-linear problem is presumed to be approximated by an ANN, provided that the required number of neurons exists in the network with well-designed network architecture. Then, the building blocks of an ANN are artificial neurons present in the model which can be represented mathematically as follows (Russell and Norvig, 2003):

$$a_i = \left(\sum_{j=1}^N w_{ji} x_j \right) + \theta_{bi} \quad (4.6)$$

where, each neuron in the network is discriminated by indices, i . This results a two dimensional vector form for the weights, w_{ji} , connecting to the artificial neuron, a_i . In Equation (4.6), x_j is either the output of a neuron determined as:

$$x_j = f_j(a_j) \quad (4.7)$$

or a direct external input determined as:

$$x_j = u_j \quad (4.8)$$

As it is seen from Equation (4.7), each artificial neuron can use different activation function, f_i associated to that particular neuron, even though in practice, it is customary to use the same activation function for all the neurons in the network in order to increase simplicity for implementation purposes.

4.3.2 ANN Architectures

The architecture of an ANN can be defined as the organizational forms of neurons in the network. In spite of having any pattern of network as a possible arrangement theoretically, there are some classifications according to the most commonly used architectural patterns. These classifications are usually based on the structure of the connections in the network. In this context, there are two fundamental architectures for ANN modeling which are widely used in practice as follows (Heaton, 2008):

- Layered feed-forward artificial neural networks, (see Figure 4.4) and
- Non-layered recurrent artificial neural networks (see Figure 4.4).

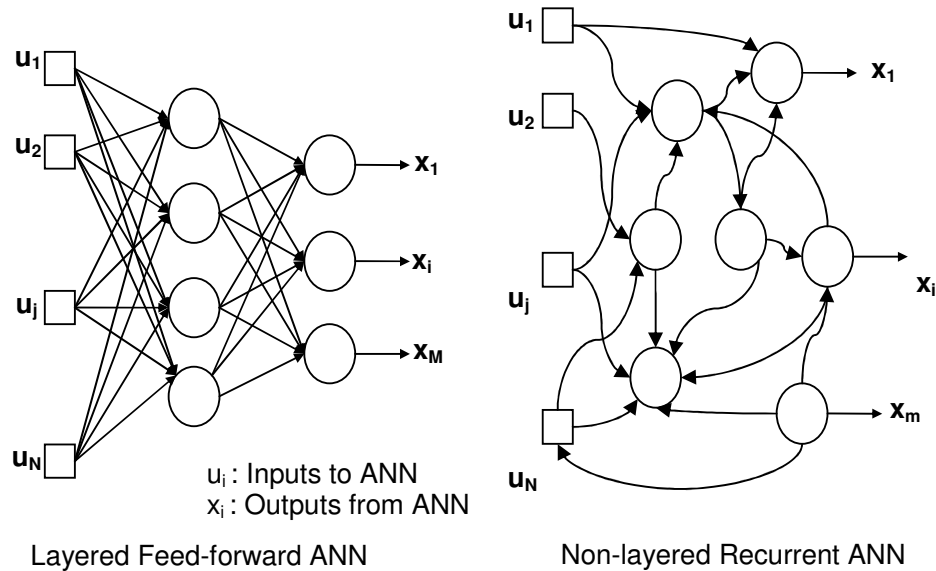


Figure 4.4. Basic types of ANN architectures (Adapted from Heaton (2008)).

As it is seen in Figure 4.4, the neurons are organized in layers in a feed-forward ANN, while in a recurrent ANN, the connections exist to the neurons of the same layer or the previous layer, which shows a much more generic behavior. However, recurrent ANN architecture is difficult to study and, for most of the practical problems it is inconvenient to use them. Therefore, wide ranges of problems in AI-based researches are associated to feed-forward neural networks.

4.3.3 Feed-Forward Artificial Neural Networks

Feed-forward artificial neural networks are the common tools for most of ANN related problems. This study also employs feed-forward ANN architecture within its methodology. In feed-forward ANN architecture, the neurons in a particular layer get input from the previous layer and the following layer is fed by their outputs. In this architecture, connections to the neurons in the same or previous layer are not allowed as its name implies (Heaton, 2008).

A feed-forward ANN is usually engaged to associate input parameters of a certain complex problem to the corresponding output parameters. Therefore, according to this conventional usage and the restrictions of its architectural definitions, the layers in feed-forward ANN can be defined in three categories as follows:

- **Input Layer:** It is made of special input neurons, directly transmitting the applied external input to the outputs without applying any transformation by an activation function. In this context, each neuron in the input layer reflects the input variables of the problem.
- **Output Layer:** It is the last layer of neurons from which the desired values of output parameters are obtained by the outputs of each neuron in the layer. Each neuron in the output layer holds the output variable of the problem.
- **Hidden Layers:** The layers between the input layer and the output layer are defined as hidden layers. The number of hidden layers and the number of neurons in each hidden layer are subject to the problem to be solved and therefore, there is not a fixed rule. These are determined in the modeling phase of an ANN.

As it is apparent from the aforementioned definitions of feed-forward ANN architecture, the formation of this type of ANN model is in layers of neurons, which institutes a simplified procedure for their implementation and usage. Therefore, there are various applications that can be solved by this type of ANN. In general, feed-forward ANNs are appreciated as black-box models in order to approximate a highly complicated nonlinear physical phenomenon without any analytical information related to that phenomenon (see Figure 4.5). In this respect, the input and output parameters of the problem are selected and reflected to the ANN as input and output layers, respectively. Therefore, the independent and dependent variables of the model to be approximated is determined in this stage. Although this is usually done intuitively, selection of

variables to be used in the model requires the following considerations (Smith, 1993):

- Firstly, the existing information or data should be transformed into a form that ANN model can process,
- Secondly, selection among the existing variables is based on prediction and covariance.

An important point for selecting the variables is such that there should not be any correlation between the input parameters. In such a case, learning capacity of the corresponding ANN decreases. Therefore, as a rule of thumb, it is required that the ANN model should be composed the independent variables that are the major predictive parameters of the dependent variables. By this way, number of data patterns required for training can be minimized, outcomes ANN models having better generalization capability.

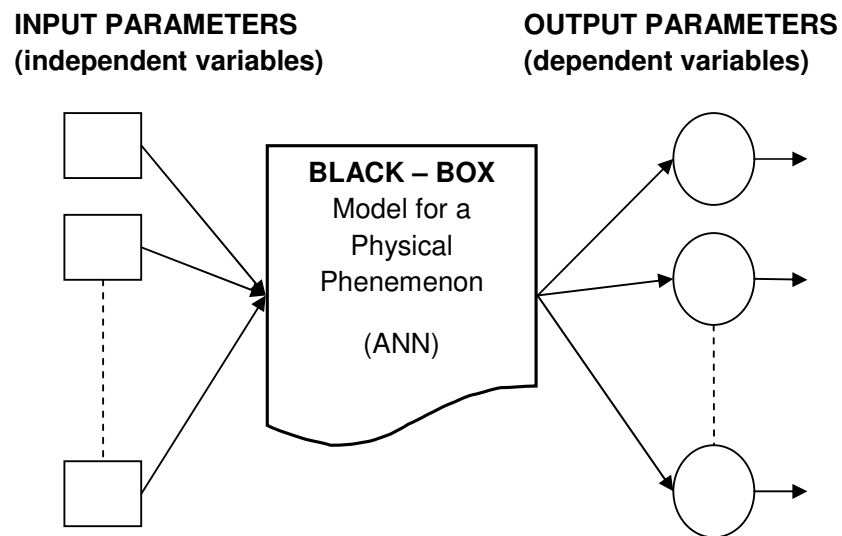


Figure 4.5. Black-box model representation of feed-forward ANN Architecture.

After the selection of the variables involved in ANN is finished, the next step is to teach the network the mathematical association between the input and output parameters by using the introduced patterns of the phenomenon. This stage is called as the learning stage of ANN at which, the connection weights between the neurons are determined. There are various forms of learning algorithms among which back-propagation algorithm is the default and commonly used one throughout most of the studies.

4.3.4 Learning (Training) in Feed-forward ANNs

Learning in feed-forward ANN architectures can be understood in a general sense that all the mathematical parameters of the ANN model are determined based on some introduced statistical data patterns such that ANN is capable of estimating the outputs of newly given input patterns. In general, there are three types of learning techniques in ANNs (Russell and Norvig, 2003):

- **Supervised Learning:** In supervised learning, the exact output value is presented by the data patterns to the ANN during training process.
- **Reinforced Learning:** In reinforced learning, it is only indicated whether the output is true or false during the training process.
- **Unsupervised Learning:** Only the input data patterns are introduced without giving any information about the output values of the data patterns. In this type of learning, ANN makes a classification on the data patterns according to the input values only.

Feed-forward ANN architectures are trained by using supervised learning algorithms. Supervised learning algorithms introduce existing data patterns into the ANN to be trained and the weights of corresponding feed-forward ANN is determined by applying appropriate training algorithm. As a result, the estimation performance of the ANN is optimally satisfied according to some predefined criteria. For that reason, training of a feed forward ANN is to calculate the values

of connection weights provided that the error between the output of the presented data and the output computed by the ANN is minimum. In this respect, feed-forward ANN training is a sort of optimization problem to be solved.

There are various training algorithms in order to find out the optimum values of the weights of the feed-forward ANN. Among these, one of the most popular one is back-propagation algorithm which is explained in the following subsection.

4.3.4.1 Back-propagation Algorithm

Back-propagation algorithm is a supervised learning technique which is based on Gradient Descent Algorithm by which the gradient of the errors with respect to the weights are minimized. In this context, the weights of the ANN are improved according to formula known as “delta rule” (Heaton, 2008):

$$w(t + 1) = w(t) + \Delta w(t) \quad (4.9)$$

in which;

$$\Delta w(t) = -\eta \nabla e(w(t)) \quad (4.10)$$

where, e is error terms of the weights, w , at a specified iteration, t . The gradient operator is denoted by ∇ . The gradient of $e(w)$ gives the direction of the steepest upward slope in search, thus a negative sign indicates the reverse direction, steepest descent. This is an iterative algorithm in which the minimum error is converged. The tuning of the stability and speed of the convergence is obtained by the constant of gradient, η . This is also called as the learning parameter in the scope of back-propagation training algorithm.

In order to compute the error terms, back-propagation algorithm requires that a number input-output data pattern of the phenomenon to be modeled by ANN are presented to ANN. In this context, back-propagation algorithm is comprised of

two main stages. By the introduction of data patterns to the ANN, the inputs taken from the data patterns are processed by the ANN so that output values can be computed. The error, which is the difference between the output values given by ANN and the exact values introduced by the data patterns, is computed. This stage is called as propagation stage. At the next stage, the computed errors are propagated backward through the ANN, which is called as error back-propagation. A brief description of the back-propagation algorithm is given as follows:

- The ANN weights are initialized.
- An input sample from the data pattern is applied to the ANN.
- Forward Phase is processed:
 - Starting from the first hidden layer and propagating toward the output layer;
 - The activation values for the units at each layer are calculated by using Equation (4.6).
 - The corresponding output values are calculated by using Equation (4.7).
 - Error term for each of the output neurons are calculated as the difference between the computed value and the exact value taken from the introduced data sample.
- Backward Phase is processed:
 - The error calculated at the previous step is propagated backward to the input layer through each hidden layer.
 - At each layer, L , the weights of ANN, w_L are updated according to the following equation (Heaton, 2008).

$$w_L(t+1) = w_L(t) + \eta \delta_L x_L \quad (4.11)$$

where; η is the learning rate, δ_L is the error term, and x_L is the output of each neuron in the layer in the matrix form.

- The above steps are repeated until a stopping criterion, such as the mean of the total error is sufficiently small.

4.3.5 Modeling Feed-forward ANNs

Modeling of a feed-forward ANN is not a straight-forward task, because the overall modeling process is not so suitable for automation. Generally, the modeling phase is accomplished by a trial and error procedure. This attribute of ANNs enforces some work load to the ANN modelers. On the other hand, some guidelines that should be followed for the modeling of ANNs were developed throughout the history of ANN usage by researchers. These guidelines plot firm procedures to be engaged and as a result, consistent ANN models with a satisfactory performance can be achieved.

The most influential parameters regarding a feed-forward ANN modeling is the number of hidden layers and the number of nodes in each hidden layer. Modeler is required to determine these parameters while designing the ANN structure. Too few hidden nodes can cause back-propagation algorithm not to converge to a solution. Similarly, too much hidden nodes may cause overfitting problem leading to poor generalization capability and a longer learning period. Therefore an optimum point should be found, suggestively; small sized networks having as few hidden units as possible is key for good generalization capability (Khan et al., 1993). In this context, despite of having no fixed rules for determining these parameters, an ANN having one hidden layer should be taken as the preliminary beginning design because most of the feed-forward ANN structures do not require more than one hidden layer. In addition to this guidance, the number of neurons in the hidden layer can be selected between the average of the number of neurons in the input and output layers and their sum (Berke and Hajela, 1991). Based on this starting design, the ANN is tuned with trial and error so that the optimum number of neurons in the hidden layer can be finalized.

4.3.6 Testing of the ANN Performance

Testing is the phase in ANN modeling in which the performance of the network is examined by the derived weights at each iteration in the learning phase. Therefore, it may be seen that how well the network can perform on data that has not been seen before training phase. The main motive for this process is to avoid the problem called as “overtraining”. Overtraining means that the ANN is too fine-tuned for the training data such that the ANN memorizes rather than learns. In other words, the error terms are highly minimized for the training data presented, however not sufficiently small for the data to be introduced for estimation. As a result, the network performs very well for training data patterns; on the other hand, it shows poor estimation capabilities for newly introduced input data. Therefore, the iteration procedure should be stopped at a particular point although the error due to training data set continues to decrease (see Figure 4.6). This can be accomplished by a testing phase in which, the learning capability of the network is evaluated.

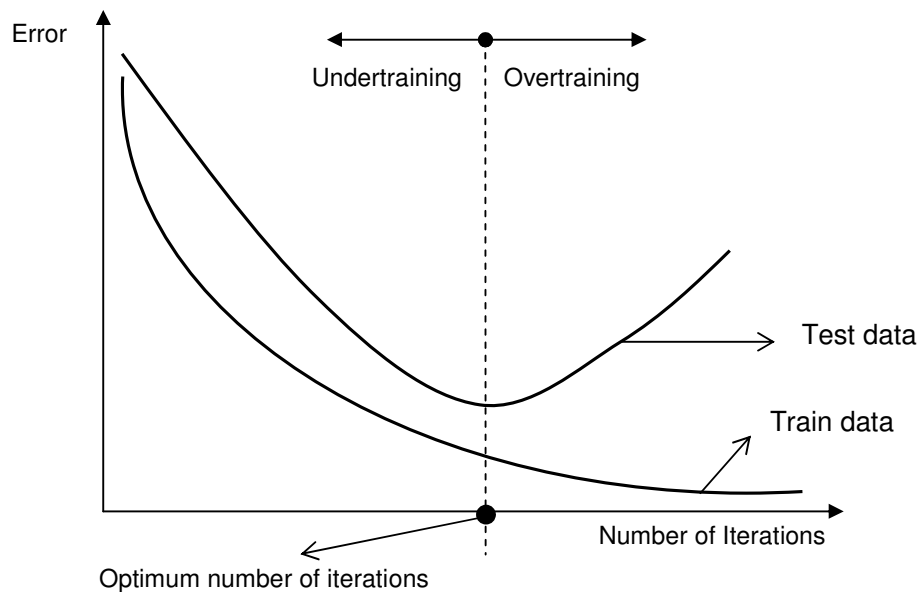


Figure 4.6. Variation of errors throughout the training and testing phases (Adapted from Demuth and Beale (2002)).

Among the available data set, some portion of the set is used for training purposes and remaining part is used for the testing purposes. In literature, it is recommended that the data set should be divided into two such that approximately 70% of the data patterns are regularly selected to be used for training purposes, while the remaining 30% is used for the testing phase. For this purpose, firstly it is a good practice to choose the training set by considering that testing set should represent the overall population (Klimauskas, 1993). The training set is selected among the remaining data patterns. The rationale behind this attitude is such that the performance of ANN is determined majorly by the test set.

4.3.7 Benefits of Using ANNs

ANNs are state of the art statistical tools having numerous capabilities over the conventional techniques. The major of these advantages can be summarized as follows (Heaton, 2008):

- They have the structure of weighted connections in parallel execution so that their learning performance is superior to many other similar AI techniques.
- They have a high capability of generalization from the complicated data patterns so that meaningful estimations can be satisfactorily done even the training data contains errors or has incomplete size.
- Nonlinear models can be approximated in a very reasonable and accurate fashion, which affords a significant power for the usage of ANNs with respect to the other conventional regression techniques.
- There is no requirement for a prior knowledge about the statistical distribution of the parameters involved in the model for the utilization of ANNs. As a result of this point, ANNs are able to model the statistical data without knowing any statistical information about the data, whereas other statistical methods, such as nonlinear regression or Fourier expansions needs to know about the

nonlinear function on which the correlation is fitted, in the beginning (Heaton, 2008).

4.4 Optimization Techniques

Optimization is one of the fundamental research areas in AI, because many practical problems involve optimization within their content. In general, optimization can be defined as the method of finding the best solution of a given objective or objectives while satisfying certain constraints. If a single-objective function is to be minimized or maximized, then the problem is of single objective optimization nature. However, there may be several conflicting objectives so that the problem is to be formulated as a multi-objective optimization, in which the goal is to minimize and/or maximize several objective functions simultaneously.

An optimization problem can be defined mathematically as the maximization or minimization of an objective function, $f(X) = f(X_1, X_2, \dots, X_N)$, subject to some constraints;

$$g_k(X) \leq 0 \tag{4.12}$$

$$h_m(X) = 0 \tag{4.13}$$

where; X 's are the decision variables of the problem, g_k and h_m are the inequality and equality constraints of the problem, respectively. Decision variables, also called as design variables are the independent variables of an optimization problem, whose alternative values form the search space in which the best solution is sought.

In mathematical optimization, there is not a universally best or most efficient method that can be applied to any type of the optimization problem. Therefore, various optimization techniques have been developed, each of which is suitable to a certain class of problems. There are several classifications of the optimization problems according to various criteria related to the formation of the

problem. A typical hierarchical categorization of optimization techniques are presented in Figure 4.7.

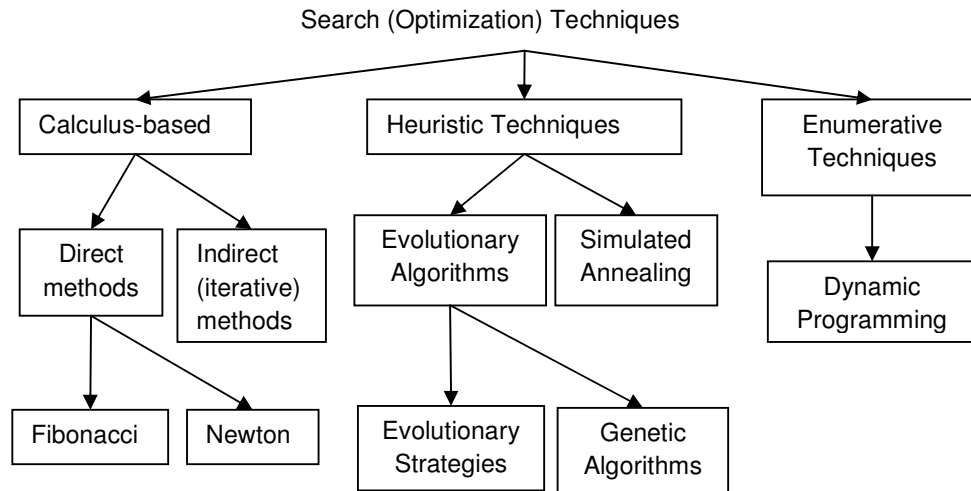


Figure 4.7. General classification of optimization techniques (Adapted from Dianati and Song (2002)).

Computational optimization techniques can be majorly categorized according to the following computational behavior in searching for the best solution (Wikipedia, 2011-b):

- **Optimization algorithms:** These are clearly defined procedures that terminate in a finite number of steps, such as Simplex Algorithm for linear programming or quadratic programming, etc.
- **Iterative methods:** These types of solution techniques converge to a solution in an iterative manner. Major examples of these techniques are Newton's method, Gradient Descent method, Interior Point methods, etc. These techniques mostly rely on calculation of the gradients of objective function.
- **Heuristic methods:** In this type of solution strategy, the solution is approximated rather than exactly achieved. Heuristic techniques are

quantified as guided search methods, in which the search for the optimum point is usually approximated by simulating some kind of physical phenomenon in nature.

In the light of above discussion about the classification of optimization techniques, some guidelines can assist for the selection of the appropriate solution strategy for optimization problems. In this context, linear optimization problems can be efficiently solved using some generic techniques, such as “Linear programming” and its extensions developed for the solution of some particular type of non-linear optimization problems such as “Quadratic programming”. However, most of the engineering problems have high degree of nonlinear characteristics due to the form of the objective function or any of the constraints, which requires other techniques to be utilized. Calculus-based methods usually depends on the calculation of the gradients of the objective function at particular points such that their applicability decreases because of the fact that many objective functions have a complicated form and their derivatives are difficult to calculate, thus their applicability is restricted for practical engineering design problems (Goldberg, 1989). As an alternative to Calculus-based techniques, enumerative based methods seek the solution by investigating almost all the points in the search space. Hence, the required level of efficiency is challenging to attain, even though some significant improvements in seeking search space can be obtained by Dynamic Programming.

Another problem is about the convexity characteristics of objective functions. When the objective function is of convex type, any local minimum also becomes the global minimum, which simplifies the solution of the problem in a great extent. However, the objective functions of most of the engineering design problems do not show this functional behavior (Goldberg, 1989).

All these restrictions impose some level of difficulty in solving design optimization problems. With the recent developments in computing technology, these restrictions are tried to be avoided by using heuristic techniques, such as evolutionary algorithms, simulated annealing, ant colony optimization, etc. The major power of heuristic techniques is that they make very few or no assumptions

about the optimization problem to be solved, therefore they can handle wide range of optimization problems regardless of their mathematical form. Although they do not guarantee an optimal solution, solutions near to optimum are usually caught by this type of methods (Goldberg, 1989). In this study, a commonly used, powerful, heuristic-based optimization technique, Genetic Algorithms are employed.

4.4.1 Characteristics of Genetic Algorithms (GA)

Genetic Algorithms is a kind of heuristic optimization technique which portrays the principals of Darwinian evolution phenomenon in nature to find the global optimum point of a given search space. The emergence of GA in terms of popularity in scientific area goes back to the studies of Holland (1975). His student, Goldberg (1989) established the formal foundations of this optimization technique with an in-depth treatment. Followed by this academic efforts, the technique have been popular among researches in various disciplines as powerful method for extensive sort of optimization problems.

GA run upon a population of alternative solutions of the problem by applying the principal of survival of the fittest iteratively, directing toward better solutions at each generation with respect to the previous one. Therefore, each generation of the algorithm yields new population by selecting some of the solution alternatives in the current population according to their fitness levels and applying some operations on them inspired by the fundamental progressions of natural evolution. As a result, the population evolves into a form having better solution alternatives by each generation. This heuristic search is called under a generic umbrella term as evolutionary algorithms.

Conventional search methods usually seek the best solution along a path within the search space from one point to another alike to series operations. However, the major characteristic of evolutionary algorithms is their exertion on a population of alternatives rather than a single solution alternative. Therefore, as an analogy, GA works on areas within the search space. This gives GA a great power in

finding global optimum point, because search is carried out in a parallel manner within the search space, which gives the algorithm a remarkable opportunity to avoid from local optima.

The procedural steps in GA can be described by a generic flowchart that can be seen in Figure 4.8. There are three main operations that constitute the progression in one single generation; selection, crossover, and mutation. In addition to these operations, the codifications of the decision variables of the optimization problem for the operations to be applied are other important tasks in the employment of GA. Brief descriptions of these principle portions of GA are given in the following sections.

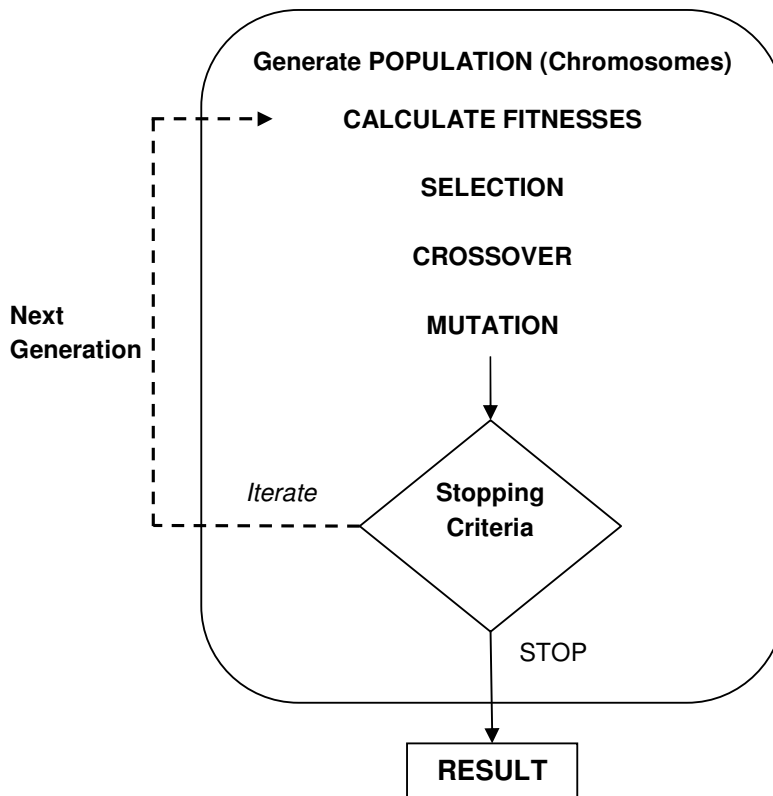


Figure 4.8. General flowchart of GA (Adapted from Weise (2009)).

4.4.1.1 Discretization and Encoding the Decision Variables

Decision variables of the optimization problem needs to be coded in a certain form in order to apply the genetic operations on them. A typical GA entails the decision variables to be coded in a binary form. After the coding is accomplished, the binary coded representation of each decision variable is concatenated to form the chromosome structure. Therefore, a chromosome structure is a representation of a solution alternative in the search space (see Figure 4.9).

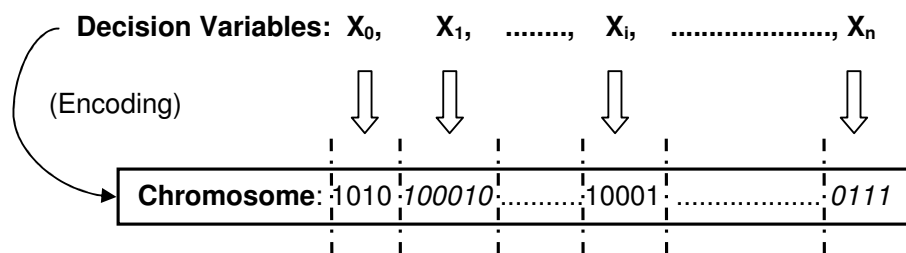


Figure 4.9. Representation of a decision variable in GA (Haupt, 2004).

The representation of decision variables in GA is associated to the discretization of these variables. In real life design problems, the decision variables are continuous, however they are represented in computing space by a process, discretization. Discretization of a variable means that the range of a variable is divided into a certain number of sub-intervals so that the possible values that can be assigned to the variable is determined. Since continuous search space means that infinite number of solution alternatives exists; discretization process transforms this infinite number of alternatives into finite number of alternatives such that it is practical to search among these.

If ϵ is the desired level of precision to be applied on the range of the decision variable, then the minimum number of bits required to represent this discretization for binary coding, n can be calculated from (Haupt, 2004):

$$2^n \geq \frac{\Delta S}{\varepsilon} \quad (4.14)$$

where, ΔS is the interval length of the decision variable to be discretized. Therefore, the level of discretization depends on the required accuracy to be achieved. Since the number of bits for a decision variable is obtained by the discretization as seen from Equation (4.14), the discretization process directly affects the number of bits of a chromosome. It is obvious that increasing the number of bits in a chromosome increases the resolution of the search space so that more detailed search can be performed. However, this adversely affect the search time as expected. Hence, all these discussions emphasize the importance of discretization process such that a reasonable discretization should be executed in a GA implementation.

4.4.1.2 Generating the Initial Population

Having accomplished the discretization and coding of the decision variables, the next step is to generate the initial population. Choice of the population size directly affects the performance of GA implementation, because as the size of population increases, the workload on the computer also increases due to the rise in the count of calculations of fitness function. It should be noted that the computation time required for the computation of the fitness value of each chromosome is an important indication of performance of a GA implementation, because GA relies upon fitness calculations. Therefore, another important parameter of a GA study is to choose a population size. There is not a fixed rule for the selection of population size in GA such that it is highly dependent on the characteristics of the optimization problem. However, as a general tendency, population sizes in the range of 50 to 200 are frequently used in GA implementations in the literature (Deb, 2001).

4.4.1.3 Selection Operation

Selection is one of the major operations of GA in which the parents that will yield offspring are chosen. In this context, selection phase comprises of two steps as the selection of the parents on which crossover is applied and the decision about the number of children each selected pair will produce. The selection process is done by imitating the survival of the fittest principal of natural evolution so that the chromosomes having the higher fitness value have the higher likelihood to survive to the next generation.

Selection operation requires the computation of fitness value of each chromosome, in order to assess the quality of a chromosome in the population. For this purpose, selection of a fitness function is essential. The only restriction for a fitness function is that fitness values cannot be negative. Moreover, a fitness function should reflect the objective values in a manner. In this context, the calculation of fitness values of each chromosome can be prepared according to either proportional fitness or rank-based fitness assignment. If proportional fitness assignments are chosen, then the fitness values of each chromosome are normalized to unity. On the other hand, in a rank-based scheme, the chromosomes are sorted according to their fitness values directly. Therefore, in a rank-based fitness assignment, the fitness values of the chromosomes are not in emphasis, instead the order of the chromosome in the population is important. As it is expected the situation is opposite for the proportional fitness based assignment. After the calculation of fitness values, a selection scheme is employed to elect the individuals to be used as parents of the offspring to survive to the next generation. There are various selection techniques in literature, of which the commonly used ones can be listed as follows (Weise, 2009):

- Roulette-wheel selection,
- Truncation selection,
- Tournament selection, and so on.

Among these, roulette-wheel selection is a widely used selection scheme due to its ease of implementation. This is a stochastic-based selection scheme such that

the probability of selection of a chromosome is calculated according to its fitness value. The selection is done by generating a random number such that if the random number falls into the selection probability span of the chromosome, the chromosome is selected. Therefore, in this scheme, each chromosome has a selection probability proportional to its fitness value. The selection operation is repeated until the desired number of chromosomes is selected for reproduction. Once the parent chromosomes are selected, the next step is applying crossover operation on them.

4.4.1.4 Crossover Operation

The creations of offspring are performed by a crossover operation applied on the selected parents. There are several crossover operators in the literature, among which single-point and two-point crossovers are popular. In a single-point crossover, a crossover location is randomly chosen on the chromosome. All the bits on the right side of the chosen location are exchanged. In a similar fashion, two-point crossovers are performed by choosing two random locations on the chromosome such that the portion of the chromosomes between these two locations is exchanged. The schematic view of these crossover techniques can be seen in Figure 4.10.

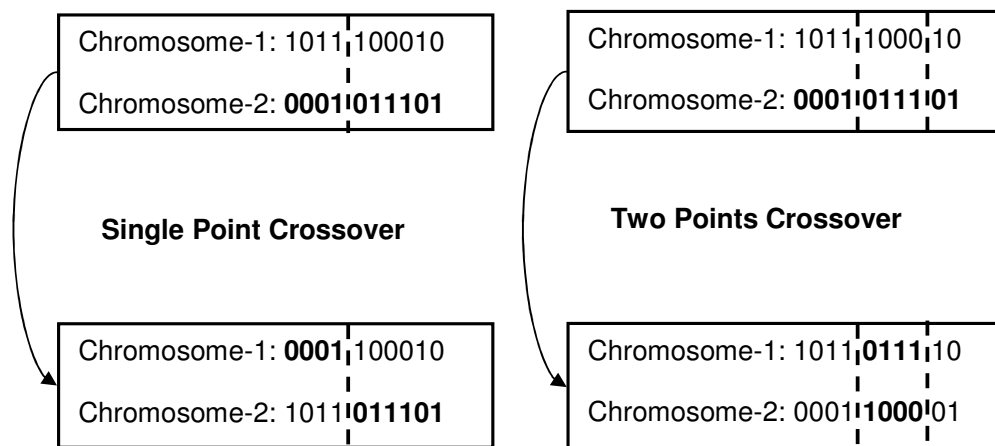


Figure 4.10. Schematic views of typical crossover operators (Haupt, 2004).

Crossover operations are the fundamental blocks of GA, which directs the search along a path conducted by evolution process. Therefore, the selection and crossover operations are the main heuristics of GA so that random searches on the search space can be avoided.

The amount of crossover operations are regulated by a parameter called as “crossover rate”. Crossover rate indicates how often the crossover operations will be performed at each generation. Therefore, if crossover rate is 100%, then all offspring is made by crossover. On the other hand, a crossover rate of 0% designates whole new generation is comprised of the exact copies of chromosomes from old population. As a general convention, some parts of the population are left to survive to the next generation by using a crossover rate of 70% to 90% approximately (Genetic Algorithms, 2011).

4.4.1.5 Mutation Operation

After the completion of crossover operations, the next stage of a GA is to apply mutation operation on the chromosomes in the pool. Mutation operator operates with one chromosome only and it just causes a random change of a bit in the chromosome. This is done in order to introduce a certain level of random search in GA. Therefore, although the population evolves along a certain path by the crossover operations, some points distant to the evolution path can also be evaluated in the search space so that a better path of evolution can be caught. A typical mutation operator changes a bit from 1 to 0 or 0 to 1 according to a given probability called as “mutation rate” (see Figure 4.11).

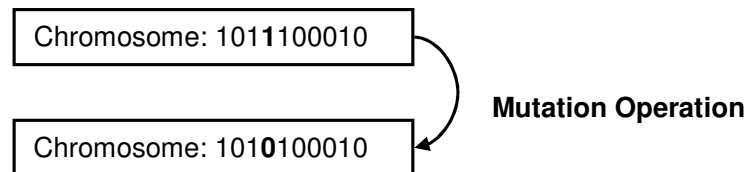


Figure 4.11. Schematic description of a typical mutation operator (Haupt, 2004).

Mutation rate indicates how often the parts of chromosomes are mutated. If there is no mutation, offspring is taken after crossover without any change. If mutation is performed, part of chromosome is changed. A mutation probability of 100% changes the entire chromosome, while a mutation rate of 0% does not perform any change on the chromosome. Conventionally, a small value, such as in the range of 1 to 10% is selected as the mutation rate to prevent the behavior of GA from resembling to a random search (Genetic Algorithms, 2011).

4.4.1.6 Regeneration

The final phase of a generation in GA is to form the new population as a result of the application of aforementioned operations. Principally, the newly created offspring replaces old population which is comprised of their parents. However, the best chromosome of the population may be lost due to the probabilistic nature of selection operations. This situation can be avoided by applying “elitism” on the population such that the best individual of the population is replicated to the next generation so that the best chromosome obtained throughout GA process cannot be lost. As a result, at each generation, the best chromosome is either the same or better than the best chromosome of the previous generation. It should be noted that elitism can increase the performance of GA very rapidly, because it holds the best found solution in the population.

4.4.1.7 Stopping Criteria

The evolution process through the generations is stopped according to some stopping criteria. A usual stopping criterion is a predefined maximum number of generations. However, some kind of intelligent behavior can also be introduced to the algorithm by dynamically checking the statistical properties of the population at each generation to decide whether to continue or halt the evolution process.

CHAPTER 5

DEVELOPMENT OF THE DESIGN FRAMEWORK

5.1 General

Advances in computing technology allow several time-consuming tasks to be handled efficiently. In this context, artificial intelligence techniques have been used popularly in various academic studies in order to take advantage of this computing power. Although the artificial intelligence topics have very wide extensions in the literature, the most widely used artificial intelligence-based civil engineering applications consider artificial neural networks and heuristic-based optimization techniques. Each of these topics has been implemented in several civil engineering studies successfully; however, the usages of these topics within a single framework are not common. The present study basically gathers these two separate artificial intelligence topics in a single framework and proposes a preliminary design method for determining the optimum dimensions of bridges crossing rivers. In this context, this study concerns two fundamental techniques of artificial intelligence studies, which can be listed as follows:

- Artificial Neural Networks (ANN),
- Heuristic optimization algorithms.

In a very brief description, ANNs are used in order to make estimations about the outcomes of a physical process which have complex mechanism, by using the past experiences as a learning tool, whereas heuristic optimization techniques are

used to find the best point of an optimization problem when all or most of the alternatives in the problem are not conveniently assessed individually.

5.2 Brief Description of Bridge Design Stages

Prior to the explanation of the details of this study, it is beneficial to review the principals of bridge design process in order to perceive the objectives and the justifications of the study in addition to its method of handling different engineering design problems within its scope. Thus, an overall view of a bridge design process is described.

A bridge design is composed of a number of progressive tasks, each of which is differentiated by the level of design or degree of detail required at any particular time (FIB, 2000). Despite the difficulties in separating these stages explicitly due to design, constructional and contraction requirements which may be interdependent, a bridge design can be mainly defined in terms of following stages (FIB, 2000):

- **Conceptual Design Stage** : In this stage, as the name implies, the conceptual considerations regarding the basic form of the bridge are determined as follows (FIB, 2000):
 - The intended function of the structure,
 - The position of the supports,
 - The distribution of the spans.
 - The choice of construction materials,
 - The type of foundations.

This stage does not involve serious analysis, rather the decisions mentioned above are given based on simple analysis and engineering judgment. Actually, the purpose of this stage is to ensure that the requirements and objective of the project can be satisfied by the selected

conceptual design among different alternatives. Detailed dimensions about the structural components are usually not specified in this stage.

- **Preliminary Design Stage:** The dimensions of the structural components are determined and based on these dimensions the corresponding reinforcement steel amounts are calculated. These computations are supported by more detailed structural analysis and designs. Therefore, at this stage, the skeleton of the design is emerged and the rest is to build the final design based on this skeleton. For this reason, the results obtained at this stage are highly important because the remaining design tasks are usually processed with respect to this stage.
- **Detailed Design Stage:** The design is finished in this stage by performing in-depth structural analysis and corresponding comprehensive design calculations. The drawings are prepared to show all the details of the structural components, such as the dimensions, the reinforcement amounts the locations of reinforcement steel, etc.
- **Execution Design Stage:** As the final stage of design process, any remaining items related to design are completed and any additional documents related to fabrication or construction are prepared (FIB, 2000). At this stage, the documentation related to subsequent inspection and maintenance works are also organized. The construction is done precisely, matching the drawings and documentations available at this stage.

These stages in a bridge design are important to understand the relative importance of the stages with respect to each other and the corresponding cooperative tasks that are involved. As it is expressed, a preliminary design is the point where all the design is built upon so that correct guidance of a preliminary design outcome a well-established bridge project. This argument is important because, this study also focuses on the preliminary design stage. In the following sections, the descriptions of the developed methodology by this study are given from the perspective of optimum preliminary design of river bridges.

5.3 Description of the Design Framework

The optimization of bridges crossing rivers involves different aspects of civil engineering which are interdependent. Therefore, in order to explain the detailed procedure of the design framework, it may be helpful to review the conventional design of a bridge crossing a river. In this context, a bridge design can be clarified concisely according to the involved sub-disciplines of civil engineering as follows:

- **Structural design:** After the topographical conditions of the valley to be passed by the bridge are obtained, the following procedure is pursued:
 - The structural model of the bridge is chosen according to the site conditions and structural requirements. There are several types of bridges, such as reinforced concrete bridges, pre-stressed concrete girder bridges, suspension bridges, truss bridges, and mixed type systems.
 - Based on the selected structural model (bridge type), the span arrangement of the bridge is proposed and preliminary dimensions for the proposed bridge system are estimated using engineering experience and intuition.
 - The preliminary dimensions of the structural components, such as abutments, piers and superstructure, along with the corresponding material properties are put into structural analysis and the final dimensions of the bridge are determined iteratively, according to the conventional design methodologies described in design specifications. A proper design imposes the necessary dimensions of these structural components to be determined concerning safety, economy, and serviceability. This stage is based on classical structural analysis and design calculations according to the structural system that is chosen. The corresponding design checks are also done in this stage.

- **Geotechnical design:** The foundation design of piers and abutments are performed by geotechnical engineers based on the required parameters of foundation soil obtained by the field studies and measurements. The choice of the necessary foundation system and its detailing is also done in this stage.
- **Hydraulic design phase:** If the bridge to be designed crosses a river, the relevant bridge hydraulics calculations are carried out and the bridge is checked according to the hydraulic conformity.

All the aforementioned design phases are mutually dependent so that the design requirement from one aspect may impose some restrictions on the other design phase. For this reason, each design phase should be arranged to work in collaboration with the other phases such that the overall design is safe and serviceable structurally, geotechnically, and hydraulically. In addition to the safety requirements, as in any engineering design, the economy is also the other important concern that should be considered so that the final design can compromise the safety and economy.

This study encompasses each of the design phases mentioned above. Among these design tasks, while the hydraulic design checks are done conventionally, the structural and geotechnical parts of the design are performed by artificial neural networks which are statistically-based artificial intelligence techniques. The details of the entire design framework and the way of handling these design problems are presented in the following subsections.

5.3.1 Structural and Geotechnical Design of Bridges

Conventional civil engineering design of a structure is aimed to determine the required dimensions of the structure such that the structure is safe for the specified design loads acting on the structure. The resistance properties of the materials, such as the modulus of elasticity, yield strength, etc., are also introduced into this progress, and based on the principles of the strength of

materials, the design is accomplished by finding the required dimensions that will make the structure safe. In this context, a safe structure is usually defined by two main criteria as follows:

- The corresponding structure material does not yield under the design loads.
- The deformation of the structure is limited according to the serviceability requirements.

In today's engineering, based on the definitions above, the most common design strategies are based on the Load and Resistance Factor Design (LRFD) (AASHTO, 1998). LRFD introduces some level of reliability considerations into the design by load and resistance coefficients. By the use of these coefficients, the design loads are increased, while the resistance parameters, such as yield strength of the material are decreased. The rest of the calculations are performed in a classical way such that the required dimension of the structure is calculated.

In a structural design, the loads and the material parameters of the structure are usually fixed in the first stage of the design. Therefore, the dimensions of the structure are the only resistance parameters that an engineer can change to achieve the required level of safety and serviceability. As a result of this fact, by designing a structure, an engineer simply calculates the required dimensions of the structure to achieve the required safety level. Of course, for some kind of composite materials, such as reinforced concrete, besides the dimensions of the structure, the amount of steel is also another variable to be computed for accomplishing the design process. Some structural analysis and design tools, such as SAP2000 (CSI, 2005) finite element analysis software facilitate these design tasks.

The above explanation about the conventional design methodology is prompted to clarify the proposed methodology of this study. Contrary to the conventional design approach, this study uses a statistical-based method for the estimation of the design dimensions of a bridge. For this purpose, artificial neural networks are chosen as the structural design tool for the following justifications:

- ANNs are used to correlate design load and resistance parameters to the required design dimensions of the structural and geotechnical components in a bridge, which are estimated rather than computing them by conventional analysis.
- This way of determining design dimensions outcomes many advantages, such as elimination of time-consuming analytical or numerical computations, and some inclusion of inherent design requirements that cannot be put in a formalized rational form.

5.3.2 Hydraulic – Structure Interaction in Bridge Engineering

Bridge hydraulics design imposes two main hydraulic criteria to be met in the design of a bridge as follows:

- The minimum net opening of the bridge is required in order to convey the stream flow hydraulically conformably; such as upstream choking is avoided through the bridge transition.
- The total scour around the bridge piers and abutments should be estimated in order to determine the required pier and abutment foundation depths so that corresponding precautions for inhibiting collapse of the foundations due to the scour should be taken.

There exists an interaction between the structural design and hydraulic design requirements in bridge engineering. Although the details of this interaction can be found in Yanmaz and Kürkçüoğlu (2000) and Yanmaz (2002-a), the concise explanation of this interaction can be stated as follows:

- As a rule of thumb in bridge engineering, substructure, abutments, piers and foundations are cheaper than superstructure for the case of longer

spans (FIB, 2000). Thus, if the number of spans in a bridge increases up to a certain level, more economical bridge design can be obtained in the overall (FIB, 2000).

- If it is more thoroughly examined; the increment of the number of spans directly decreases the span lengths causing a more economical superstructure design. Besides, when the span length is decreased, the number of piers may increase, which results an additional cost of pier. However, as an overall, economic gain by shortening the superstructure lengths can be higher than the economic gain by the reduction of the number of piers in case the superstructure lengths are increased. Therefore, an optimum point exists where the specified number of spans yields optimum design regarding the total cost of the bridge. This is the inherent optimization problem of bridge engineering in the context of girder bridge types (FIB, 2000).
- In addition to the structural point of view; hydraulic criteria imposes additional constraints on the optimization of the distributions of bridge spans. If the number of spans is increased, the hydraulic conformity of the bridge transition is disturbed. In other words, more piers decrease the net flow area through the opening, and hence leads to more flow disturbances. This disturbance has mainly two basic effects as choking and possible hydraulic jump occurrence and scouring problem. The protection for these problems causes additional costs, such as increment of the foundation depths, using pile foundations, and application of conservative scour countermeasures.
- As a result, an optimum point in the design should be caught up so that the optimum bridge span arrangement can be found among several different alternatives by considering both structural and hydraulic criteria.

5.3.3 Definition of the Optimization Problem

In the light of the structural, geotechnical design aspects and the hydraulic-structure interaction phenomenon, this study is grounded on an optimization problem which can be defined formally as follows:

- Minimize the objective function; the total cost of the bridge,
- Subject to the design constraints among which hydraulic design checks taken in a probabilistic way.

The objective of this study is to find the optimum bridge span arrangements which will be safe and functional from viewpoints of structure, geotechnics, and hydraulics. The study aims to propose a preliminary bridge design, which is optimized for the hydraulic effects. For this reason, although the structural and geotechnical design dimensions are also proposed by a statistical-based method, the emphasis is on the bridge hydraulics concepts that will identify the hydraulic - structure interaction for given input data. A definition sketch for typical cross-section of a bridge crossing a river can be seen in Figure 5.1.

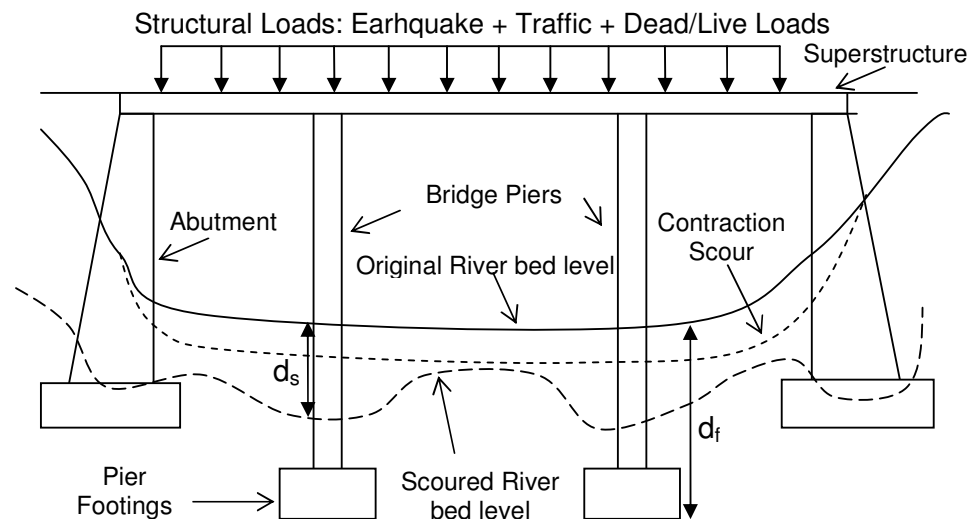


Figure 5.1. Typical cross-section for a river bridge.

Based on this methodology, a design framework, named as AIROB was developed. This framework is used to propose preliminary design outputs for pre-stressed concrete bridges crossing rivers provided that the relevant input data are given. In summary, the framework can provide the following design outputs:

- The optimum bridge span arrangement,
- The corresponding basic dimensions of bridge structural components, such as pier width, abutment width, pier and abutment foundation width, superstructure girder depth, and amount of steel reinforcement.
- The costs of each bridge structural components and the approximate total cost of the bridge.

Before going through the implementation details of AIROB, some guidelines regarding the structural design aspects are instructive for the efficient and precise utilization of the methods involved in the study. Therefore, some rule of thumbs based on engineering experience and design criteria are given in the following section.

5.4 Guidelines for the Structural Design of Bridges

This study follows a statistical-based approach for structural design of the bridge components. Therefore, some general structural design principals are incorporated to the methodology for capturing the lack of design information that may exist in a statistical-based approach. These design principals are based on engineering experiences and some design specifications, such as ASSHTO (1998).

A bridge structural type is an important decision. Different structural types impose various criteria on the design tasks. In this study, only pre-stressed concrete

girder types of bridges are concerned, of which the details regarding AIROB are presented in the following sections. At this point, some structural guidelines for pre-stressed concrete girder bridges are presented.

A pre-stressed concrete girder bridge is composed of a set of pre-stressed girders and reinforced concrete type abutments and piers. Although the structural model that how the girders and piers are connected may be different according to various purposes, vast majority of a typical pre-stressed concrete girder bridge has the following structural properties shown in Figure 5.2:

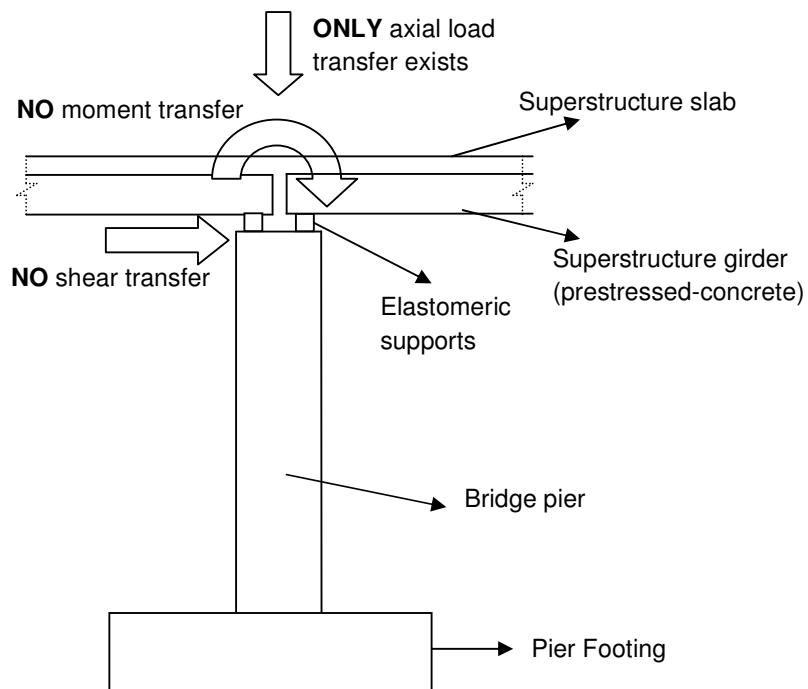


Figure 5.2. Descriptive sketch for the connection nodes.

- The internal force transfer among the pier and the girders or abutment and the girders are very small. In other words, practically, there is no shear and moment transfer between a pier and its adjacent connected girders or between the abutment and its neighboring girder (see Figure 5.2). Thus, the girders can be assumed as simple-supported beams, while the

abutments and piers can be assumed as cantilever type structural walls or columns.

- Therefore, it is practically reasonable to analyze and design each of these structural components independently. In other words, the designs are carried out for each pier, abutment and superstructure separately rather than performing a wholly connected monolithic bridge design analysis.

Another important point in bridge structural design is the proportioning of the dimensions of piers. A bridge pier of reinforced concrete type, the most important dimension proportioning is the ratio of the height of the pier, H_p to the bridge width, b_s called as “column aspect ratio”. Column aspect ratio has an important effect on the ductility of columns suspect to the dynamic loading especially. For this reason, some design criteria are developed for the design of bridge piers where earthquake effects are considerably important. Figure 5.3 shows the influence of column aspect ratio on the ductility of columns designed to the Caltrans confinement requirements (ATC-32-1, 1999).

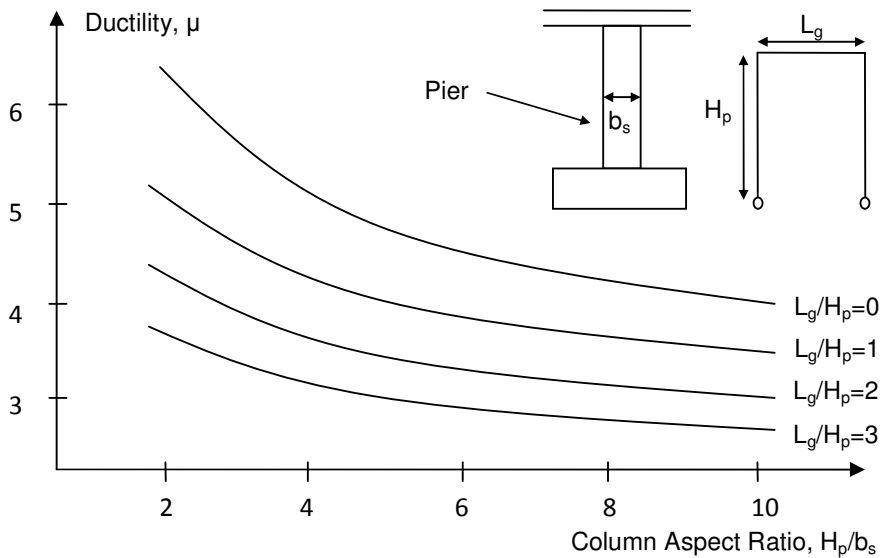


Figure 5.3. Influence of column aspect ratio on the ductility of columns designed to the Caltrans confinement requirements (Adapted from ATC-32-1 (1999)).

As seen in Figure 5.3; for a given amount of confining reinforcement, the structure ductility capacity reduces as the aspect ratio of the pier increases (ATC-21-1, 1999). Thus, required level of ductility should be achieved by designing the pier according to the corresponding column aspect ratio given in Figure 5.3.

As a consequence; the minimum required value of H_p/b_s is suggested to be 10. However, a more robust design requires H_p/b_s values in the range of 6 to 8. An important point that should be noted is that if these criteria impose b_s value to be higher than 3.5 or 4.0 meters, then special structural sections for piers are used due to economical justifications, such as using hollow sections. Therefore, this limiting design case for a typical pre-stressed concrete girder should be considered in the design process.

5.5 Design of Bridge Structural Components by Feed-forward Artificial Neural Networks

A bridge can be categorized according to different criteria. There are various types of bridge structural models. In this study, only the bridges that have pre-stressed concrete superstructure are considered. The reason for the selection of this type of structural model is their widely usage in many countries to pass small to medium span lengths, such as 10 ~ 40 meters interval approximately. In Turkey, most of the existing bridge designs are in this category such that collection of different bridge design projects of this type is practical to build a bridge database.

Since an ANN model is based on statistics, a database of bridge designs are required to be used in learning phase of the artificial neural network. Therefore, construction of a bridge database is one of the central tasks in this study. For this purpose, several existing bridge design projects were collected from different sources, as project firms and Turkish General Directorate of Highways. Among these design projects, elimination was performed to accomplish a database which consists of consistently qualified bridge designs. Table 5.1 presents the brief description about this bridge database in which $H_{30}-S_{24}$ denotes the truck loading

type, whereas C_{40} and C_{45} are the concrete types having compressive strength of 40 MPa and 45 MPa respectively.

Table 5.1. Characteristic information about the bridge design database.

Total number of bridge projects processed by the database	118
The earthquake regions of the bridges in the database	High earthquake regions
The traffic loading type on the bridges in the database	H_{30} - S_{24}
Concrete and Reinforced Concrete material Types	C_{25}
Pre-stressed concrete material types	C_{40} and C_{45}
Pre-stressed concrete girder shapes	I shape
The abutment shapes in the bridge projects	Vertical wall
The pier shapes in the bridge projects	Rectangular piers (rounded corners)
Maximum bridge total length in the database	266.80 m
Minimum bridge total length in the database	13.00 m
Maximum bridge width in the database	56.00 m
Minimum bridge width in the database	9.00 m
Maximum number of spans in the database	8

In the second stage of the study, the bridge projects in the database were examined and the relevant parameters that would represent the required input – output variables of the artificial neural network models were extracted. For this reason, the pre-stressed concrete bridge design was analyzed in collaboration with experienced structural bridge engineers.

Based on the conclusions mentioned above, all the bridge designs in the database were divided into three sub-databases, such as pier, abutment, and superstructure databases (see Table 5.2). This way of design approach makes possible a complete bridge design as follows:

- When a bridge is to be designed, each component of the bridge is designed according to its corresponding database. For example, if a pier of the bridge is to be designed, then the ANN model trained by the pier database is used to estimate the design dimensions of the pier and the same approach is followed for both the abutments and superstructures.
- The overall bridge design is accomplished by designing each component by its corresponding ANN model and thus, the total cost of the bridge is obtained by the summation of the costs of each individual component that composes the bridge.

Table 5.2. Characteristic information of the databases for bridge components.

Abutment Database	
Total number of records in the database:	57
Maximum abutment height in the database:	9.95 m
Minimum abutment height in the database:	2.07 m
Pier Database	
Total number of records in the database:	46
Maximum pier height in the database:	2.10 m
Minimum pier height in the database:	36.78 m
Superstructure Girder Database	
Total number of records in the database:	78
Maximum superstructure girder span length:	40.00 m
Minimum superstructure girder span length:	12.50 m

Since the bridge design is divided into design of individual structural components, the study has separate corresponding ANN models for each of these databases. Consequently, each of the databases establishes the underlying training data for each of the corresponding ANN models.

5.5.1 Modeling of the Artificial Neural Network Architectures

The main idea behind the ANN model used in this study is to estimate the design dimensions of the bridge. For this purpose, all the piers, abutments, and superstructures in each of the bridge projects in the database are examined and three databases; abutment database, pier database, and superstructure database are constructed by the extraction of relevant information as seen in Table 5.2. Then, the next step was to choose the input and output parameters to be correlated for each of these databases among the extracted information. For this purpose, the designed dimensions are selected to be the main output variables, while the parameters that represent the loadings and material properties are selected as the input variables. The aim is to build a black-box model to represent the relation between the selected input and output variables. The parameters selected for these black-box function models that are constructed to estimate the design dimensions of the structural components can be examined in Figures 5.4, 5.5, and 5.6.

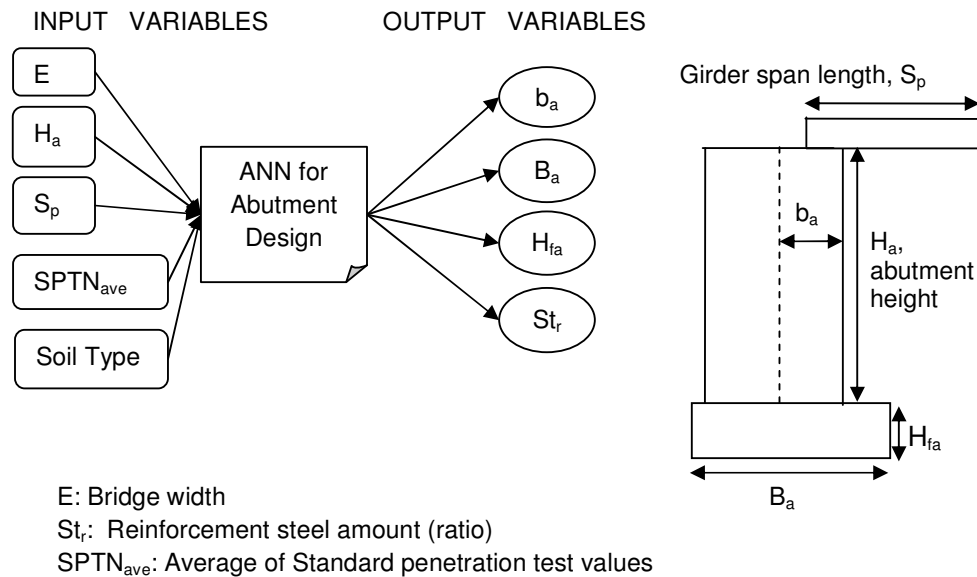


Figure 5.4. Schematic representation of selected parameters in ANN model for the design of abutments.

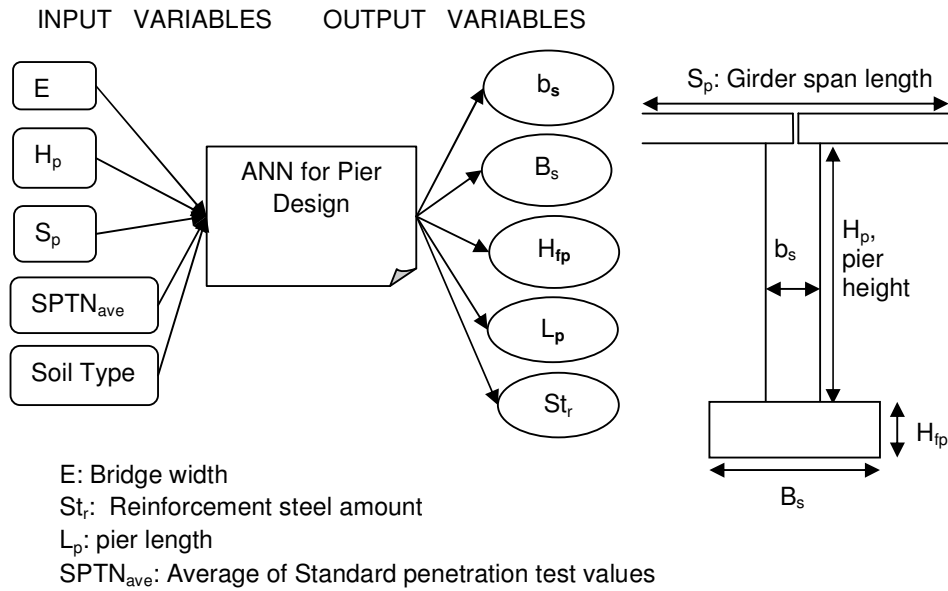


Figure 5.5. Schematic representation of selected parameters in ANN model for the design of piers.

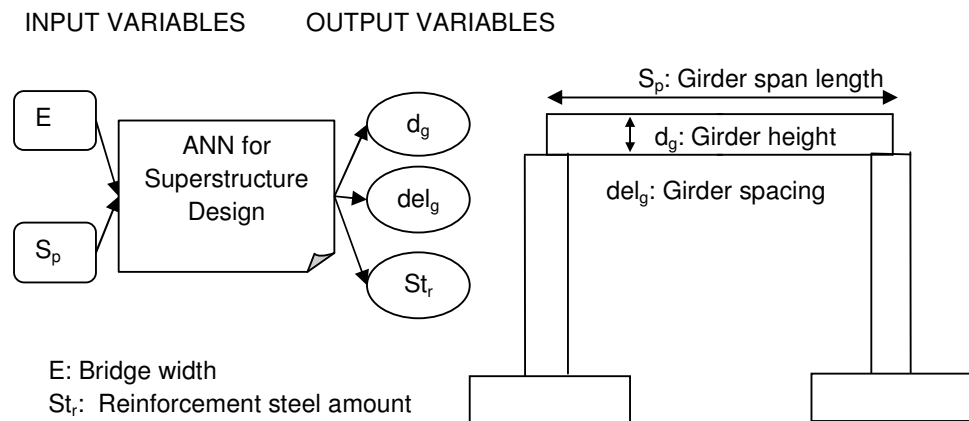


Figure 5.6. Schematic representation of selected parameters in ANN model for the design of superstructure.

In the selection of input and output parameters for the design of components of the bridge, some input variables are ignored due to the lack of sufficient data regarding the related parameter in the database. In this context, the earthquake regions, the traffic loading type, reinforced concrete and steel material types, pre-stressed concrete material types, pre-stressed concrete girder shapes are eliminated in the contents of ANN models, because there is not any variability for each of these parameters in the database of bridge projects as presented in Table 5.1. Therefore, the developed ANN models for design of bridge components should be used within the range of these calibration data presented in Table 5.1.

Similar to the estimation of design dimensions, the cost estimation for each of the components is handled by additional ANN models. These ANN models are only used to guess the cost of the structural component given the required dimensions. In this respect, after determining the design dimensions of a component by the corresponding ANN model, the next step is to estimate its cost by inserting the compute design dimensions as the inputs for the ANN cost model. For this purpose, for all the records in each of the database, the cost of the structure is calculated based on the relevant data in the projects. The detailed tabular representation of cost calculations for an abutment, a pier and a superstructure is given in Appendix B as an example. Based on the calculated costs, for each structural component; separate ANN models are designed in order to perform cost calculations. The parameters selected for these ANN models involved in cost calculations can be examined in Figures 5.7, 5.8 and 5.9.

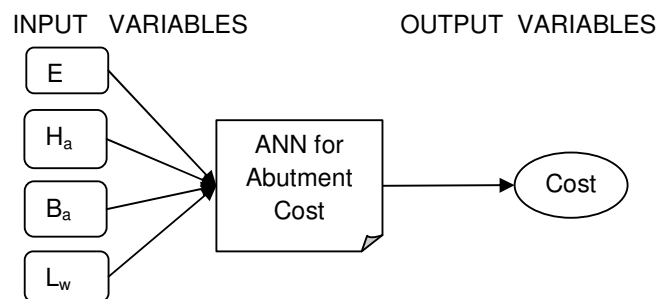


Figure 5.7. Schematic representation of selected parameters in ANN model for the cost of abutments.

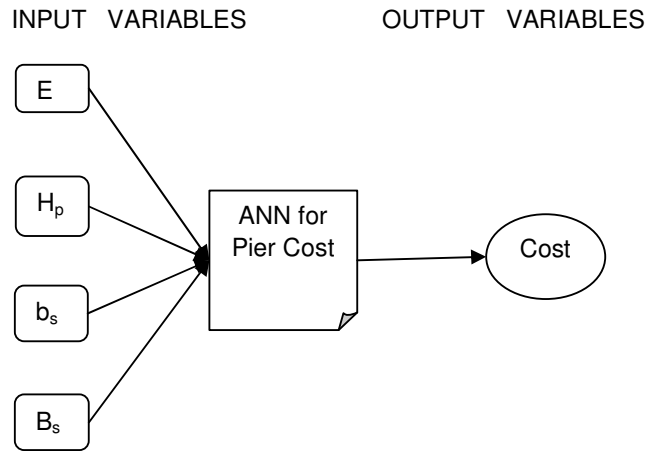


Figure 5.8. Schematic representation of selected parameters in ANN model for the cost of piers.

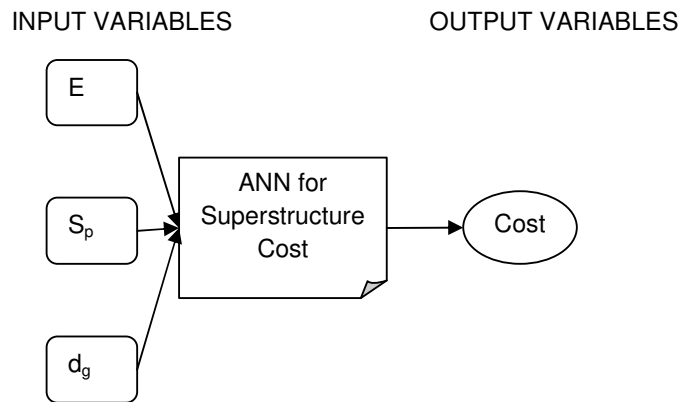


Figure 5.9. Schematic representation of selected parameters in ANN model for the cost of superstructure.

As a result, totally six separate feed-forward ANN models are constructed to be trained by the corresponding database. Among these ANN models, three of them are modeled for estimation of design dimensions for abutment, pier, and superstructure separately, remaining three of them are used to estimate cost of each corresponding component. For this purpose, The Neural Network Toolbox in the MATLAB software package was used (Demuth and Beale, 2002). For each of the ANN model, the back-propagation learning algorithm is selected. Each of the databases is also divided into two parts such that approximately 70% of the database is to be used in the training phase, while remaining 30% of the database is to be used in validation phase of artificial neural networks. As a result, these data patterns were put into The Neural Network Toolbox in MATLAB and six ANN models corresponding to each of the black-box models is constructed. The design of an ANN model is usually done by trial and error procedure until obtaining the desired functional mapping between the input and output variables. For this reason, the following principles were used in the final design of the ANN models:

- The LogSigmoid function was selected as the activation function,
- One hidden layer is considered to avoid over-fitting phenomenon in the modeling of ANN architectures,
- The number of nodes in the hidden layer are determined by trial and error (see Figures 5.10 through 5.15),
- The optimum numbers of epochs for each of the ANN models are determined by the validation phase of the training data to avoid over-fitting.

Based on the above principles, the various alternatives for each ANN model are evaluated and among these alternatives, the optimum ones are decided to be used in the further parts of the study. The summarized information about the finalized ANN models is presented in Table 5.3.

Table 5.3. Characteristic information for the final ANN models.

Finalized ANN Model	Number of Hidden Nodes	Epochs	MSE (Mean Squared Error)
Abutment Design	7	130	1.85E-03
Abutment Cost Estimation	7	47	2.02E-05
Pier Design	12	1500	2.96E-05
Pier Cost Estimation	5	140	1.01E-05
Superstructure Design	7	500	6.08E-03
Superstructure Cost Estimation	7	53	2.46E-05

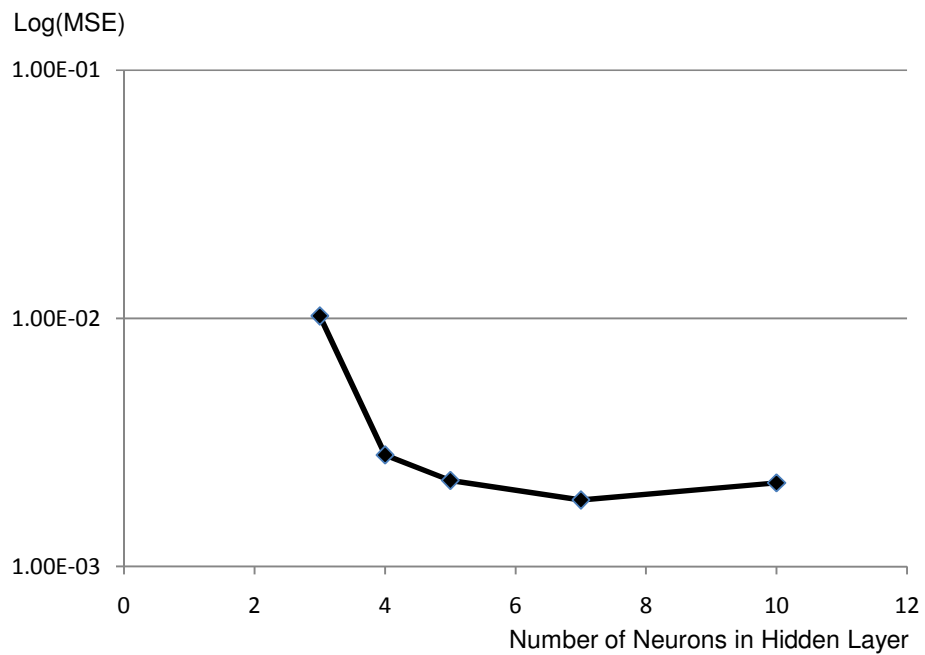


Figure 5.10. Variation of MSE values with respect to the amount of nodes in the hidden layer (For abutment design model).

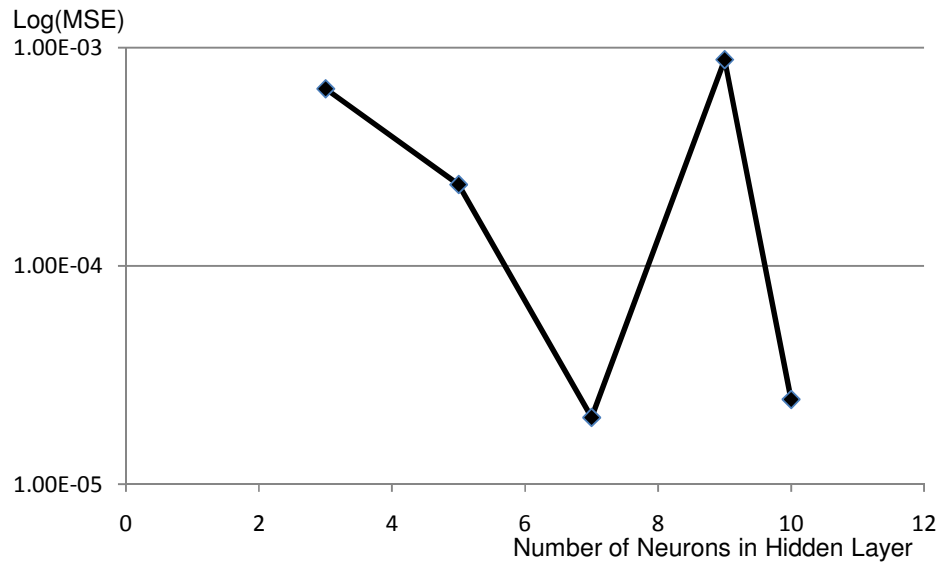


Figure 5.11. Variation of MSE values with respect to the amount of nodes in the hidden layer (For abutment cost model).

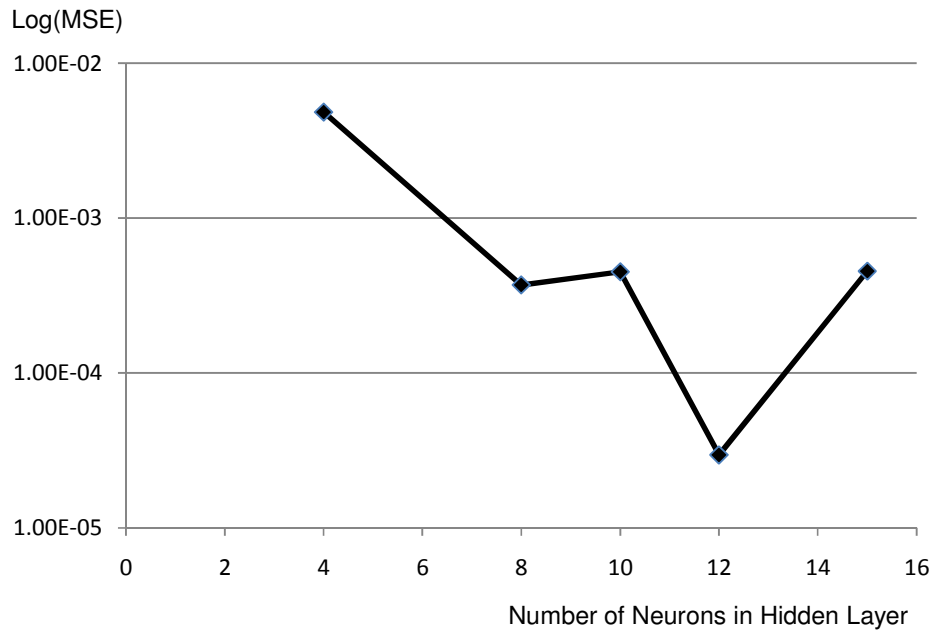


Figure 5.12. Variation of MSE values with respect to the amount of nodes in the hidden layer (For pier design model).

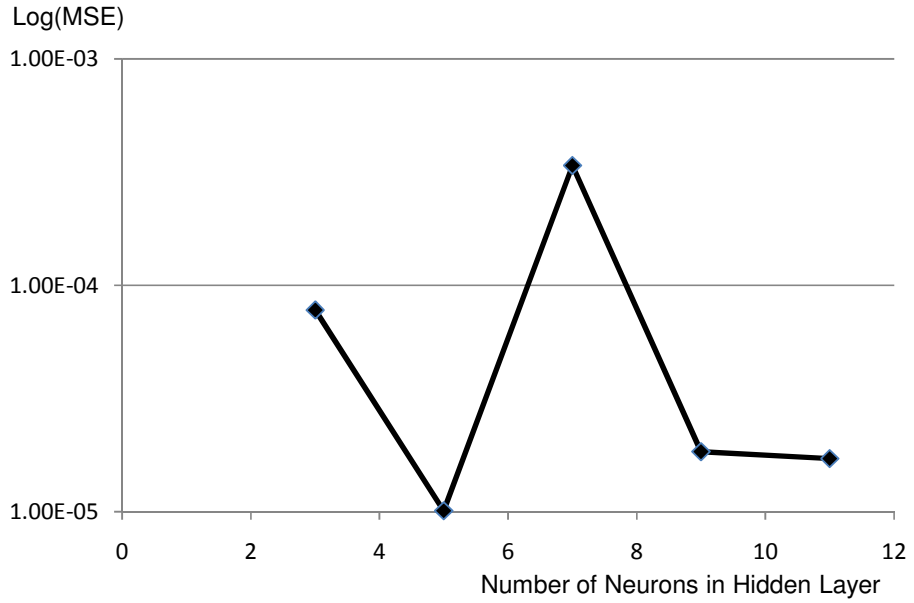


Figure 5.13. Variation of MSE values with respect to the amount of nodes in the hidden layer (For pier cost model).

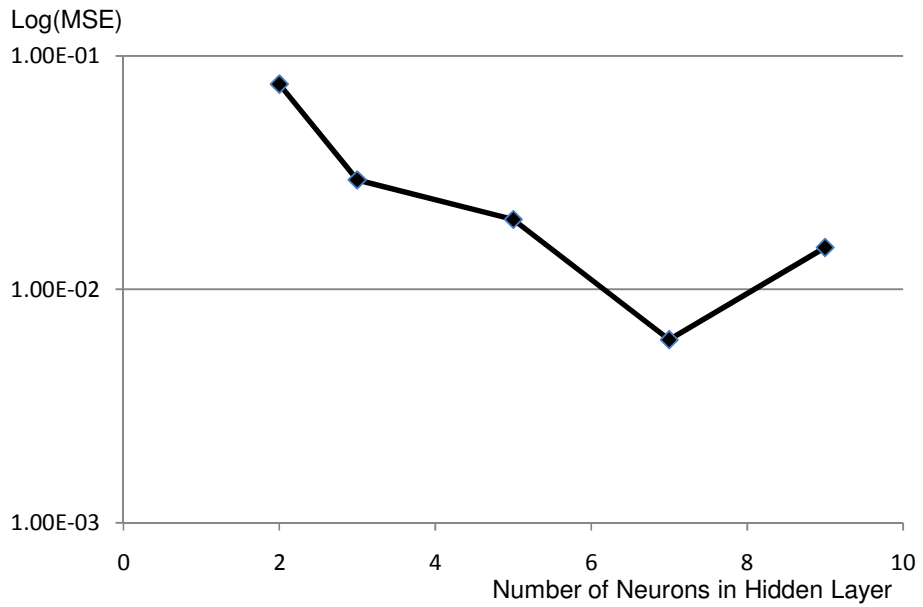


Figure 5.14. Variation of MSE Values with respect to the amount of nodes in the hidden layer (For superstructure design model).

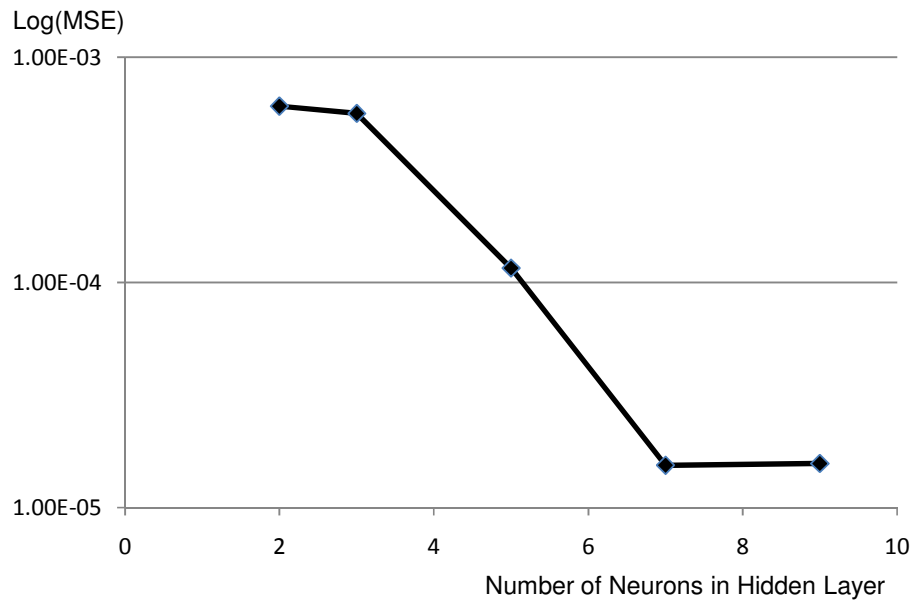


Figure 5.15. Variation of MSE values with respect to the amount of nodes in the hidden layer (for superstructure cost model).

As it is seen from the Figures 5.10 to 5.15, the mean squared error (MSE) of an ANN model varies according to the number of hidden nodes. In general, when the number of hidden neurons increases, MSE error decreases due to increment of non-linear capacity of ANN. But this does not mean the best ANN model, since overtraining should be avoided. For this reason, for some ANN models, less number of hidden neurons gives better ANN performance. Therefore, for each trial, the ANN model is trained up to the optimum number of epochs where overtraining begins. As a result, each ANN model is modeled by avoiding overtraining phenomenon. The optimum number of hidden neurons is selected as the ANN model which gives the smallest MSE value among the alternatives.

All these ANN models are the key tools to perform the structural and geotechnical design of the bridge components and estimating their costs. The following assumptions should be kept in mind in structural and geotechnical designs:

- Since, ANN models are based on statistical data of existing bridge projects, it is assumed that all designs are safe and within the economical range in terms of civil engineering perspectives.
- The estimated designs by ANN models reflect the above assumption such that the proposed design outputs by ANN model are inherently safe and within the serviceable limits. For this reason, any additional design checks are not required.
- The economy of the designs estimated by ANN models are accepted within the reasonable economical range, because all the real-life projects are assumed to be reasonably economical. However, it should be noted that it is not possible to make a conclusion that the design proposed by ANN models are the most economical structural and geotechnical designs, because it is believed that real-life projects are designed using conventional practices without optimization of the structural components. On the other hand, it can safely be stated that they are expected within the acceptable economical range due to the final checks done by the General Directorate of Highways.
- Consequently, this study does not include the detailed structural and geotechnical optimization of the bridge components. The internally detailed optimizations of the bridge components from the perspectives of structural and geotechnical engineering are beyond the scope of this study.

5.6 Bridge Hydraulics Computations

In order to calculate the mean values of the hydraulic parameters involved in reliability calculations, bridge hydraulics fundamentals are used throughout the bridge opening. For this reason, two additional cross-sections in addition to the bridge cross-section are given as input to the software to perform the hydraulic calculations through the bridge. These cross-sections are:

- Cross-section downstream of the bridge where the disturbed flow due to bridge is no longer available,
- Cross-section upstream of the bridge where the flow is not disturbed due to bridge.

The cross-sections just upstream and just downstream of the bridge are automatically generated by the framework based on the bridge cross-section. The framework is capable of applying the following hydraulic computational procedures whose details are explained in Chapter 2:

- Energy Method (Standard Step Method),
- Momentum Approach,
- Yarnell Equation (Yarnell, 1934)

Although the principles of the computation algorithms are based on average sectional flow variables, such as average velocity, spatial distribution of velocity across the cross-section can also be calculated by applying the flow distribution algorithm according to sectional conveyances as described in USACE (1998). The developed software framework implements this algorithm and therefore has the capability of calculating the local flow velocities for abutments and piers according to their relative locations at the corresponding cross-section.

5.6.1 Reliability Analysis

The complexities in the scouring phenomenon raise the uncertainties involved in the mechanism. These uncertainties were not reflected to the conventional design methodologies due to the lack of sufficient information. Therefore, conventional deterministic methodologies for the design of bridge foundations are subject to an

unknown level of scouring risk. For this purpose, the conventional deterministic approaches impose high factor of safeties to avoid this unknown risk level. In recent times, this situation even results in designing pier footings as pile foundations in order to elude this hydraulic risk without making appropriate economic analysis.

Reliability analyses are superior to conventional deterministic analyses because of the inclusion of many uncertainties. Therefore, provided that the statistical properties of related parameters are known, it is highly preferable to perform reliability analyses. In literature, there exist a number of studies for the reliability of the bridge piers and abutments. The primary of these are Johnson and Ayyub (1992), Johson (1992), Johnson and Ayyub (1996), Johnson (1998), Yanmaz and Çiçekdağ (2001), Yanmaz and Üstün (2001), Yanmaz (2001), Yanmaz (2002-b), and Yanmaz and Çelebi (2002). In these studies, different techniques for calculation of the reliabilities of the bridge piers and abutments are proposed.

In general context, reliability can be stated as the probability that the resistance of the system is equal to or higher than the loading imposed on the system. In bridge hydraulics, reliability of a bridge pier or abutment is defined as the survival probability of the pier or abutment without overturning due to excessive scouring action. Thus, the probability of failure, P_f , for bridge piers or abutments can be formalized by the following equation.

$$P_f = P_r(d_f < d_s) \quad (5.1)$$

where; P_r is the probability and d_f is the depth of footing. Reliability, R_L , means survival probability of the system which is simply the complement of the failure probability, i.e. $R_L=1-P_f$. There are various techniques that can be considered in reliability calculations ((Ang and Tang, 1984), (Mays and Tung, 1992)). The exact calculation of reliability of a system is difficult to perform since the exact probability distributions of the random variables are required and the computation of the integral equations may be very difficult and cumbersome. For this reason,

simpler approximate methods were developed details of which are out of the scope of this thesis. In a very brief logic, these analytical-based solutions are achieved by expanding the failure function by Taylor Series around the mean values up to a desired level of accuracy. In addition to these analytical-based approximate solutions, a numerical-based solution, “Monte Carlo Simulation” technique may be applied very conveniently as a computerized solution. In this study, Monte-Carlo Simulation technique is used to calculate the reliability values. A brief description of Monte-Carlo Simulation technique is given in the following paragraph.

Monte-Carlo simulation technique is based on the “Law of Large Numbers”; which says that if large number of samples are generated, eventually the desired probability distribution is approximated. Monte-Carlo simulation concerns with generation of random numbers from some given probability distribution. The principle of Monte-Carlo technique lies beneath the generation of any type of probability distribution based on uniform distribution random number. Then, uniformly distributed random numbers are transformed into the desired distribution by a method called “Inverse Transform Sampling”. The main steps using this technique can be listed as follows with reference to Figure 5.16:

- Let x_R be a random variable whose distribution can be described by the cumulative distribution function F_{CDF} .
- It is desired to generate values of x_R which are distributed according to this distribution,
- For this purpose, a random number from the standard uniform distribution is generated; called as u_R .
- The value of x_R is computed such that $F_{CDF}(x_R) = u_R$;
- The computed value of x_R becomes the random number drawn from the distribution described by F_{CDF} .

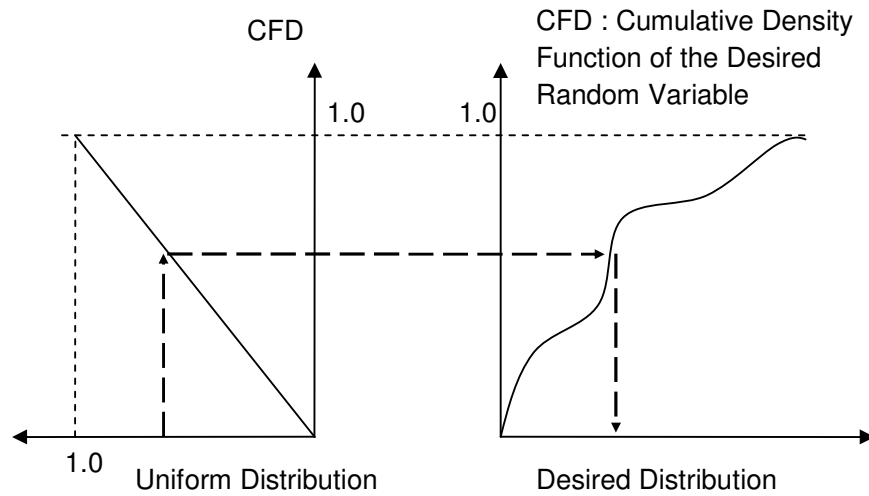


Figure 5.16. Graphical Description of Inverse Transform Sampling Procedure

By using the “Inverse Transform Sampling” procedure, a random variable of any probability distribution can be obtained via uniform distribution. This is especially very useful for computerized solutions because almost all programming environments have the capability of producing uniformly distributed random values.

$$P_f = P_r (f(x_R) < 0) \tag{5.2}$$

In the light of the above procedure, the Monte-Carlo Simulation technique can be performed as follows: For a probability equation of the form Equation (5.2), Monte-Carlo simulation technique can be applied provided that the random variables involved in the equation are independent. Thus, for any random variable, the corresponding values are generated subsequently, according to its probability distribution function based on the Inverse Transform Sampling process. Then, in each iteration, these values are put into the probability equation and the results of this equation are classified as positives and negatives. The ratio

of the number of negatives to the total number of iterations gives the probability of the equation being less than zero.

The number of simulation cycles in Monte-Carlo analysis directly influences the value of the calculated reliability. Therefore, sufficiently large number of iterations should be run in order to obtain a significant sampling of simulation events such that the results are close to the exact values. For this purpose, by using the coefficient of variation of the reliability value, Ω_R in each cycle, the accuracy of the mean reliability should be assessed so that the decision whether to continue or stop the simulation can be given. If the simulation cycles are increased, the value of Ω_R decreases and after some point it converges to a certain value so that the simulation can be stopped. According to Johnson (1999), $\Omega_R < 0.1$ can be taken as a criterion to indicate that simulation can be ended.

The statistical data i.e. probability density functions (PDF) of the random variables involved in the reliability calculations and their coefficient of variation (Ω) for the necessary hydraulic parameters which are taken into consideration in the software are presented in Table 5.4 with reference to Yanmaz and Çiçekdağ (2001) and Yanmaz (2003). In Table 5.4, "NI" stands for no information.

Table 5.4. Statistical properties of the parameters in reliability calculations.

Parameter	Ω	PDF
u, average flow velocity	0.2	Symmetrical Triangular
D ₅₀ , median size of bed material	0.01	Normal
y, flow depth	0.2	Symmetrical Triangular
W, channel width	0.01	Normal
u _c , critical mean threshold velocity	0.2	Symmetrical Triangular
K _s , correction factor	NI	Uniform
K _θ , correction factor	NI	Uniform
K _d , correction factor	NI	Uniform

The equations used in the reliability calculations for computing local scour around piers, abutments, and contraction scour are given in Chapter 3. Using the mean

values along with the given coefficient of variation and the corresponding probability density functions for each of the corresponding random variable given in Table 5.4, the simulation is run to compute the reliability values within the constraints of the problem.

5.7 Formulation of the Optimization Problem

The kernel of this study is an optimization problem that is described in Section 5.3.3. This optimization problem is done by focusing on hydraulic–structure interactions so that the optimum arrangement of bridge spans is calculated as the result of the optimization problem. Besides the optimum arrangement of the bridge spans, the required dimensions of the structural components of the bridge, such as the pier width, abutment width, superstructure girder depth, etc., are also estimated by the developed software framework. For this reason, the central part of the algorithm of the developed software is based on an optimization problem.

The objective of this optimization problem is to minimize the total cost of the bridge by satisfying the imposed constraints. In this fashion, it is essential to define the corresponding cost function of the problem mathematically. The cost function is heavily dependent on the ANN models developed, because costs of the bridge components are estimated by an ANN approach. In this context, the total cost of a bridge, $C(X)$ is calculated by the following mathematical expression within the contents of this study:

$$C(X) = \sum_{i=1}^2 \text{ANNc}_a(\text{Input}_{a-i}) + \sum_{i=1}^{N_s-1} \text{ANNc}_p(\text{Input}_{p-i}) + \sum_{i=1}^{N_s} \text{ANNc}_{ss}(\text{Input}_{ss-i}) + \text{Cost}_{\text{add}} \quad (5.3)$$

where;

ANNc_a : artificial neural network model for abutment cost estimation,

$ANNc_p$: artificial neural network model for pier cost estimation,
 $ANNc_{ss}$: artificial neural network model for superstructure cost estimation,
 $Cost_{add}$: additional costs due to excavation, fixed costs, etc.,
 $Input_a$: Input array for $ANNc_a$,
 $Input_p$: Input array for $ANNc_p$,
 $Input_{ss}$: Input array for $ANNc_{ss}$,

Above mathematical expressions show that the total cost of the bridge is found by the addition of the cost of each structural member in the bridge estimated by the ANN cost models, each of which is built for corresponding structural component types; abutments, piers, and superstructure. In this context, the costs of each abutment, pier, and superstructure girders are added to find out the estimated total cost of the bridge.

Having defined the cost function of the optimization problem, it is appropriate to formulate the optimization in the light of the verbal definitions of the optimization software defined in Section 5.3.3. Therefore, the mathematical formulation of this optimization problem can be written and explained in details as follows:

- Minimize the objective function: $O(X_i) = C(X_i) + P_c(X_i)$ (5.4)

- Subject to the following constraints;

$$h_1(X_i) = \sum_{i=1}^n X_i - L_t = 0 \quad (5.5)$$

$$g_1(X_i) = \Gamma_c - \Gamma < 0 \quad (5.6)$$

$$g_2(X_i) = P_r(d_{sa-1} - d_f > 0) < P_{f_max} \quad (5.7)$$

$$g_3(X_i) = P_r(d_{sa-2} - d_f > 0) < P_{f_max} \quad (5.8)$$

$$g_{3+j}(X_i) = P_r(d_{sp-i} - d_f > 0) < P_{f_max} ; j = 1, 2, \dots, N_s. \quad (5.9)$$

where;

N_s : the number of spans in the bridge,

L_t : total width of the bridge valley (total length of the bridge),

Γ_c : critical contraction ratio,

Γ : existing contraction ratio,

d_{sa-1} , d_{sa-2} : total depth of scour around abutment-1 and abutment-2 respectively,

d_{sp-i} : total depth of scour around each pier in the bridge,

d_f : depth of footing for abutments and piers,

X_i : the decision variables,

$O(X_i)$: objective function,

$C(X_i)$: total cost of the bridge,

$P_c(X_i)$: penalty cost function for the violation of the constraints,

$h_1(X_i)$: the equality constraint due to the cross-sectional geometry that the sum of the span lengths must be equal to the valley width (total bridge length),

$g_1(X_i)$: the probabilistic inequality constraint for the hydraulic choking,

$g_2(X_i)$: the probabilistic inequality constraint for to the reliability of abument-1 due to the total scour around abutment-1,

$g_3(X_i)$: the probabilistic inequality constraint for to the reliability of abument-2 due to the total scour around abutment-2,

$g_{3+j}(X_i)$: the probabilistic inequality constraints for the reliability of piers due to the total scour around each pier.

P_{f_max} : maximum allowed failure probability for probabilistic constraints,

Given the number of spans in the bridge, N_s , the optimization definition shows that there are one deterministic equality constraint and total of $(3+N_s)$ inequality constraints among which one of them is deterministic and the rest of them are probabilistic. The probability constraints put the optimization problem into reliability-based form whose details are discussed in section 5.6.1. The software solves the optimization problem defined above for different number of spans, N_s , and chooses the one with the smallest total cost of the bridge as the final optimum result of the problem. Therefore, the software framework solves a

number of optimization problems in parallel in order to obtain the overall best result. Each optimization problem gives the optimum arrangement of the spans in the bridge for the given number of spans.

5.7.1 Selection of the Optimization Technique

When the optimization problem is examined thoroughly, it is easily seen that, objective function consists of ANN models which have inherently very non-linear behavior. Therefore, this is a non-linear optimization problem due to both the non-linearity of the objective function and most of the constraints. Hence, non-linear nature of this optimization problem imposes some restrictions on the selection of the optimization algorithm to be used. In this study, heuristics-based optimization techniques are found conveniently applicable to this problem, so among various heuristic-based optimization techniques, Genetic Algorithms was chosen as the major optimization technique to be implemented by the developed software framework, AIROB. The fundamentals of the genetic algorithms are expressed in Chapter 4.

In addition to Genetic Algorithms, AIROB is also capable of solving the optimization problem by “Dynamic Programming” approach. The comparison of the results and implementation details of GA and Dynamic Programming approaches are given in Appendix C in detailed fashion by a case study. A brief description of Dynamic Programming in the context of this study and the inspection of the fundamental characteristics of the optimization problem regarding to the preference of GA are presented in the following sections.

5.7.1.1 Dynamic Programming Approach

Dynamic programming is an enumerative based optimization technique as described in Figure 4.7 and mentioned in Chapter 4. The basic strategy in the implementation of dynamic programming lies on solving a complex problem into

simpler sub-problems (Wikipedia, 2011-c). Therefore, it is conveniently applicable to optimization problems which can be easily divided into sub-problems so that each of the sub-problems is solved in order to achieve the optimization of the whole problem. In this context, Dynamic Programming approach is based on the Bellman's Principle of Optimality principle (Bellman, 1957) as follows:

“An optimal policy has the property that whatever the initial state and initial decision are, the remaining decisions must constitute an optimal policy with regard to the state resulting from the first decision.”

As a result of the above definition, it is obvious that the formulation of the optimization problem is performed in recursive manner so that the solution of the problem consists of solution of the sub-problems which have the same structure of the whole problem. In this context, a Dynamic Programming problem is composed of two fundamental terms such as “stage” and “state” (Sniedovich, 2010). “Stage” is the position of the sub-problems where a decision is required, whereas “States” are the alternative solutions of a certain stage. Thus each stage of the problem involves finite number of states linked to it.

The optimization problem of the study can be formulated by a Dynamic Programming approach as the following recursive equation with reference to Figure 5.17 :

$$F_{d_n}(S_{p_{tot}}) = \min\{f_d(X_d) + F_{d_{n+1}}(S_{p_{tot}} - X_d)\} \quad (5.10)$$

where; F_{d_n} : the total cost of the bridge up to the current Stage_n.

$S_{p_{tot}}$: total span length covered up to the current Stage_n.

X_d : the decision (span length) to be taken for the current Stage_n.

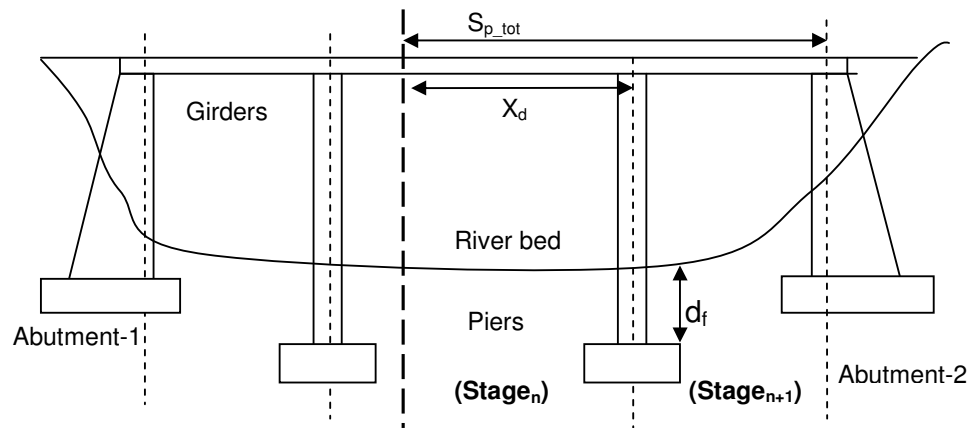


Figure 5.17. Descriptive sketch illustrating the dynamic programming formulation of the river bridge optimization problem.

By the above formulation, the problem is solved by starting from one of the abutments and continued in a series fashion in order to reach to the other abutment. Therefore, when the total bridge length, which is equal to the summation of the all span lengths, are covered, the dynamic programming approach stops by giving the optimum span arrangement. In this formulation, each stage is defined to be the span to be passed, thus the total number of stages are simply equal to the total number of spans in the optimization problem. Computational details of this approach along with its comparison with GA are described in Appendix C.

5.7.1.2 Characteristics of the Optimization Problem in terms of GA

The optimization engine of AIROB utilizes GA by means of a fitness function, F , which is simply equal to the inverse of the objective function given in equation (5.4), because the optimization problem is a minimization type and the objective function values have always positive signs.

$$F(X) = \frac{1}{O(X)} \quad (5.11)$$

After selecting the fitness function, it is essential to select the appropriate values for the parameters of GA. Since GA is a probabilistic-based technique, their parameters affect the probabilistic behavior of the algorithm. Therefore, when using a genetic algorithm, it is very important to select the appropriate parameters so that the technique can find out the optimized results efficiently. As a result of this sensitive behavior, GA are said to be very problem-dependent (Genetic Algorithms, 2011). For this purpose, sensitivity analyses are beneficial in order to utilize the method superiorly. Based on the results of the sensitivity analyses, an insight for the selection of these parameters can be rationalized. A sensitivity analysis was carried out for a certain application problem in Chapter 6.

5.7.1.2.1 Examination of Search Space

Search space is an important parameter in GA. Although, there is not a limitation for using GA in terms of search space, its major power comes from the effective search performance in large search spaces. In this context, the search space of this problem is examined to perceive the problem from this perspective.

The optimization problem formulated for this study is defined for a predefined number of spans. Therefore, when the number of spans changes, the corresponding size of search space also changes. Size of the search space is also dependent on the discretization used by GA. For a rough discretization with 5 bits, a decision variable can have $2^5=32$ discrete values. For a span range of 10 to 40 meters, this discretization gives 1 meters of precision approximately. For depths of scour ranging from 0 to 5 meters, gives 0.15 meters precision approximately when the number of discretization is equal to 32.

Based on the explanations about the discretization in GA, the size of the search space for a given number of spans, N_s can be calculated by the following equation:

$$S = 32^{2N_s + 1} \quad (5.12)$$

where, S is the size of the search space for a certain number of spans. This equation is obtained by multiplying the discretization amount for each decision variable to find out the total number of alternatives in the problem. In this context, the total number of decision variables is equal to $2N_s+1$, of which N_s amount is for the spans and remaining is for the depth of footings for each abutment and pier.

If equation (5.12) is computed for various N_s values, the size of the search space with respect to the number of spans can be obtained. Therefore, the variation of the size of the search space with respect to various numbers of spans can be seen in Figure 5.18. As it is seen for $N_s=3$, the size is approximately 10^{10} , however, it increases linearly in “logarithmic scale”, such that the size of the search space is about 10^{20} for $N_s=6$.

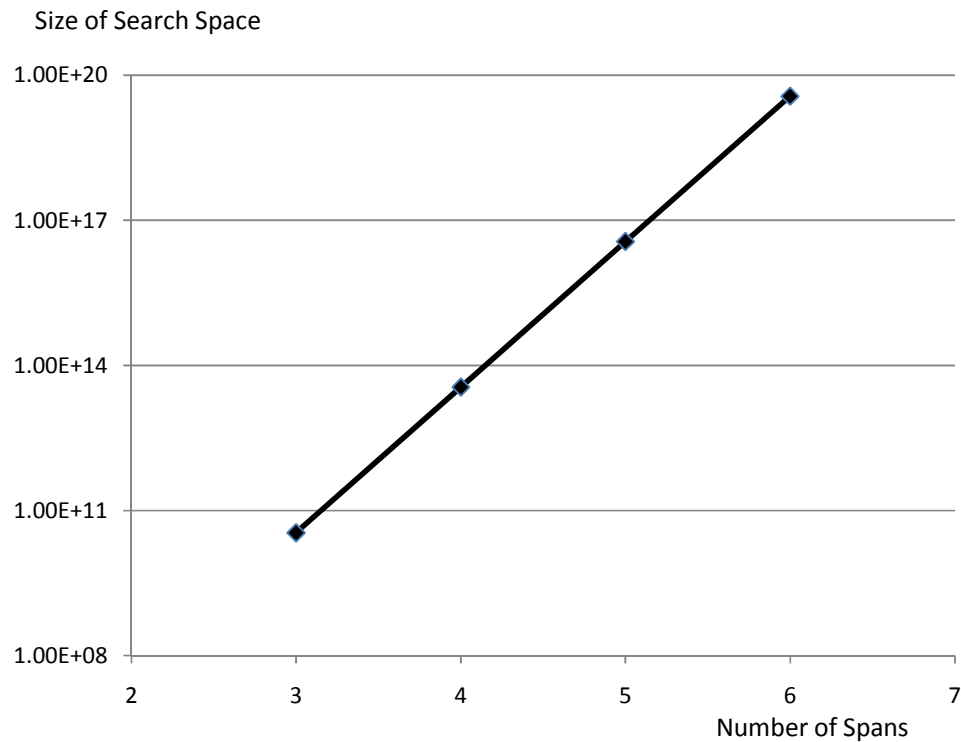


Figure 5.18. Variation of search space according to the number of spans (Size of search space axis is in logarithmic scale).

5.7.1.2.2 Handling of the Constraints of the Optimization Problem

The constraints of the problem are handled by penalty functions, in which violation of each constraint is taken as a penalty cost to the total cost of the bridge. Therefore, by the generations of GA, the infeasible solutions are expected to converge within the feasible region where all the constraints are satisfied.

The penalty function used in this study is of the following form (Gen and Cheng, 2000):

$$P_c = \sum_{i=1}^{N_c} \delta_i r_i \quad (5.13)$$

where, P_c is the total penalty cost amount, N_c is the total number of constraints, δ_i is the penalty coefficient for each violation amount, which is denoted by r_i .

In this problem, geometry constraint which is given in equation (5.5) has higher importance relative to the other constraints, because the total length of the bridge must match the summation of the span lengths. Therefore, if this constraint is not satisfied, the problem becomes meaningless. The significance of this constraint requires higher value of penalty coefficient for this constraint. The values of the coefficients are determined by trial and error so that the optimum value is approximated by converge the GA population with a good performance.

5.8 Programmatic Details of AIROB

AIROB, as its name implies an **A**rtificial **I**ntelligence based computation framework for the **R**eliability-based **O**ptimization of **B**ridges. It includes many number of software libraries, almost all of which have been coded throughout the

period of this study. Among these software libraries, there are a number of categories related to the computational part of this study.

The framework, AIROB has been implemented by Microsoft's C# programming language. The reason behind the choice of C# is its strong capabilities in terms of object-oriented programming and code development efficiency in Microsoft Windows environment. The object-oriented programming paradigm has been highly utilized in the design of AIROB so that the extensibility of the framework can be accomplished efficiently.

AIROB consists of mainly five libraries that encapsulate the associated computational tasks as follows:

- Optimization Library: It is composed of the classes related to GA majorly and also dynamic programming.
- Structural – Geotechnical Design Library: This is the main library in which ANN models are computationally generated and utilized.
- Bridge Hydraulics Library: This is the library where all bridge hydraulics related computations are performed, such as water surface profile computations, bridge scouring computations, etc.
- Reliability Library: The Monte – Carlo simulation technique are implemented in the contents of this library.
- Open Channel Hydraulic Library: It consists of simulation of open channel flows very similar to HEC-RAS (USACE, 1998) procedure for regular and irregular channels with floodplains. Flow distribution calculations for a cross-section are also encapsulated within this library.
- Other Helper Libraries: Some computational procedures which are not explicitly related to this study, but used in this study exist in this library.

The major ones are “Root Finding” classes and “Polygon Geometry” classes which are mostly utilized associated with “Open Channel Library”.

All of these aforementioned libraries are assembled in the framework, AIROB from which various applications can be developed. In this study, reliability-based optimization of river bridges was studied based on AIROB. However different studies can be done within the scope of the libraries of AIROB. Therefore, it is highly extendible to serve for wide range of civil engineering requirements.

AIROB consists of approximately 20,000 lines of code and it is open to be extended. AIROB also has a graphical user interface (GUI) for its ease of usage and a brief user manual for using AIROB through this GUI is presented in Appendix D.

5.8.1 Algorithmic Description of AIROB

This study makes use of many different computational techniques and each of which is explained separately in the previous chapters. However, there are intricate connections between each of these techniques in the implementation of the software and this might make the understanding of the overall behavior of the software difficult. This is mainly due to the employment of different AI techniques, Artificial Neural Networks and Genetic Algorithms in a collaborative manner. For this reason, presenting a general view of the flowchart of the software is worthy to clarify the overall mechanism of the software framework (see Figure 5.19).

Figure 5.19 shows the basic steps in the implementation of GA and the positions where ANN models are called within the algorithm. Also, the reliability based hydraulic computations performed for the computation of the cost of the problem for each generation can be observed by the flowchart presented in Figure 5.19. As it can easily be observed, the inherent structure of these calculations require considerable amount of computing time due to involvement of various iterative tasks in the algorithm.

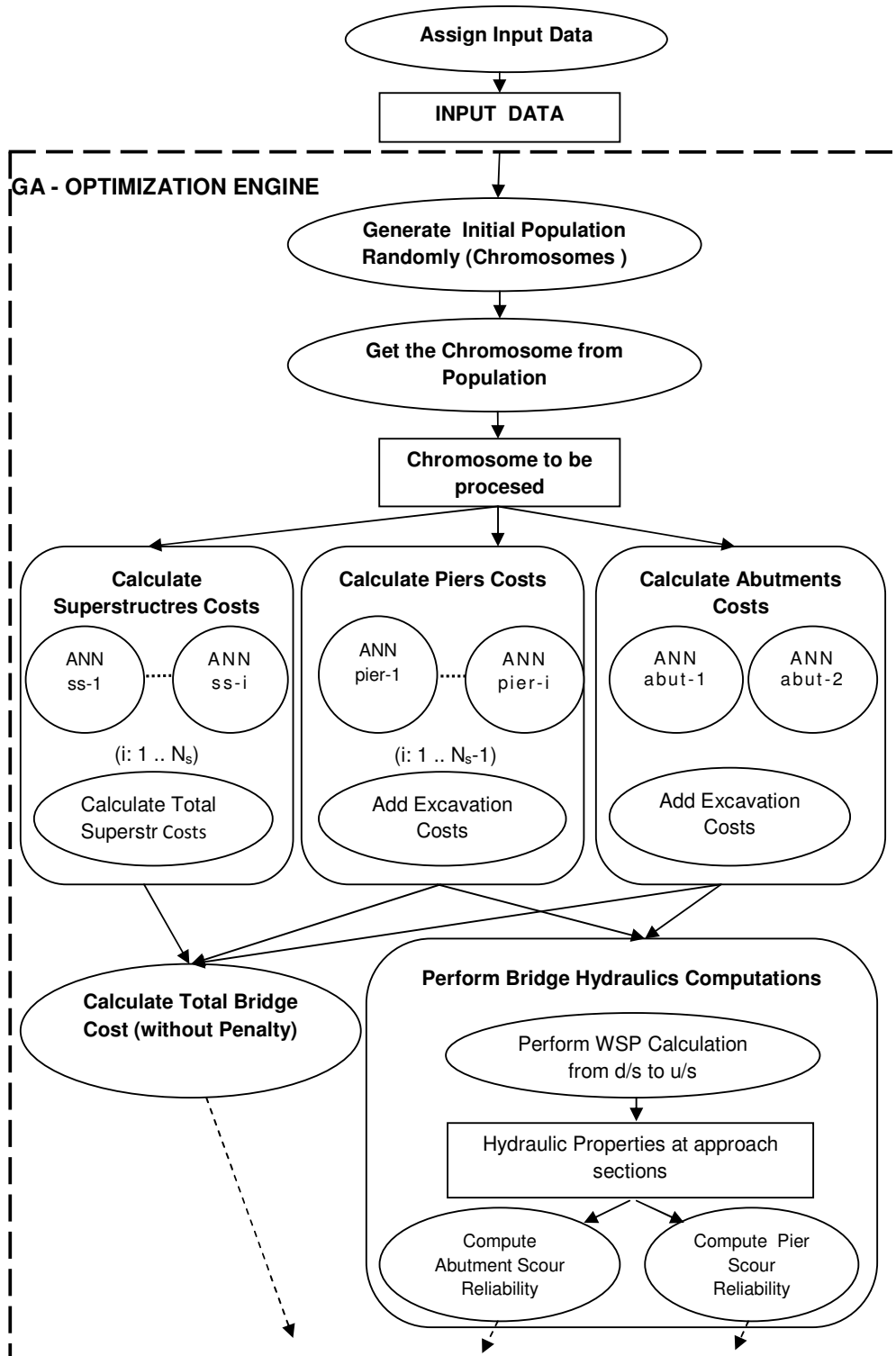


Figure 5.19. General flowchart of AIROB.

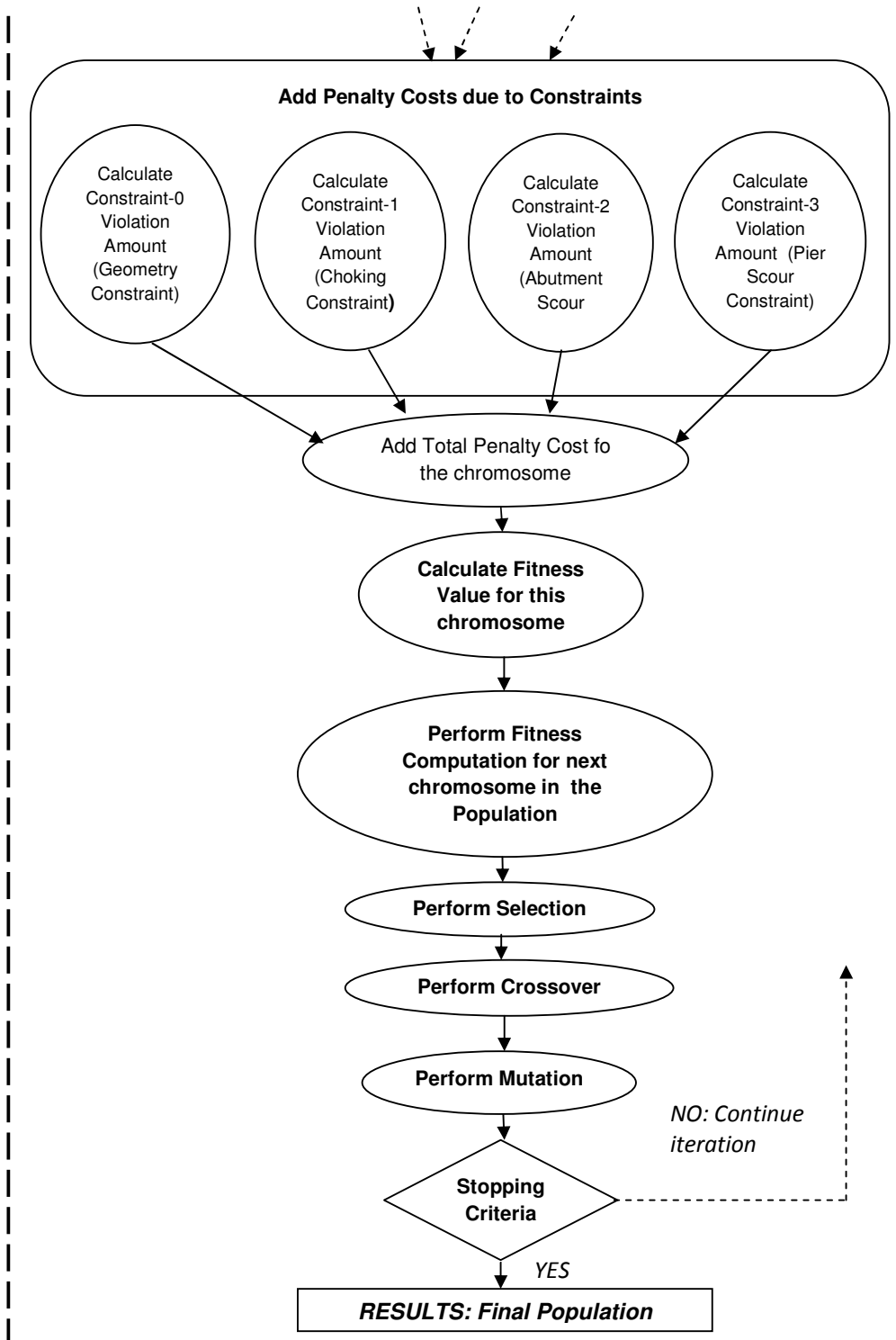


Figure 5.19 (Continued). General flowchart of AIROB.

The main input data and explanations of the symbols used in Figure 5.22 are listed below:

- Number of spans in the bridge, N_s
- River discharge, Q ,
- Manning's roughness coefficients; n_{Mann} ,
- Median sediment size, D_{50} ,
- Bridge Deck Height, El_{bridge} ,
- Embankment Length, L_{em} ,
- Bridge width, E ,
- River width, L_t ,
- Bridge Expansion Length, L_e ,
- Bridge Contraction Length, L_c ,
- Average River Bed Slope, S_o ,
- Unit Cost for Excavation, UC_e ,
- Soil Type, S_{type} ,
- Average SPTN value of the soil, $SPTN_{\text{ave}}$,
- Min value for Depth of Footing for Abutments, $d_{f\text{amin}}$,
- Max value for Depth of Footing for Abutments, $d_{f\text{amax}}$,
- Number of discretization points for Abutment, $N_{d\text{fa}}$,
- Min value for Depth of Footing for Piers, $d_{f\text{pmin}}$,
- Max value for Depth of Footing for Piers, $d_{f\text{pmax}}$,
- Number of discretization points for Piers, $N_{d\text{fp}}$,
- Min value for Span Lengths, $S_{p\text{imin}}$,
- Max value for Span Lengths, $S_{p\text{imax}}$,
- Number of discretization points for Span Lengths: $N_{S\text{pi}}$,
- Weights of ANN Abutment Design Model: $WANN_{d\text{a}}$,
- Weights of ANN Pier Design Model: $WANN_{d\text{p}}$,
- Weights of ANN Superstructure Design Model: $WANN_{d\text{ss}}$,
- Weights of ANN Abutment Cost Model: $WANN_{c\text{a}}$,
- Weights of ANN Pier Cost Model: $WANN_{c\text{p}}$,
- Weights of ANN Superstructure Cost Model: $WANN_{c\text{ss}}$,
- Population Size for GA, N_{pop} ,

- Maximum number of generations for GA, Gen_{max} ,
- Crossover Rate for GA, R_{cross}
- Mutation Rate for GA, R_{mut}
- Selection Method for GA, M_{select} ,
- Elitism for GA, elitism,
- Crossover Type for GA, Typ_{cross} .

Application of the proposed software framework, AIROB is illustrated in Chapter 6.

CHAPTER 6

APPLICATION

6.1 Application Problem

An example is presented to illustrate the use of the methodology and the software, AIROB. This example considers a river reach having a cross-section and a plan view shown in Figures 6.1 and 6.2, respectively. The problem is solved for a design flood discharge of $Q = 200 \text{ m}^3/\text{s}$. The cross-section of the river, where a bridge of 24 m width is to be constructed, has an irregular shape with floodplains at both sides of the main channel (see Figure 6.1).

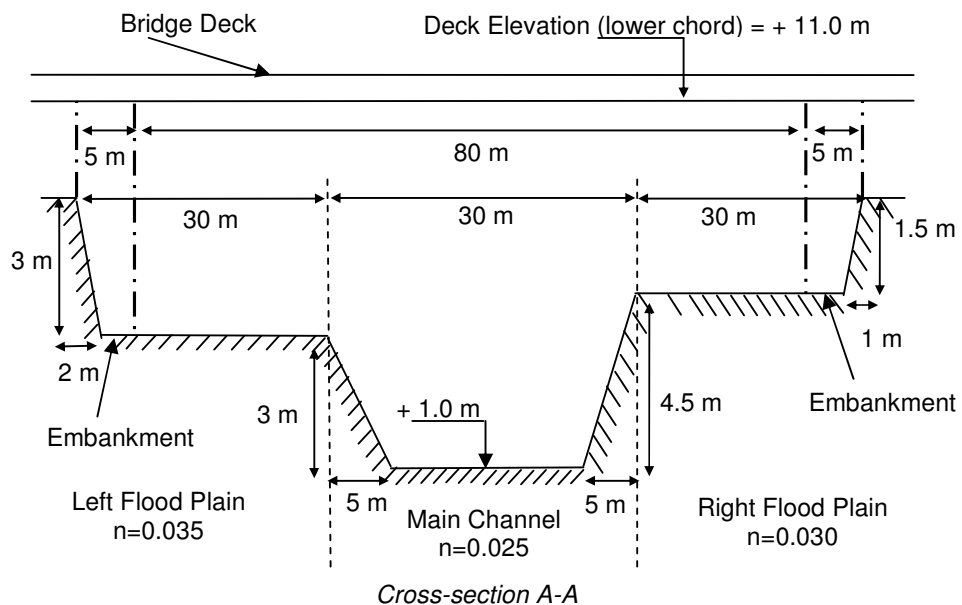


Figure 6.1. River cross-section details at bridge opening for the application problem (Not to scale).

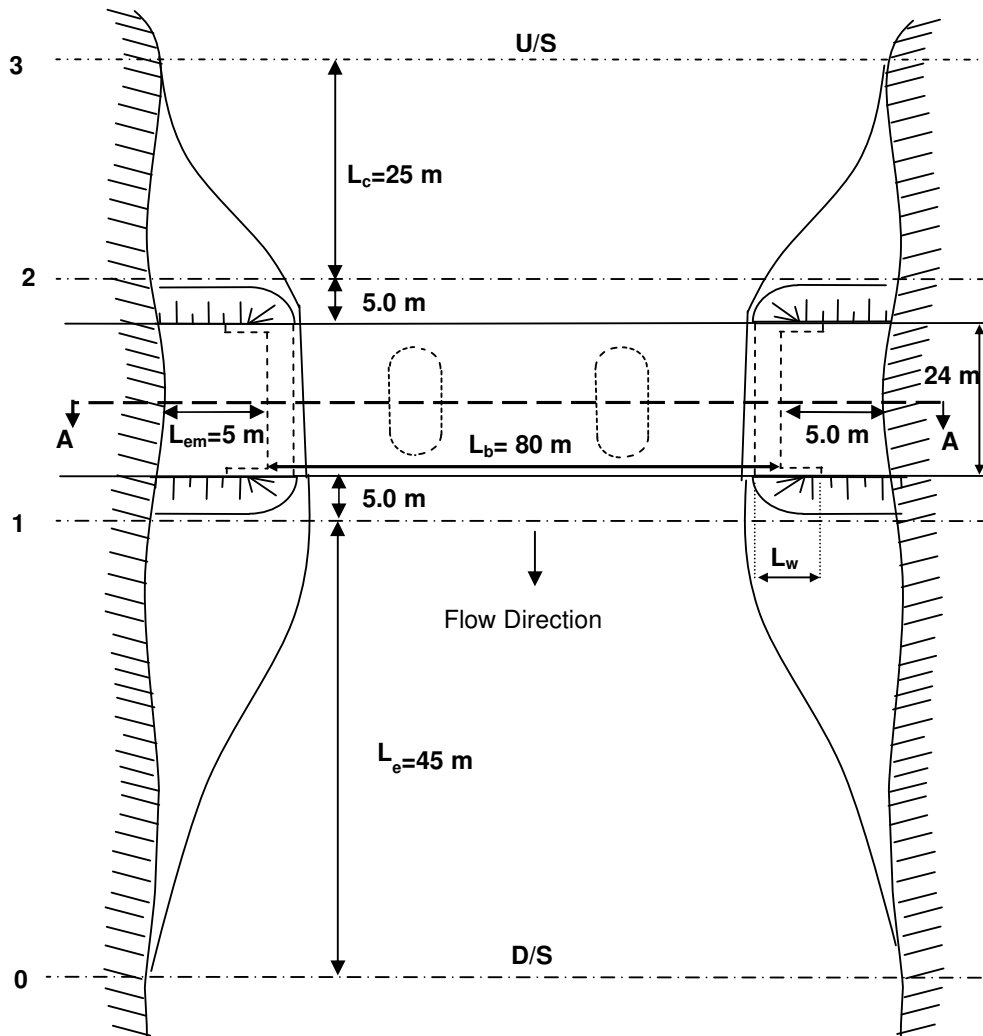


Figure 6.2. Plan view of the river reach at bridge opening for the application problem (Not to scale).

The embankment lengths for both sides of the bridge are taken as 5 m. Accordingly, the total length of the bridge to be designed is 80 m by subtracting the embankment lengths from the total width of the river cross-section. This bridge can be designed with different number of spans as two to six since the statistical data include minimum span length, 12.50 m and maximum span length, 40 m (see Table 5.2). The span arrangements are required to be symmetrical with respect to the centerline of the bridge as a design constraint. The aim of this problem is to find the most economical bridge span arrangement by considering

the constraints that will satisfy the desired hydraulic conformity. The remaining explanatory input data for the problem are given as follows:

- Both the downstream cross-section (cross-section 0 in Figure 6.2) and the upstream cross-section (cross-section 3 in Figure 6.2) have geometrically the same form as the river cross-section in Figure 6.1. The thalweg elevations for the downstream and upstream cross-sections are +1.1 m and +0.9 m, respectively.
- The water surface profile calculations are assumed to be in low flow conditions so that the flow is in subcritical regime leading to the calculations to be performed with the downstream boundary condition with a normal depth corresponding to a mild river bed slope of 0.0001.
- The flow contraction length, L_c is equal to 25 m, whereas the flow expansion length, L_e is equal to 40 m (see Figure 6.2).
- The cross-sections just downstream of the bridge and just upstream of the bridge are generated by AIROB automatically from the given river cross-section in Figure 6.1.
- For the just downstream and just upstream of the embankments, the flow is assumed to be ineffective by AIROB.
- The lower chord elevation of the bridge deck is constant as + 4.0 m due to the constraint of a highway alignment at the bridge site.
- The river reach has an alluvial bed whose bed is composed of sandy-gravel soil, having a median size, D_{50} of 2.5 mm and average SPTN value of 40.
- The bridge location is assumed to be in an earthquake zone where the corresponding dynamic forces dominate on the design calculations, complying with the underlying bridge database of AIROB. In this manner

the traffic loading is also assumed to be $H_{30}\text{-}S_{24}$ and all the materials are assumed to be of the types presented in Table 5.1.

- It is assumed that the topographic conditions enforce both abutments to have a wall length, L_w equal to 1.65 m along the cross-section.
- For the reliability based constraints, the minimum value of reliability is taken as 0.999 for both the abutments and the piers. The probability distribution functions and the corresponding coefficient of variation values for the hydraulic random variables are taken according to Table 5.4.

Genetic Algorithms library of AIROB is utilized for the solution of this application problem with a population size of 40, crossover rate of 0.8 and mutation rate of 0.1. Binary coding scheme is used such that each decision variable of the problem, span lengths and depth of footings are encoded with 8 bits. The selection scheme used in GA is “Roulette wheel selection” by providing “elitism” in the GA evolution process. Therefore, the convergence rate to the best solution is improved within a maximum number of 250 generations.

Based on the declarations of the input data above, the AIROB is executed for five different optimization problems, each of which is the assigned number of spans that can be chosen. As a result, for each number of spans, the optimized span arrangement is given by the software output. Among all these cases, the one which gives the minimum total cost is proposed to be chosen as the overall optimized design such that the optimum number of spans and the corresponding span arrangements are given. The optimum span arrangements for each number of span cases are given in Table 6.1. The proposed dimensions of the bridge components for the best solution are tabulated in Table 6.2. Finally, the variation of the total cost of the bridge according to the number of spans is presented in graphical form in Figure 6.3 for both the reliability-based and deterministic constraints. When the constraints are taken as deterministic, only the mean values of the scour depths are computed, which is the direct result of the corresponding scour equation. Thus, the constraint is satisfied when the depth of footing is greater than the mean value of the corresponding scour depth.

Consequently, the probability distributions of the scour depths are not taken into account for the cases with deterministic constraints.

Table 6.1. The optimum span arrangements for each case (Reliability-based constraints).

N_s	Span Arrangements (m)	Depth of Footings, d_f (m) (in order from Abutment-1 to Abutment-2)
2	40 - 40	d_f : (4.776 - 6.982 - 1.682)
3	22.5 - 35 - 22.5	d_f : (4.757 - 4.320 - 4.117 - 1.815)
4	20 - 20 - 20 - 20	d_f : (4.776 - 3.518 - 4.929 - 2.806 - 2.388)
5	15 - 15 - 20 - 15 - 15	d_f : (4.565 - 2.953 - 6.729 - 5.282 - 2.894 - 1.894)
6	12.50 - 12.50 - 15 - 15 - 12.50 - 12.50	d_f : (4.776 - 5.4 - 6.976 - 5.141 - 5.906 - 2.888 - 2.389)

Table 6.2. Basic dimensions of the structural components of the optimized bridge for reliability-based constraints ($N_s=3$).

Total Bridge Cost:	1,869,057 US\$
Number of Spans:	3
Span Arrangement (m) :	22.5 - 35 - 22.5
Abutments	
b_a (abutment width)	1.15 m
B_a (abutment footing width)	5.50 m
H_{fa} (abutment footing height)	1.50 m
St_r (reinforcement amount)	0.085 tons/m ³
P_f for Abutment-1	9.83E-04
P_f for Abutment-2	9.71E-04
Piers	
b_s (pier width)	1.20 m
B_s (pier footing width)	5.90 m
H_{fp} (pier footing height)	1.90 m
St_r (reinforcement amount)	0.15 tons/m ³
P_f for Pier-1	9.91E-04
P_f for Pier-2	9.63E-04
Girders	
d_g (depth of girders)	120 cm
del_g (Girder spacing)	130 cm

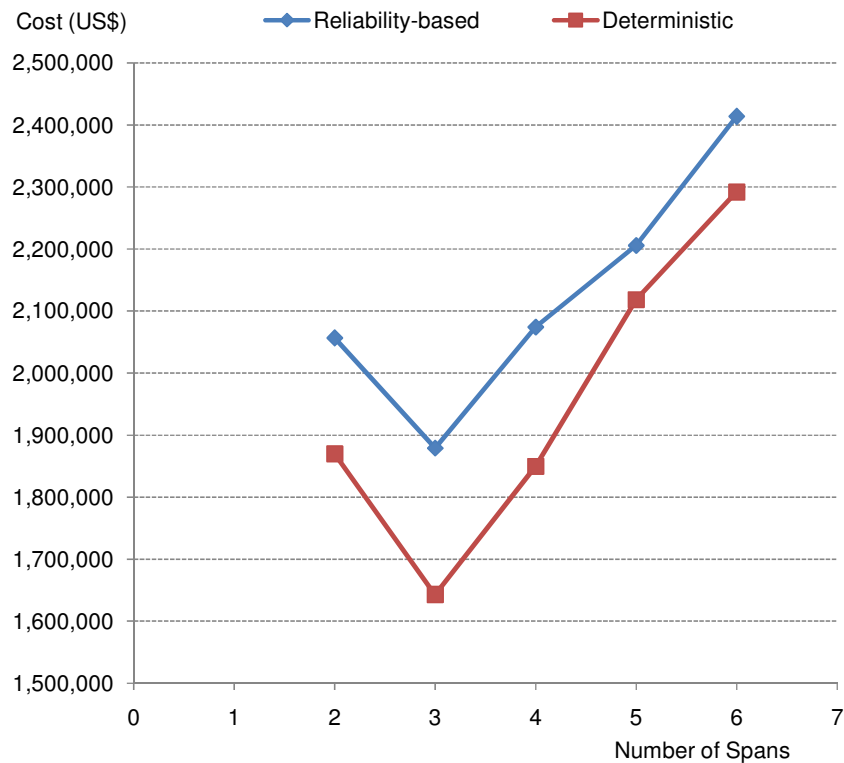


Figure 6.3. Variation of total cost of the bridge according to the number of spans.

As it is seen from the tabulated and graphical results, for a single pier located at the mid-location of the cross-section, the cost is high due to high span lengths. Moreover, in this alternative, the location of the pier is within the high flow velocity zone, causing a considerable amount of increase in scour depth. As a consequence of this phenomenon, AIROB increases the depth of the pier footing in order to satisfy the corresponding hydraulic constraint which is involved in the problem to avoid the collapse of the pier. This requirement yields a higher pier, and consequently a higher pier imposes a wider pier width, b_s due the structural requirements, such as the satisfaction of minimum column aspect ratio, of which, the details are discussed in Chapter 5. As a result, the total cost of the bridge also increases due to the enlarged pier dimensions.

The overall optimal span arrangement case is a bridge having two piers located 22.5 meters from both embankments (see Table 6.1 and Table 6.2). In this alternative, the smaller span lengths decreases the total cost of the superstructure. Although it may seem at first sight that two piers are more costly than a single pier, the piers are shifted to low flow velocity zones by AIROB to have smaller scour depths and pier heights. Therefore, the cost of two piers does not add an uneconomic situation with respect to the first alternative.

When the number of spans increases further, the total cost increases more abruptly, because it is much more difficult to avoid a pier from a high velocity zone in this case. When a pier is within a high velocity zone, the consequence of this is enlarged dimensions which also impose increase in the dimensions of the other piers, because structural design requirements state that the width of each pier should be equal in a bridge. As a result, the total cost of the bridge increases, although the total cost of the superstructure decreases due to smaller span lengths.

As a result of the above discussion about the outcomes of the application problem, the optimum alternative is found to be the one having three spans as seen in Figure 6.3. The scaled graphical representation of this alternative is presented in Figure 6.4.

Figure 6.4 shows that the optimum span arrangements are achieved when the piers are located within the floodplains, having smaller flow velocities. The velocity distribution across the cross-section for this case is also given in Figure 6.4, which implies that pier locations are free from excessive velocity zones. When the proposed locations of the piers are near to the slope corners such as in this problem (see Figure 6.4), "stone pitching" can be constructed to prevent the slope instability due to erosion of these regions, with almost no economical overload with respect to the total cost of the bridge.

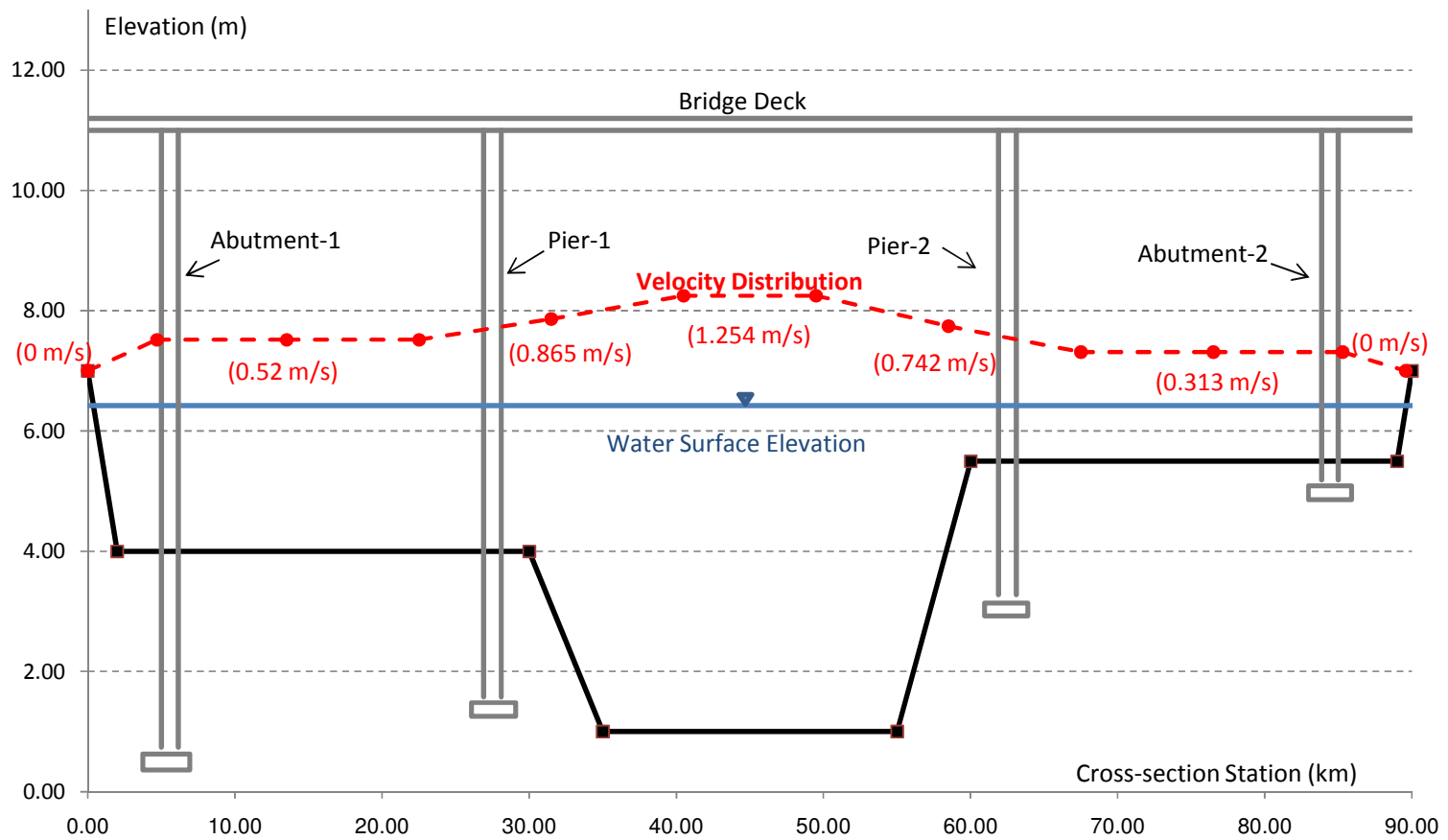


Figure 6.4. Velocity distribution across the bridge cross-section for the optimum alternative (in scale)
(Footings not to scale).

The results of AIROB can also be examined from the outcomes of reliability - based calculations. The application problem is executed for both conventional deterministic case and probability-based case. As it is seen from Figure 6.3, it is obvious that reliability-based calculations give higher costs with respect to the deterministic cases, because probabilistic based constraints impose higher footing depths. This is an anticipated outcome, for the reason that, in deterministic approach, fixed values are used for variables, whereas worst possible combinations of variables can be tested in probabilistic approach. As a result, the vertical distance between the curves in Figure 6.3 stands for the cost of the risk taken due to the uncertainties of the scouring phenomenon. In other words, the extra costs for the reliability-based approaches compensate the probable adverse effects of the uncertainties on the safety of the structure. In this example, the average cost of this risk is computed as 171,441 US\$. For the comparison of the reliability-based cases to the deterministic cases, the results of AIROB for deterministic-based executions are tabulated in Table 6.3. It should be noted that the optimized span arrangements for the deterministic cases are calculated as identical with the results of the reliability-based cases, however the depth of footings are smaller when the constraints are deterministic as it is expected (see Tables 6.1 and 6.3).

Table 6.3. The optimum span arrangements for each case (Deterministic constraints).

N_s	Span Arrangements (m)	Depth of Footings, d_i (m) (in order from Abutment-1 to Abutment-2)
2	40 - 40	d_i : (3.927 - 4.255 - 1.502)
3	22.5 - 35 - 22.5	d_i : (3.897 - 2.503 - 1.956 - 1.502)
4	20 - 20 - 20 - 20	d_i : (4.0 - 2.503 - 4.131 - 2.51 - 1.322)
5	15 - 15 - 20 - 15 - 15	d_i : (4.146 - 2.503 - 2.736 - 4.46 - 4.7 - 1.503)
6	12.50 - 12.50 - 15 - 15 - 12.50 - 12.50	d_i : (4.269 - 2.51 - 2.093 - 4.7 - 2.531 - 2.51 - 1.429)

6.2 Examination of Bridge Hydraulic Computations

The bridge hydraulic calculations through the bridge opening are the major computational components of the framework, AIROB. For each optimization case, the water surface profile calculations are carried out from the downstream cross-section (cross-section 0 in Figure 6.2) to the approach cross-section (cross-section 1 in Figure 6.2) for any arrangement of the piers within the bridge cross-section. The “momentum approach” is utilized for the calculation of the hydraulic information at each cross-section, of which the details are represented in Chapter-2. The boundary condition for the calculations is downstream water surface elevation of +6.347 m which corresponds to a uniform flow with a bed slope of 0.0001 as seen in Table 6.4. The detailed hydraulic information for each cross-section is tabulated in Tables 6.4 through 6.7 with reference to Figure 6.2.

Table 6.4. Hydraulic information for the cross-section 0.

Hydraulic Parameters	Average	Left Flood Plain	Main Channel	Right Flood Plain
Discharge, Q (m^3/s)	200	34.888	156.359	8.759
Water surface elevation, EL_w (m)	+6.347	+6.347	+6.347	+6.347
Maximum flow depth, y (m)	5.447	2.447	5.447	0.947
Flow Area, A_m (m^2)	242.933	70.511	144.66	27.762
Average Flow velocity, u (m/s)	0.823	0.495	1.081	0.316
Hydraulic depth, D (m)	2.722	2.380	4.822	0.937
Thalweg elevation, EL_{min} (m)	+0.9	+3.9	+0.9	+5.4
Energy Head, EGL (m)	+6.39	+6.36	+6.407	+6.352
Hydraulic Head, HGL (m)	+6.347	+6.347	+6.347	+6.347
Velocity Head (m)	0.044	0.012	0.055	0.005
Froude Number, Fr	0.159	0.102	0.157	0.104
Conveyance, K (m^3/s)	20003.74	3488.82	15638.83	876.09
Wetted perimeter, P (m)	93.636	30.941	32.558	30.138
Hydraulic radius, R (m)	2.594	2.278	4.443	0.921
Friction Slope, S_f	0.0001	0.0001	0.0001	0.0001
Top width, T (m)	89.262	29.631	30.0	29.631
Energy correction coefficient, α	1.266			
Momentum correction coefficient, β	1.096			

Table 6.5. Hydraulic information for the cross-section 1.

Hydraulic Parameters	Average	Left Flood Plain	Main Channel	Right Flood Plain
Discharge, Q (m^3/s)	200	34.33	157.74	7.927
Water surface elevation, EL_w (m)	+6.346	+6.346	+6.346	+6.346
Maximum flow depth, y (m)	5.373	2.373	5.373	0.873
Flow Area, A_m (m^2)	223.613	68.333	142.452	25.583
Average Flow velocity, u (m/s)	0.894	0.502	1.107	0.310
Hydraulic depth, D (m)	2.508	2.309	4.748	0.865
Thalweg elevation, EL_{min} (m)	+0.973	+3.973	+0.973	+5.473
Energy Head, EGL (m)	+6.397	+6.359	+6.408	+6.351
Hydraulic Head, HGL (m)	+6.346	+6.346	+6.346	+6.346
Velocity Head (m)	0.052	0.013	0.063	0.005
Froude Number, Fr	0.180	0.106	0.162	0.106
Conveyance, K (m^3/s)	19326.52	3317.35	15243.13	766.034
Wetted perimeter, P (m)	82.557	30.852	33.56	30.05
Hydraulic radius, R (m)	2.709	2.215	4.375	0.851
Friction Slope, S_f	0.000107	0.000107	0.000107	0.000107
Top width, T (m)	89.164	29.582	30.0	29.582
Energy correction coefficient, α	1.267			
Momentum correction coefficient, β	1.097			

Table 6.6. Hydraulic information for the cross-section 2.

Hydraulic Parameters	Average	Left Flood Plain	Main Channel	Right Flood Plain
Discharge, Q (m^3/s)	200	34.40	157.57	8.03
Water surface elevation, EL_w (m)	+6.423	+6.423	+6.423	+6.423
Maximum flow depth, y (m)	5.383	2.383	5.383	0.883
Flow Area, A_m (m^2)	224.363	68.604	142.726	25.853
Average Flow velocity, u (m/s)	0.891	0.501	1.104	0.311
Hydraulic depth, D (m)	2.516	2.319	4.758	0.874
Thalweg elevation, EL_{min} (m)	+1.040	+4.040	+1.040	+5.540
Energy Head, EGL (m)	+6.475	+6.436	+6.486	+6.482
Hydraulic Head, HGL (m)	+6.423	+6.423	+6.423	+6.423
Velocity Head (m)	0.0513	0.0128	0.0621	0.005
Froude Number, Fr	0.179	0.105	0.162	0.106
Conveyance, K (m^3/s)	19409.66	3338.44	15291.87	779.346
Wetted perimeter, P (m)	82.557	30.864	32.557	30.061
Hydraulic radius, R (m)	2.718	2.222	4.384	0.86
Friction Slope, S_f	0.000106	0.000106	0.000106	0.000106
Top width, T (m)	89.178	29.589	30	29.589
Energy correction coefficient, α	1.266			
Momentum correction coefficient, β	1.096			

Table 6.7. Hydraulic information for the cross-section 3.

Hydraulic Parameters	Average	Left Flood Plain	Main Channel	Right Flood Plain
Discharge, Q (m^3/s)	200	34.023	158.50	7.481
Water surface elevation, EL_w (m)	+6.434	+6.434	+6.434	+6.434
Maximum flow depth, y (m)	+1.100	+4.100	+1.100	+5.600
Flow Area, A_m (m^2)	232.855	67.168	141.27	24.418
Average Flow velocity, u (m/s)	0.859	0.051	1.122	0.306
Hydraulic depth, D (m)	2.613	2.273	4.709	0.826
Thalweg elevation, EL_{min} (m)	+1.100	+4.100	+1.100	+5.600
Energy Head, EGL (m)	+6.482	+6.448	+6.498	+6.439
Hydraulic Head, HGL (m)	+6.434	+6.434	+6.434	+6.434
Velocity Head (m)	0.048	0.013	0.064	0.005
Froude Number, Fr	0.17	0.107	0.165	0.108
Conveyance, K (m^3/s)	18969.22	3226.90	15032.81	709.50
Wetted perimeter, P (m)	93.365	30.805	32.558	30
Hydraulic radius, R (m)	2.494	2.180	4.340	0.813
Friction Slope, S_f	0.000111	0.000111	0.000111	0.000111
Top width, T (m)	89.112	29.556	30	29.556
Energy correction coefficient, α	1.268			
Momentum correction coefficient, β	1.097			

The summarized information about the conservation of energy between the cross-sections 0 and 1 (see Figure 6.2), and between the cross-sections 2 and 3 (see Figure 6.2) are given in Table 6.8, whereas, the details of the conservation of momentum between cross-sections 1 and 2 (see Figure 6.2) are given in Table 6.9. The illustration of the water surface profile results are presented in Figure 6.5.

Table 6.8. Hydraulic information about conservation of energy calculations.

Conservation of Energy	Between cross-sections 0 and 1	Between cross-sections 2 and 3
Contraction / Expansion loss, HL_{ce} (m)	0.00397	0.00108
Friction loss, HL_f (m)	0.0066	0.0049
Total energy loss, HL_e (m)	0.0026	0.0059

Table 6.9. Hydraulic information about conservation of momentum calculations.

Conservation of Momentum (Between cross-sections 1 and 2)	Hydraulic Forces
Total Hydraulic Force on cross-section 1, F_{ds} (kN)	468,188.386
Total Hydraulic Force on cross-section 2, F_{us} (kN)	470,777.412
Resisting force by piers and abutments, F_R (kN)	1,799.536
Wall friction force between cross-sections, F_f (kN)	857.941

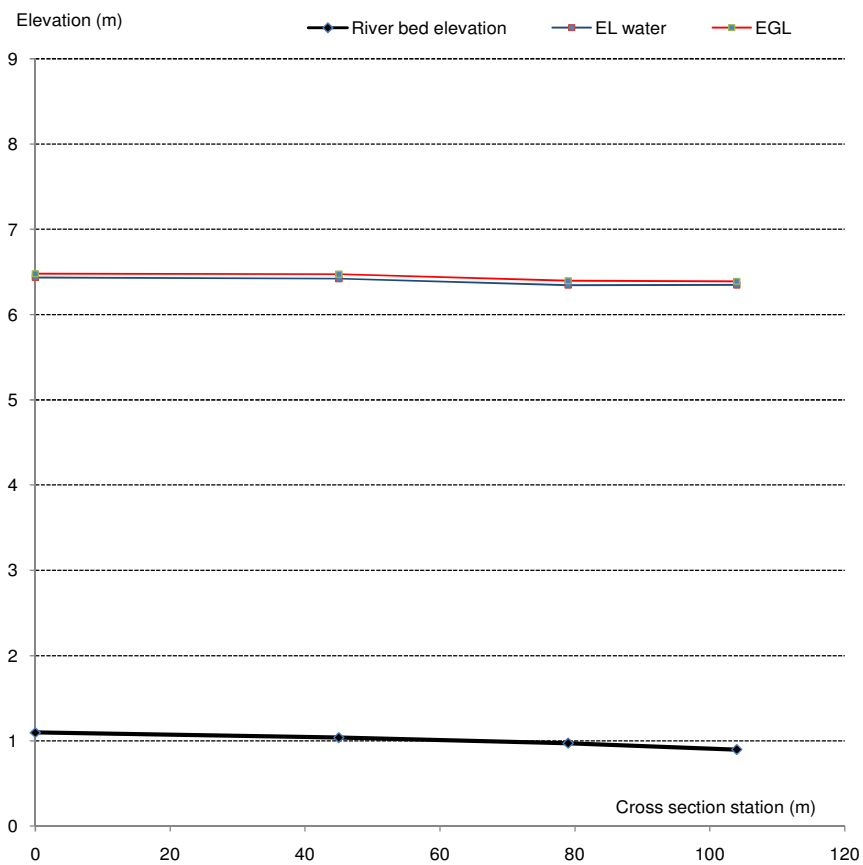


Figure 6.5. Water surface profile through the bridge for the application problem.

6.3 Examination of Genetic Algorithm Results

The application problem is solved by using GA, which is the default optimization method of AIROB framework. In this application, the major GA related input parameters are as follows:

- Each decision variable is binary encoded with 8 bits, and a population of 40 chromosomes is chosen.
- “Roulette-wheel selection” is used as the default selection strategy, along with the “elitism” approach in order not to lose the best solution through the successive generations.
- Crossover rate is taken as 0.80, whereas mutation rate is chosen as 0.1.
- The range for footing depth is taken as 0 to 9.0 meters, whereas the range for the span lengths is taken as 12.50 to 40.0 meters.

These entire GA related input data are taken as constant for all the optimization calculations of this application. Tables 6.10 and 6.11 shows the initial and successive populations for $N_s=3$ with probabilistic constraints. Each row in these tables presents an alternative solution within the search space of the problem, which are sorted from the one having highest fitness to the lowest fitness (see Tables 6.10 and 6.11).

In this problem, binary encoding is used to represent the decision variables in GA processes. Each decision variable is encoded by 8 bits, which can hold $2^8=256$ discrete values within the range of the corresponding decision variable. The total number of decision variables is equal to $2N_s+1$. Thus, if it is multiplied by the number of bits used in encoding, which is equal to 8 in this problem, the total length of a chromosome is found.

Table 6.10. Initial GA population of the application problem
(For $N_s=3$ and reliability-based constraints).

No	Chromosome (binary coded)	S_p-3 (m)	S_p-2 (m)	S_p-1 (m)	d_f (m)	d_f (m)	d_f (m)	d_f (m)	Fitness
					(P-2)	(P-1)	(A-2)	(A-1)	
0	10000010110011110101100001100110101001100101000010001100	26.52	34.82	21.99	3.60	5.86	2.82	4.94	4.44E-07
1	1110010010000011011111001000001101101000101111010111111	37.09	26.63	26.09	2.29	6.35	3.32	6.74	6.49E-08
2	100011101000011101000111110000110010100001011110000010	27.92	19.73	30.08	7.94	7.13	0.81	4.59	2.44E-08
3	0100100010101101010100001010110101011000111111111111	20.27	31.16	21.13	6.11	3.21	5.05	9.00	1.80E-08
4	1101100101000000100101000010011100001111001011111000010	35.90	19.40	28.46	1.38	0.53	1.66	6.85	1.07E-08
5	00000110000110001100111001110101110000110101001001101100	13.15	15.09	34.72	4.13	6.88	2.89	3.81	8.69E-09
6	100011001010011101001100010010010011001101111101101100	27.60	30.51	20.70	2.58	2.68	7.87	3.81	8.06E-09
7	0111100011110110110011110011101111011100011110000011100	25.44	39.14	23.61	5.54	8.40	2.12	0.99	6.90E-09
8	1011111110100110111110100001110101101000011011100011101	33.10	35.26	25.98	0.49	6.35	1.94	1.02	5.44E-09
9	10101000010111010111101100001001001101001101010000001011	30.62	22.53	25.77	0.32	1.84	7.48	0.39	5.39E-09
10	0000101111111100001110000011111101010111111001000010111	13.69	39.89	15.52	1.09	6.04	8.54	0.81	4.85E-09
11	01111000010011111100000001010101000001110000000101001010	25.44	21.02	33.21	3.00	0.25	0.04	2.61	4.47E-09
12	10001011011001101011100100010111001010100110000110110000	27.49	23.50	32.45	0.81	1.48	3.42	6.21	4.18E-09
13	001101000001011011011100110001001000101111111100000001	18.11	14.87	36.23	6.92	4.91	9.00	0.04	3.92E-09
14	1101110001001111010110101010111001010101001100100100111	36.23	21.02	22.21	6.14	3.00	5.40	1.38	3.82E-09
15	000011000001011101111100101110101011110111101101010101	13.79	14.98	25.87	6.57	6.67	8.72	3.00	3.68E-09
16	101000110001110101101011100110111000110000101100000001	30.08	15.63	24.04	5.86	8.01	0.39	0.04	3.54E-09
17	10010001110100101000001000010110011100111100100101010111	28.14	35.15	26.52	0.78	4.06	7.09	3.07	3.42E-09
18	000011011010111100011111100001010010101001100010010110	13.90	31.37	15.84	6.85	5.26	5.37	5.29	3.28E-09
19	11000100011101111100001001001110000001011011101110011	33.64	25.33	33.42	2.58	6.78	6.46	4.06	3.24E-09
20	00110100000001100111111000001100110001101001000111101	18.11	13.15	26.09	0.21	3.11	7.41	2.15	3.14E-09
21	00101101001000011111000110110001110110100000100001110001	17.35	16.06	38.49	6.25	7.69	0.28	3.99	3.13E-09
22	01000101001111100100000111000101101100011010010100101011	19.94	19.19	19.51	6.95	6.25	5.82	1.52	2.51E-09
23	00110000011100010001110011101000001001110011110001100010	17.68	24.69	15.52	8.19	1.38	2.12	3.46	2.42E-09
24	0101110110100110000011011100010010110101000100110101011	22.53	30.40	13.90	6.92	6.39	4.84	6.04	2.36E-09
25	01111101100000000001010100001100001000110101101101010101	26.09	33.21	13.58	4.73	0.60	6.11	6.11	2.32E-09
26	110110101110110100011000001010000000111111111010101111	36.01	38.17	27.60	0.71	0.18	8.97	6.18	2.29E-09
27	00010001010111100010010001000000000011110010011011000101	14.33	22.64	16.38	2.26	0.53	1.34	6.95	2.19E-09
28	10001000000001110101101000010001101001011001111010110011	27.17	13.26	22.21	0.60	5.82	5.58	6.32	2.14E-09
29	00000001011100011101101000100001101001011100010111100101	12.61	24.69	36.01	1.17	5.82	6.95	8.08	2.12E-09
30	00111000001011110010001101000001101000010011010001100100	18.54	17.57	16.28	2.29	5.68	1.84	3.53	2.01E-09
31	0101110100111001001111001001100010000111101001011010000	22.53	18.65	19.19	2.68	2.37	7.41	7.34	1.97E-09
32	01010011001010100001011011001001111100100001001110100010	21.45	17.03	14.87	7.09	8.54	0.67	5.72	1.75E-09
33	00100100110011111101100000001100011101110000011100100101	16.38	34.82	35.79	0.42	4.20	0.25	1.31	1.72E-09
34	10011100010001000000011100100001110000010011011011000001	29.32	19.83	13.26	1.17	6.81	1.91	6.81	1.70E-09
35	01111010000010100011111101111001001010001111101011001111	25.66	13.58	19.29	4.27	1.41	8.82	7.31	1.62E-09
36	10010110001010000000110000001000101110011011010100100100	28.68	16.81	13.79	0.28	6.53	6.39	1.27	1.59E-09
37	10100001000011110000101000011111000111101011000100100011	29.86	14.12	13.58	1.09	1.06	6.25	1.24	1.57E-09
38	10000001000001110001011111110111110000101011011011100	26.41	13.26	14.98	8.86	8.47	6.11	7.77	1.26E-09
39	0011011111010111101101111000100011110001011101111010110	18.43	36.12	36.12	6.92	4.24	6.60	7.55	1.19E-09

Table 6.11. GA population after the first generation
(for $N_s=3$ and reliability-based constraints).

No	Chromosome (binary coded)	S_p-3 (m)	S_p-2 (m)	S_p-1 (m)	d_f (m)	d_f (m)	d_f (m)	d_f (m)	Fitness
					(P-2)	(P-1)	(A-2)	(A-1)	
0	1000010110011110101100001100110100001100101000010001100	26.52	34.82	21.99	3.60	4.73	2.82	4.94	5.05E-07
1	10000010110011110101100001100110101001100101000010001111	26.52	34.82	21.99	3.60	5.86	2.82	5.05	5.02E-07
2	10000010110011110101100001100110101001100101000010111111	26.52	34.82	21.99	3.60	5.86	2.82	6.74	4.85E-07
3	10001010110011110101100001100110101001000101111010111111	27.38	34.82	21.99	3.60	5.79	3.32	6.74	4.72E-07
4	11100100100000110111111001100110101001100101000010001100	37.09	26.63	26.09	3.60	5.86	2.82	4.94	4.53E-07
5	10000010110011110101100001100110101001100101000010001100	26.52	34.82	21.99	3.60	5.86	2.82	4.94	4.44E-07
6	10000010110011110101100001100110101001100101000010001100	26.52	34.82	21.99	3.60	5.86	2.82	4.94	4.44E-07
7	10000010110011110101100001100110101001100101000010001100	26.52	34.82	21.99	3.60	5.86	2.82	4.94	4.44E-07
8	10000010110011110101100001100110101001100101000010001100	26.52	34.82	21.99	3.60	5.86	2.82	4.94	4.44E-07
9	10000010110011110101100001100110101001100101000010001100	26.52	34.82	21.99	3.60	5.86	2.82	4.94	4.44E-07
10	10000010110011110101100001100110101001100101000010001100	26.52	34.82	21.99	3.60	5.86	2.82	4.94	4.44E-07
11	10000010110011110101100001100110101001100101000010001100	26.52	34.82	21.99	3.60	5.86	2.82	4.94	4.44E-07
12	10000010110011110101100001100110101001100101000010001100	26.52	34.82	21.99	3.60	5.86	2.82	4.94	4.44E-07
13	10000010110011110101100001100110101001100101000010001100	26.52	34.82	21.99	3.60	5.86	2.82	4.94	4.44E-07
14	10000010110011110101100001100110101001100101000010001100	26.52	34.82	21.99	3.60	5.86	2.82	4.94	4.44E-07
15	10000010110011110101100001100110101001100101000010001100	26.52	34.82	21.99	3.60	5.86	2.82	4.94	4.44E-07
16	01100010110011110101100001100110101001100101000010001100	23.07	34.82	21.99	3.60	5.86	2.82	4.94	4.44E-07
17	10000010110011110101100001100110101001100101000010001100	26.52	34.82	21.99	3.60	5.86	2.82	4.94	4.44E-07
18	10000010110011110101100001100110101001100101000010001100	26.52	34.82	21.99	3.60	5.86	2.82	4.94	4.44E-07
19	10000010110011110101100001100110101001100101000010001100	26.52	34.82	21.99	3.60	5.86	2.82	4.94	4.44E-07
20	10000010110011110101100001100110101001100101000010001100	26.52	34.82	21.99	3.60	5.86	2.82	4.94	4.44E-07
21	10000010110011110101100001100110101001100101000010001100	26.52	34.82	21.99	3.60	5.86	2.82	4.94	4.44E-07
22	10000010110011110101100001100110101001100101000010001100	26.52	34.82	21.99	3.60	5.86	2.82	4.94	4.44E-07
23	10000010110011110101100001100110101001100101000010001100	26.52	34.82	21.99	3.60	5.86	2.82	4.94	4.44E-07
24	10000010110011110101100001100110101001100101000010001100	26.52	34.82	21.99	3.60	5.86	2.82	4.94	4.44E-07
25	(10000010110011110101100001100110101001100101000010001100)	26.52	34.82	21.99	3.60	5.86	2.82	4.94	4.44E-07
26	01110010110011110101100001100110101001100101000010001100	24.79	34.82	21.99	3.60	5.86	2.82	4.94	4.44E-07
27	10000010110011110101100001100110101001100101010010001100	26.52	34.82	21.99	3.60	5.86	2.97	4.94	4.37E-07
28	1110010010000011011111001000001101101100101000010001100	37.09	26.63	26.09	2.29	6.42	2.82	4.94	6.85E-08
29	1110010010000011011111001000001101101000101111010001100	37.09	26.63	26.09	2.29	6.35	3.32	4.94	6.60E-08
30	1000001011001111010110000100000110110100010111101011111	26.52	34.82	21.99	2.29	6.35	3.32	6.74	6.57E-08
31	(111001001000001101111100100000110110100010111101011111)	37.09	26.63	26.09	2.29	6.35	3.32	6.74	6.49E-08
32	(10001111010000111010001111100001110010100001011110000010)	27.92	19.73	30.08	7.94	7.13	0.81	4.59	2.44E-08
33	(010010001010110101010000101011010101011000111111111111)	20.27	31.16	21.13	6.11	3.21	5.05	9.00	1.80E-08
34	100000101100001101111100100000110110100010111101011111	26.52	33.53	26.09	2.29	6.35	3.32	6.74	9.65E-09
35	11100100100011110101100001100110101001100101000010001100	37.09	27.92	21.99	3.60	5.86	2.82	4.94	8.70E-09
36	01111000010011111100000001010101000001110000000101001010	25.44	21.02	33.21	3.00	0.25	0.04	2.61	4.47E-09
37	10011000010011111100000001010101000001100000000101001010	28.89	21.02	33.21	3.00	0.21	0.04	2.61	4.46E-09
38	0111101000001010001111101111001001010001111101011001100	25.66	13.58	19.29	4.27	1.41	8.82	7.20	1.62E-09
39	1000101000001010001111101111001001010001111101011001111	27.38	13.58	19.29	4.27	1.41	8.82	7.31	1.62E-09

Table 6.10 shows the initial population for $N_s=3$. Thus, a chromosome consists of 56 bits. If the first row of Table 6.10 is examined, the structure of the chromosomes can be observed in Figure 6.6.

DECISION VARIABLES						
S_p-3 (m)	S_p-2 (m)	S_p-1 (m)	d_f (P-2) (m)	d_f (P-1) (m)	d_f (A-2) (m)	d_f (A-1) (m)
10000010	11001111	01011000	01100110	10100110	01010000	10001100
↓	⇓	↓	⇓	↓	⇓	↓
26.52	34.82	21.99	3.60	5.86	2.82	4.94

S_p : span length

P-1: pier-1

A-1: abutment-1

d_f : depth of footing

P-2: pier-2

A-2: abutment-2

(Decision variables are ordered from right to left in the chromosomes.)

Figure 6.6. Chromosome structure depicting decision variables.

The value of a decision variable in the search space is required to be translated from its binary representation. Although there are different types of conversion formulas as options in the framework, AIROB uses the following conversion equation as default:

$$X = X_{\min} + \frac{(X_{\max} - X_{\min})}{2^b - 1} X_b \quad (6.1)$$

where, X is the value of the decision variable. X_{\min} and X_{\max} are the lower and upper bounds of the range of the decision variable, respectively. The decimal value of the decision variable in binary format is denoted by X_b and the number of encoding bits is represented as b .

As an example to examine the structure of the chromosomes and the containing decision variables, the first decision variable of the problem is checked as follows. The depth of footing for abutment-1 is represented by the first decision variable in the chromosomes (see Figure 6.6). Thus, with reference to Figure 6.6, $X_b=(10001100)_2 = 140$. The input data for the range of footing depths are, $X_{min}=0$, and $X_{max}=9.0$ m. According to Equation (6.1), the corresponding value of the decision variable is calculated as 4.94 m for 8 bit binary coding, $b=8$.

After the encoding of the variables is completed, the next step is to generate an initial population randomly as seen in Table 6.10. In the beginning of the generations, there is a high variability among the alternatives, whereas each generation constricts the alternatives in the population in order to converge to a solution close to the exact optimum solution of the problem. This situation can also be verified by the increase of average fitness value of the population in each generation. While the initial population has an average fitness value of 1.69E-08, the average fitness of the successive generation increases up to 3.24E-07 due to the selection, crossover and mutation operations in GA.

In Table 6.11, the chromosomes in bold font indicates the ones on which a crossover operation is applied, whereas the italic font refers to the application of the mutation operation. In this context, a chromosome in both bold and italic font means that a crossover operation followed by a mutation operation is performed after the selection. Table 6.11 shows that 32 offspring are created as a result of crossover operations. Mutation operation is applied to four chromosomes, which is 10% of the population size, which is equal to the mutation rate. These inter-generations information also confirms the proper execution of the GA procedures. Table 6.11 shows that crossover operation yields a number of identical offsprings. This situation can be avoided if the related option is selected in the GA engine of AIROB. However, in this problem, the duplications of the offsprings are permitted to exist.

The effect of elitism approach can also be seen in Table 6.11 such that a certain portion of the best chromosomes of the preceding generation is survived to the current generation. The chromosomes in parenthesis in Table 6.11 specify the

best chromosomes of the previous generation replicated by the “elitism” approach. In this application, best four chromosomes of the previous population are directly survived to the next generation. Thus, it can be observed that the best four chromosomes of the initial population are also present in the next generation according to Tables 6.11 and 6.12.

As the number of generations increases, both the average and maximum fitnesses in the population shows an increasing trend as seen in Figure 6.7. As it is expected, after a certain number of iterations, average fitness values fluctuate around an equilibrium value as the population converges to a minimum point. However, the maximum fitness value monotonically increases by the effect of the elitism strategy. As a result, an optimum point is achieved at generation no, 250 as seen in Figure 6.6. The corresponding final converged population can also be examined in Table 6.12.

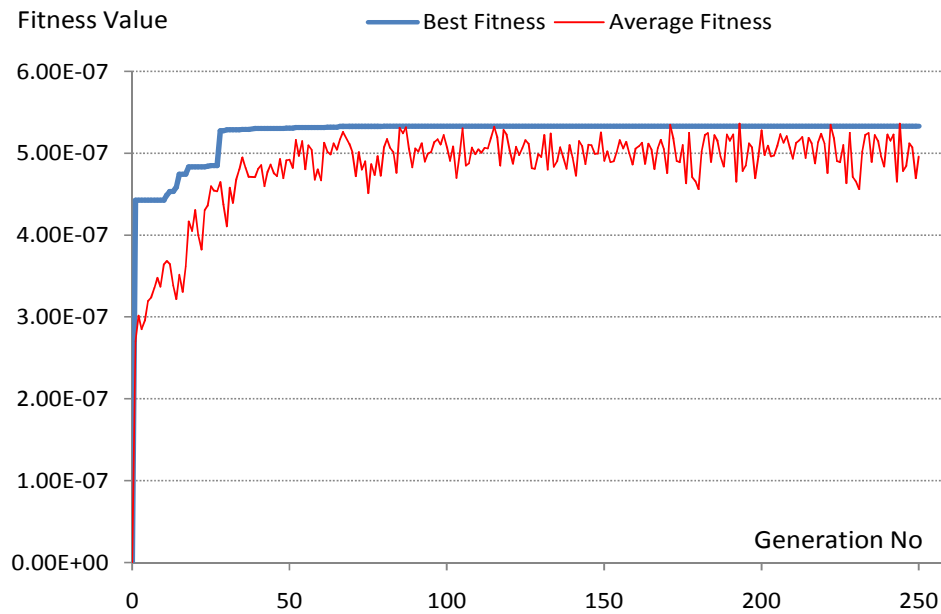


Figure 6.7. Variation of average and maximum fitness values at each generation.

6.3.1 Sensitivity Analysis of Genetic Algorithm Parameters

A sensitivity analysis is performed on the application problem in order to assess the effects of the GA parameters on the optimized results. For this purpose, the application problem with the optimal span arrangement is preferred as the reference problem of the sensitivity analysis. Thus, the reference problem has three spans and the constraints are conducted as deterministic due to their faster execution performance.

Crossover rate and type, mutation rate, and population size are chosen to be the parameters of GA, of which their effects are to be observed. For this purpose, the developed software framework, AIROB was run for a number of times, by changing the value of the parameter concerned and the statistical data of these solutions are obtained, such as the mean, maximum and minimum fitness values given by the software. This process is repeated for each of the aforementioned parameters of GA. Based on these statistical data, the effects of these parameters on the optimization results are assessed. The obtained graphical results are shown in Figures 6.8 to 6.11.

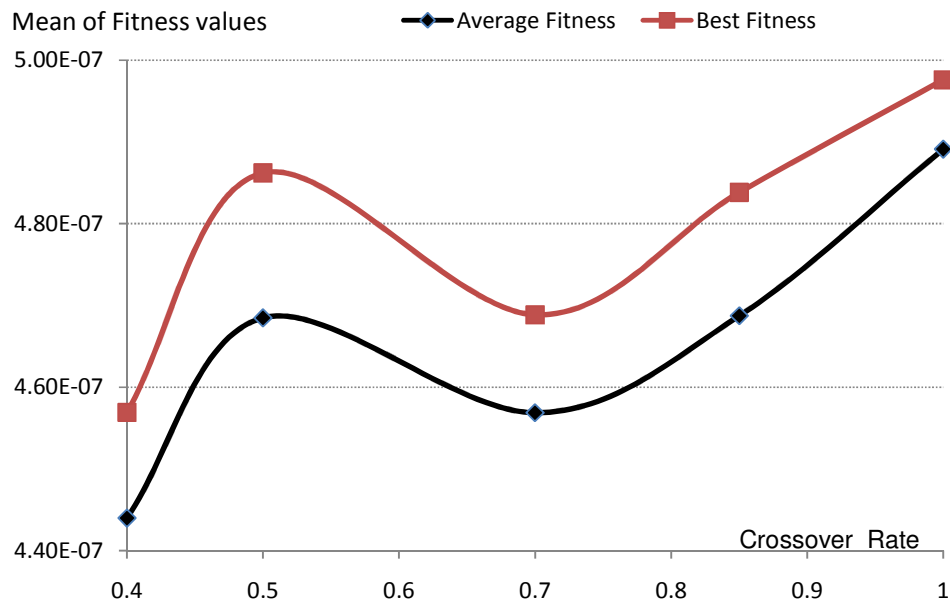


Figure 6.8. The effect of the crossover rate on the optimization results.

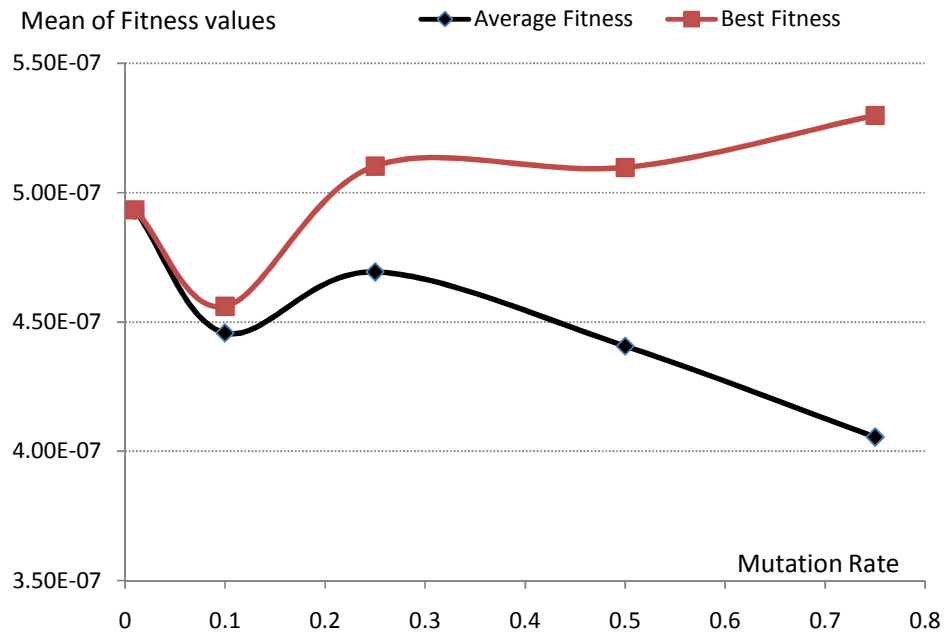


Figure 6.9. The effect of the mutation rate on the optimization results.

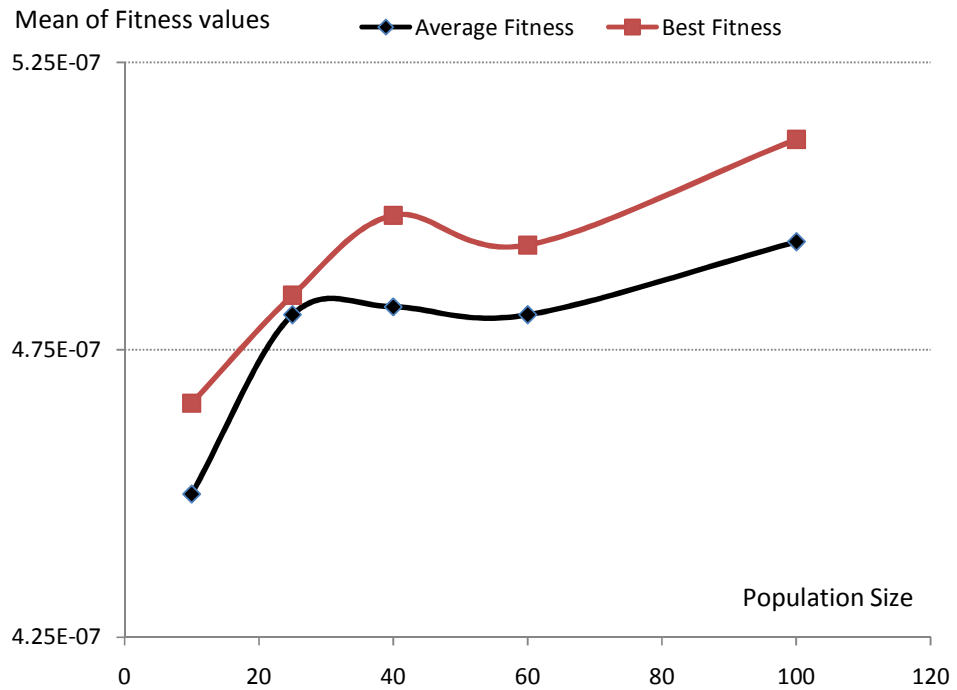


Figure 6.10. The effect of the population size on the optimization results.

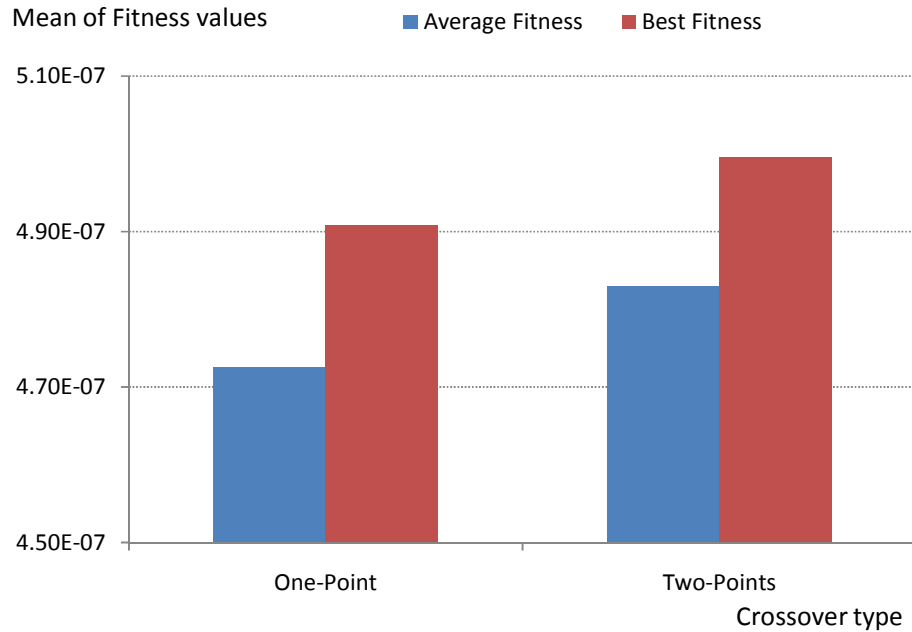


Figure 6.11. The effect of the crossover type size on the optimization results.

An acceptable statistical sample for a certain value of GA parameter is gathered by executing the problem 20 times. This process is done due to the probabilistic nature of GA, which gives different results at each execution. Thus, the statistical sample consists of the average and best fitness values of the trials for each parameter value. Accordingly, the graphs are constructed by taking the dependent variable as the concerned GA parameter value and the independent variable as the corresponding mean of the fitness values, which are the mean of the statistical sample gathered by the trials. Thus, the mean values of both average and best fitness of the population which corresponds to the parameter values are specified in Figures 6.8 to 6.11. As a result, the variation of the fitness information of the converged population with respect to each GA parameter is achieved. The decisions on the value of the parameters are mainly taken according to the average fitness value of the population, since average values reflect the behavior in a more expected fashion. Brief discussions about the results of this sensitivity analysis are as follows:

Figure 6.8 shows that after a crossover rate, 0.7 the fitness values tends to increase. Therefore, 70% should be taken as a minimum crossover rate for this type of problem. When the crossover rate increases beyond this value, fitness values also increases, however crossover operation is a costly operation in terms of computer's CPU performance. Therefore, it seems that a cross over rate of 0.85 can be considered as an optimal value as seen in Figure 6.8

Sensitivity analysis results show that a relatively high value of mutation rate achieve better results. After a mutation rate of 0.25, average fatnesses tend to decrease as seen in Figure 6.9. Thus, an optimal decision for the value of mutation rate seems to be between 0.20 and 0.30.

According to Figure 6.10, a population of 30 chromosomes indicates that although larger population sizes product better fitness results, the effect of population size on CPU performance is very much, therefore it seems unreasonable to select a population size greater than 50.

Finally, two points crossover operator indicates better results as seen in Figure 6.11. Thus, it is preferable to apply crossover operations of two-points-sliced type in this type of problems.

As a result of the discussions above, the proposed intervals for the values of GA parameters for a similar problem can be outlined as follows:

- Crossover rate = 0.80 – 0.90
- Crossover type = Sliced from two points,
- Mutation rate = 0.20 – 0.30
- Population size = 30 – 50

6.3.2 Sensitivity Analysis of Penalty Function Coefficients

In the scope of this study, penalty functions were used for the constraint handling method of which its basic form is given in Equation (5.13). The penalty function simply adds an extra cost to the total cost of the bridge when the constraints are violated. The amount of this penalty cost depends on the violation of each constraint; therefore the violation amount of each constraint is multiplied by a coefficient in order to find the best form of the penalty function in terms of convergence performance and achieved minimum cost.

For this purpose, the penalty functions are assessed in two forms. The first form of these employs directly the violation amounts, whereas the second form employs a more generic way by using violation percentages.

A violation percentage of a constraint, perc_i , is defined as follows:

$$\text{perc}_i = \frac{\delta_i}{Cv_i} \quad (6.2)$$

where δ_i is the violation of the constraint- i , where Cv_i is the limiting value of the constraint. In this manner violation amounts are normalized, put into non-dimensional form.

For this example problem, firstly the direct violation amounts are used and found that for geometry constraint (see Equation 5.5), the proposed value of the coefficient is 0.05 and for the rest of the constraints, 0.04. But, all constraints should have the coefficients in the range of 0.03 and 0.06. Outside this range, the GA cannot converge within the trials of 500 generations. However, recommended values tend to converge within the first 100 iterations and give well optimized results. It should be noted that these values are tried for this example and for any other example it may be needed to perform a different sensitivity analysis for the coefficient values.

If the penalty function is used in the form of violation percentages, it is much more generic and give consistent results for the problems different than the application example also. It is observed that for the geometry constraint, the corresponding coefficient should be in the range of 5 to 10, whereas the remaining constraints have the coefficient value of 1.0.

6.4 Examination of Reliability Calculations

AIROB performs the reliability-based calculations by utilizing Monte-Carlo simulation method as described in Chapter 5. As a result, for each depth of footing, a corresponding failure probability is calculated. In this application, when the probability failure is below 0.001, the scouring constraints are satisfied. The variation of probability failure with respect to the depth of footing for $N_s=3$ is illustrated in Figures 6.12 and 6.13.

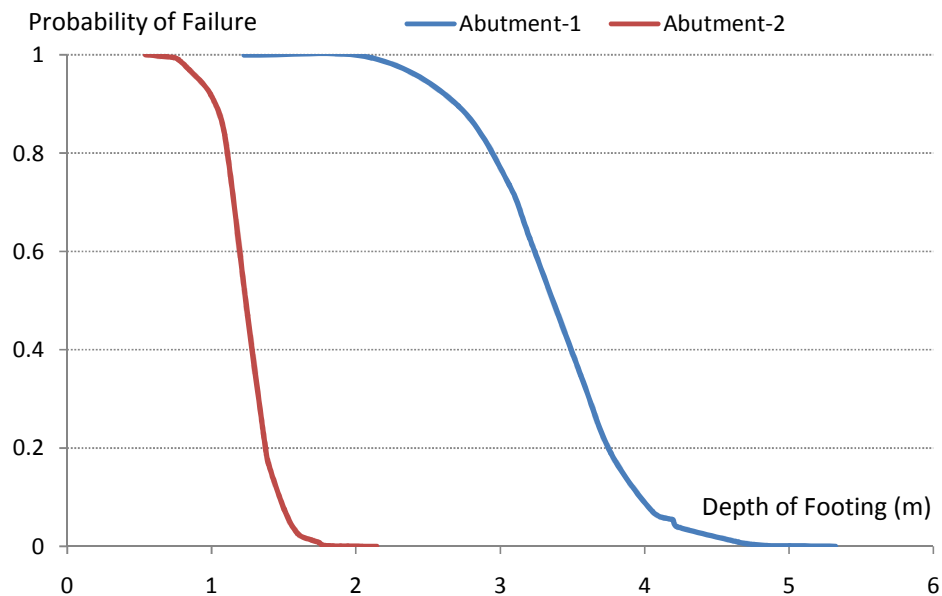


Figure 6.12. Variation of failure probability of abutment footings with respect to the footing depth ($N_s=3$).

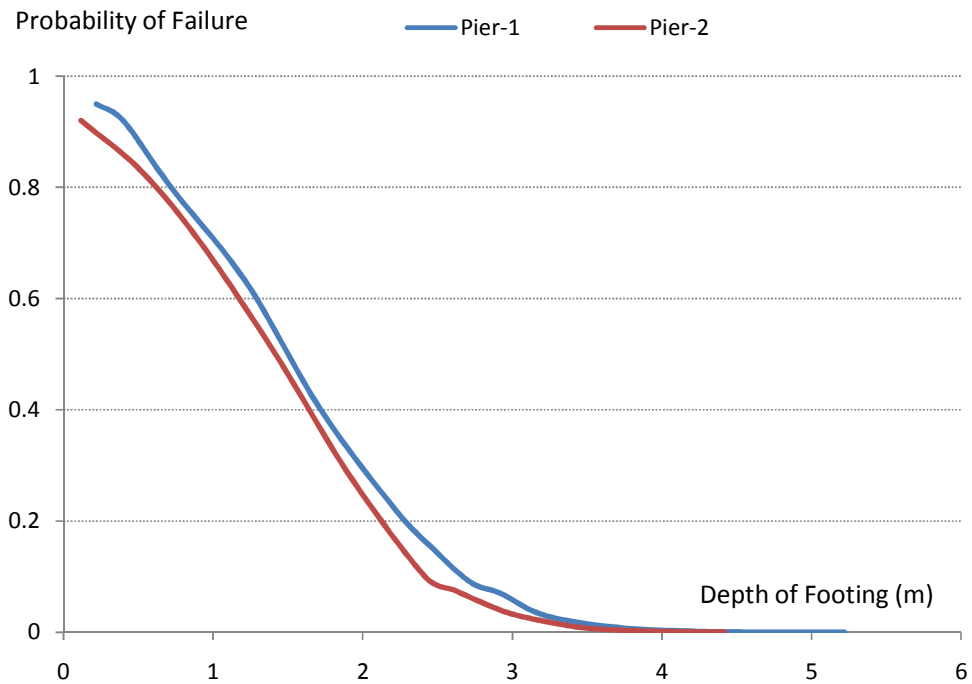


Figure 6.13. Variation of failure probability of pier footings with respect to the footing depth . ($N_s=3$).

As it is seen in Figure 6.12, for abutment-1 the required depth of footings are greater than abutment-2 due to adverse hydraulic conditions that cause deeper scours. It is observed that; for abutment-1 the depth of footing converges to 5 m with nearly zero failure probability, whereas for abutment-2 it is close to 2 m. Similar situation exist for the piers. However in this case, the converged footing depth for both piers is close to each other, approximately 4.5 m, which corresponds to almost zero failure probability. The detailed results are presented in Table 6.2. As it is observed from Table 6.2, the failure probabilities are very close to 0.001, which is the desired limiting value for both abutments and piers. The corresponding depths of footings are also indicated in Table 6.2.

CHAPTER 7

DISCUSSION, CONCLUSIONS AND RECOMMENDATIONS

Optimum design of river bridges by the use of innovative artificial intelligence techniques has been carried out in this study. The study proposes a new methodology for preliminary design of bridges by taking advantage of the state of the art computational techniques in the literature. In this context, the proposed methodology was solidified by introducing a computing framework from which a computer software, AIROB, for the applicability of the methodology is developed.

Integration of the artificial intelligence techniques are one of the prominent features of this study. In this context, the major rationale for the utilization of ANN techniques in this study can be understood by examining the implementation issues of the optimization engine of the framework. An efficient implementation of the optimization algorithm of this study requires avoiding time consuming conventional structural design computations. Besides, inclusion of conventional structural analysis and design calculations imposes a huge amount of implementation workload, which would be unreasonable for this kind of study giving the emphasis to hydraulic design. Thus, it is advantageous to find an alternative approach for handling the structural design computations. As a result, utilization of ANN models are found to be a reasonable solution to eliminate the conventional structural design processes. Capturing intrinsic design conventions by real design projects is also another advantage of employing an ANN strategy. For the optimization part of the study, usage of ANN models for cost estimation imposes to select a more generic technique such that the non-linear forms of ANN equations are not problematic to deal with. Besides, computational overburden of calculating reliability values by Monte-Carlo simulation along with

bridge hydraulic computations having iterative-based solutions leads to selection of a heuristic based search technique, GA, as the optimization technique.

Built on the aforementioned justifications for the integration of AI approaches, this study encompasses various areas of engineering and scientific disciplines. This broad structure of the study enables to perceive the corresponding consequences from different viewpoints. Therefore, the outcomes of this study should be examined from two perspectives basically; the first perspective is bridge engineering point of view, whereas the other one is a concretized integration of artificial intelligence techniques into civil engineering discipline. Thus, the results of this study should be discussed along these two different paths of thinking.

The study assembles different bridge engineering aspects into a unified design basis. Structural and geotechnical design tasks are handled by a statistical based approach, artificial neural networks, while hydraulic design is incorporated into the model by conventional analytical based design methods reinforced by included reliability techniques. Therefore, various design philosophies are also inherently embedded into the proposed methodology and the resulting computing framework. The extensive usages of these various pioneering engineering design approaches highlight the power of the methodology and the corresponding computing framework, AIROB.

From a bridge engineering perspective, which is more practical point of view, the study mainly ambitions to analyze the hydraulic – structure interaction in bridges crossing rivers. Interaction of structural and hydraulics design aspects is one of the parts of bridge engineering in which detailed researches are lacking. Therefore, simulation software was constructed in order to investigate this interaction. This simulation model is built upon the computing framework developed for embodying the proposed methodology. The simulation software solves one dimensional hydraulic flow equations by integrating the structural and geotechnical design tasks with the use of some AI techniques so that the hydraulic-structure interaction can be examined within the scope of an optimization problem. This optimization problem is searching for the best span arrangement of a river bridge in terms of both design and economy

considerations. As expected, the simulation software results show that the hydraulic effects are also important aspects in design of river bridges because of the scour effects around the piers and abutments that may cause fatal collapse of the bridge. The simulation results indicate that the width of the opening of a river bridge does not have a major effect, unless the total length of the bridge is unreasonably small. Therefore, as expected, local scour phenomenon in bridge engineering has the prominent influence on the design of river bridges. In this context, the locations of piers across the bridge cross-section are important parameters because the scour depths are directly affected by the velocity distribution across the cross-section. Thus, the heights of the piers increase by the rise of footing depths in order to avoid the adverse effects of local scour. This may have considerable effect on the total cost of the bridge according to the topographical properties of the bridge site. Also, the locations of the piers directly affect the span lengths of the superstructure, which has also a significant influence on the economy of the bridge. Although for a bridge site having almost a regular cross-section, an engineering experience may be greatly helpful for estimating span arrangement, it is an intricate problem for bridges crossing rivers having irregular cross-sectional geometry especially. Therefore, the developed simulation software can impressively facilitate span arrangement decisions for the preliminary design of such bridges.

In addition to the capability of offering an optimum span arrangement, AIROB has also been developed in order to estimate the basic dimensions of the structural and geotechnical components provided that some required structural and geotechnical parameters are given. In this respect, the software framework replaces the conventional cumbersome analytical computational tasks with a much more clear and elegant way, artificial neural networks. This capability of the software makes the inherent design considerations that cannot be formalized by conventional methods possible. In this context, since ANNs are built on statistical data, they can also reflect the past engineering experiences. The study constructed a database of existing real design projects for the development of ANN models, thus any design experience used for the designs of these bridges in the database was also involved implicitly in the built ANN models. It should be noted that, the development of the current database was done by filtering many

designs and enriched by gathering bridge projects from various sources which the details are stated in Chapter 5. Therefore, this study is built on a sufficiently qualified database from which the reliable and reasonable results were obtained as shown by the applications.

If the study is examined from an AI perspective, the outcomes are also very promising. Thus, it is possible to categorize the developed framework as similar to an expertise or decision support systems. As mentioned previously, the integration of AI techniques also embed some sort of intelligent behavior to the methodology, such as reflecting the past experiences implicitly. Hence using these experiences, new designs can be offered. This has been accomplished by assembling two fundamental topics of AI; estimation and optimization. Estimation part was implemented by ANNs, while optimization part was fulfilled by Genetic Algorithms. The applications of the study show that both parts work well integrated, giving reasonable outputs. The integration of various AI techniques within a unified model has not been commonly seen in civil engineering, thus this study proposes an innovative design methodology by developing associated computing framework. One of the results of this study is such that; by the use of AI techniques, engineering designs can lead to a more consistent and reliable fashion by diminishing the engineer-oriented mistakes. It is obvious that AI researches are at an infant stage such that there are lots of progressions that should be completed. However, this study shows that the principles of AI can be successfully applied to the solutions of civil engineering problems with an integrated fashion. Thus, the results taken from these studies can supply rationalized guidelines to civil engineers.

Finally, some recommendations are specified for the enlightenment of future researches regarding this study. First of all, it should be noted that the quality of the outputs given by the software is highly dependent on the quality and abundance of the design projects in the database. For this reason, if the bridge database is increased based on the requirements of the ANN models, more qualified outputs can be obtained. Besides, different structural and geotechnical design perspectives that are desired to be introduced to the software framework can be accomplished by insertion of the corresponding design projects into the

database and making related modifications on the ANN models in order to capture the corresponding design aspects. For example, if the effects of pile foundations on the hydraulic – structure interactions are desired to be observed by the developed software framework, it is possible to consider the bridge projects having footings with piles and refining the related ANN models by reflecting pile effects as a new input variable of the ANN models of abutments and piers. Therefore, the economy of pile foundations can be studied to observe the circumstances for which use of piles becomes more economical than increasing the footing depths. In addition to geotechnical design related studies, structural design oriented studies can also be extended based on the methodology offered by this study. This study considers only pre-stressed superstructures with reinforced concrete piers and abutments. However, the principles of the methodology are the same if bridges having different structural models are to be studied.

As a final recommendation; the AI techniques within the scope of the study can be changed in order to observe the efficiencies of other techniques within the context of this study. An example may be integrating different optimization procedures other than Genetic Algorithms. Consequently, the optimization engine of the study may be improved by considering the efficiency, performance, and applicability features of corresponding optimization techniques.

REFERENCES

AASHTO (American Association of State Highway and Transportation Officials), 1998. Standard Specifications for Highway Bridges, Washington, D.C.

Aguilar, R.J., Movassaghi, K., and Brewer, J.A., 1973. Computerized optimization of bridge structures. *Computers and Structures*, 3(3): 429–442.

Anderson, J.A., 1983. "Cognitive and psychological computation with neural models". *IEEE Transactions on Systems, Man and Cybernetics*, Vol. SMC-13, No. 5, pp. 799-814.

Ang, A.H.S., and Tang, W.H., 1984. *Probability Concepts in Engineering Planning and Design, Volume 2 Decision, risk and reliability*, John Wiley and Sons, New York.

ATC-32-1 (Improved Seismic Design Criteria for California Bridges Resource Document), 1999. Applied Technology Council, California Department of Transportation.

Bellman, R.E., 1957. "Dynamic Programming". Princeton University Press, Princeton, NJ. Republished 2003: Dover.

Berke, L., and Hajela, P., 1991. "Application of neural networks in structural optimization." *NATO/AGARD Advanced Study Institute*, 23(I-II), 731-745.

Chow, V.T., 1959. "Open Channel Hydraulics.", McGraw Hill, New York.

CSI (Computers and Structures Inc.), 2005. "CSI Analysis Reference Manual for SAP2000, ETABS, and SAFE", Computer and Structures, Inc. Berkeley, California, USA.

Deb K., 2001. "Multi-Objective Optimization using Evolutionary Algorithms", John Wiley & Sons, Chichester.

Demuth, H., and Beale M., 2002. "Neural Network Toolbox for Use with MATLAB", The MathWorks, Inc.

Dianati, M. and Song, I., 2002 " An Introduction to Genetic Algorithms and Evolution Strategies", University of Waterloo , Canada.

French, R.H., 1987. "Open Channel Hydraulics", Singapore, McGraw Hill.

FHWA (Federal Highway Administration), 1998. "User's Manual for WSPRO – A Computer Model for Water Surface Profile Computations", Publication No: FHWA-SA-98-080, U.S. Department of Transportation, Washington, U.S.A.

FHWA (Federal Highway Administration), 2001. "Evaluating Scour at Bridges – Fourth Edition", Publication No: FHWA NHI 01-001, U.S. Department of Transportation, Washington, U.S.A.

FIB (Fédération Internationale de la Précontrainte), 2000. "Guidance for good bridge design", bulletin 9: guide to good practice, fib bulletins, Lausanne, Switzerland.

Gen, M. and Cheng, R., 2000. "Genetic Algorithms & Engineering Optimization". , John Wiley & Sons, Inc.

Genetic Algorithms, 2011. "VII. Parameters of GA".
<http://www.obitko.com/tutorials/genetic-algorithms/parameters.php>, last visited on January 2011.

Goldberg, D. E., 1989. "Genetic Algorithms in Search, Optimization, and Machine Learning", Reading, Addison-Wesley...

Hassanain, M.A and Loov, R.E., 2003. "Cost optimization of concrete bridge infrastructure", Canadian Journal of Civil Engineering, 30(5): 841–849.

Haupt, R.L. and Haupt, S.E., 2004. "Practical Genetic Algorithms", Second Edition, John Wiley & Sons, Inc.

Heaton, J., 2008. "Introduction to Neural Networks with C#, Second Edition", Heaton Research, USA.

Holland, J.H., 1975. "Adaptation in Natural and Artificial Systems". Ann Arbor, MI: The University of Michigan Press.

Hopfield, J., J., 1982, "Neural networks and Physical Systems with Emergent Collective Computational Abilities". Proc. Natl. Acad. Sci., V.79, pp. 2554-2558.

Johnson, P.A., and Ayyub, B.M., 1992. "Assessment of Time-variant Bridge Reliability due to Pier Scour", Journal of Hydraulic Engineering, ASCE, 118(6): 887-903.

Johnson, P.A., 1992. "Reliability-based Pier Scour Engineering", Journal of Hydraulic Engineering, ASCE, 118(10): 1344-1358.

Johnson, P.A., and Ayyub, B.M., 1996. "Modeling Uncertainty in Prediction of Pier Scour", Journal of Hydraulic Engineering, ASCE, 122(2): 66-72.

Johnson, P.A., 1998. "Fault Tree Analysis of Bridge Scour", Proceedings International Water Resources Engineering Conference, ASCE, 1:110-114, Memphis, USA.

Johnson, P.A., 1999 "Fault Tree Analysis of Bridge Failure Due to Scour and Channel Instability", Journal of Infrastructure Systems, ASCE, 5(1), 35-41.

Khan, A.I., Topping, B.H.V., Bahreininejad, A., 1993. Parallel training of neural networks for finite element mesh generation. In: Khan,A.I., Topping,B.H.V. (Eds.), NeuralNetworks and Combinatorial Optimization in Civil and Structural Engineering. Civil-Comp Press, Edinburgh, pp. 81–94.

Klimasauskas, C. (1993). “Applying neural networks, Part II: A walk through the application process”, in Trippe, R. R. and E. Turban (eds), Neural Networks in Finance and Investing, Chicago: Probus Publishing Company, pp54-63.

Kohonen, T., 1982. “The self-organized formation of topography correct feature maps”. Biological Cybernetics, Vol.43, pp.59-69.

Lagasse, P.F., Zevenbergen, L.W., Schall, J.D., and Clopper, P.E., 2001. “Bridge Scour and Stream Instability Countermeasures”. Publication No: FHWA NHI 01-003, U.S. Department of Transportation, Federal Highway Administration, VA, USA.

Matthai, H.F., 1976. “Measurement of Peak Discharge at Width Contractions by Indirect Methods”, Techniques of Water Resources Investigations of the United States Geological Survey, U.S. Geological Survey, Washington, USA.

Mays, L.W., and Tung, Y.K., 1992. “Hydrosystems Engineering and Management”. McGraw Hill Inc., Singapore.

Richardson, E.V. and Davis, S.R., 2001. “Evaluating scour at bridges.” Hydraulic engineering Circular No:18, Publication No: FHWA NHI 01-001, FHWA, US. Dept. of Transportation, Washington, D.C., USA.

Rumelhart, D.E., Hinton, G., E., Williams, R., J., 1986. Learning representations by back-propagation error, Nature, Vol. 32, pp. 533-536.

Russel, S.J., and Norvig, P., 2003. “Artificial Intelligence: A Modern Approach”, Prentice Hall, USA.

Sniedovich, M., 2010. "Dynamic Programming – Foundations and Principles – Second Edition", CRC Press, USA.

Smith, M., 1993. "Neural networks for statistical modeling". Van Nostrand Reinhold, New York.

USACE (United States Army Corps of Engineers), 1998. "HEC-RAS (User's Manual: Version 2.2)", US Army Corps of Engineers. Hydrologic Engineering Center, Davis, California.

Weise, T., 2009. "Global Optimization Algorithms – Theory and Application -", Second Edition, <http://www.it-weise.de/>.

Wikipedia, 2011-a. "Artificial Intelligence".
http://en.wikipedia.org/wiki/Artificial_intelligence, last visited on January 2011.

Wikipedia, 2011-b. "Optimization (mathematics)".
[http://en.wikipedia.org/wiki/Optimization_\(mathematics\)](http://en.wikipedia.org/wiki/Optimization_(mathematics)), last visited on January 2011.

Wikipedia, 2011-c. "Bellman Equation".
http://en.wikipedia.org/wiki/Bellman_equation, last visited on January 2011.

Yanmaz, A.M., and Kürkçüoğlu, S., 2000. "Assessment of Hydraulic and Structural Interactions for Bridges", CD-ROM Proc. 4th International Conference on Hydrosience and Engineering, Seoul, Korea.

Yanmaz, A.M., 2001. "Uncertainty of Local Scouring Parameters Around Bridge Piers", Turkish Journal of Engineering and Environmental Sciences, 25(2), 127-137.

Yanmaz, A.M., and Çiçekdağ, Ö., 2001. "Composite Reliability Model for Local Scour Around Cylindrical Bridge Piers", Canadian Journal of Civil Engineering, 28(3), 520-535.

Yanmaz, A. M., and Bulut, F., 2001. "Computer Aided Analysis of flow Through River Bridges", CD-ROM Proceedings of World Water and Environmental Resources Congress, ASCE, Orlando, USA.

Yanmaz, A.M., and Üstün, İ., 2001. "Generalized Reliability Model for Local Scour Around Bridge Piers of Various Shapes", Turkish Journal of Engineering and Environmental Sciences, Turkish Scientific and Technical Research Council, 25, 6, 687-698.

Yanmaz, A. M., 2002-a. "Köprü Hidroloği", Metu Press, Ankara (in Turkish).

Yanmaz, A.M., 2002-b. "Dynamic Reliability in Bridge Pier Scouring", Turkish Journal of Engineering and Environmental Sciences, Turkish Scientific and Technical Research Council.

Yanmaz, A.M., and Çelebi, T., 2002. "Assessment of Uncertainties for Local Scouring Parameters Around Bridge Abutments", CD-ROM Proceedings of 2002 Conference on Water Resources Planning and Management, ASCE, Roanoke, USA.

Yanmaz, A.M., 2003. "Reliability Simulation of Scouring of Outlet Facilities", Turkish Journal of Engineering and Environmental Sciences, Turkish Scientific and Technical Research Council, 27, 65 – 71.

Yarnell, D.L., 1934. "Bridge Piers as Channel Obstructions", Technical Journal No:442, U.S. Department of Agriculture, Washington, USA.

APPENDIX A

BRIDGE DATABASE

Table A.1. Summarized information of the bridges in the database.

Bridge Name	EQ Region	Total Length (m)	Width (m)	No. of Spans	Span Arrangement
Akoren	1	13.00	12.75	1	1 x 13.00
Karasu-8	1	15.70	13.50	1	1 x 15.70
Dagdelen	1	20.00	13.70	1	1 x 20.00
Tersakan-II	1	27.00	12.75	1	1 x 23.00
Ibrahimaga	1	27.50	13.25	1	1 x 27.50
BitlisCreek-4	1	27.80	24.00	1	1 x 27.80
BitlisCreek-8	1	30.00	14.00	1	1 x 30.00
BeylerbeyiCreek	1	32.40	13.30	3	3 x 10.40
CumayeriJunction Overpass	1	41.10	27.05	2	2 x 20.00
Sarıcaçay	1	46.50	28.00	3	3 x 15.50
Carsak	1	52.20	13.70	3	3 x 17.00
BitlisCreek-14	1	52.30	10.50	2	27.80 + 22.80
KarasuCreek	1	53.00	13.00	3	3 x 17.00
Karasu-7	1	55.50	13.50	2	2 x 27.00
Uluderbent	1	56.80	11.00	3	3 x 18.60
BitlisCreek-16	1	57.31	24.00	2	2 x 27.80
Karasu-6	1	61.60	13.50	3	3 x 20.00
BitlisCreek-9	1	64.80	30.00	3	2 x 23.00 + 16.00
Gaziosmanpaşa Uni. Junction Bridge	1	70.70	16.00	4	4 x 17.00
BitlisCreek-17	1	87.40	18.00	3	3 x 27.80
BitlisCreek-7	1	90.40	17.50	4	3 x 23.00 + 16.00
Degirmendere	1	106.00	12.00	6	6 x 17.00

Table A.1 (Continued). Summarized information of the bridges in the database.

Bridge Name	EQ Region	Total Length (m)	Width (m)	No. of Spans	Span Arrangement
BitlisCreek-5	1	16.70	24.00	1	1x16.70
BitlisCreek-10	1	107.80	24.00	4	22.80 + 2 x 27.80 + 22.80
BitlisCreek-20	1	110.00	28.40	4	22.80 + 27.80 + 22.80 + 30.00
BitlisCreek-21	1	112.20	28.40	4	22.80 + 30.00 + 22.80 + 30.00
BitlisCreek-22	1	126.60	28.40	4	4 x 30.00
Namnam	1	171.50	11.25	8	18.40 + 6 x 20.80 + 16.40
BitlisCreek-19	1	183.80	28.40	6	5 x 30.00 + 22.80
BitlikCreek-15	1	20.00	24.00	1	1x20.00
IrrigationCanal Underpass	1	20.00	35.00	1	1x20.00
Kocabas-1Junction	1	24.30	20.00	1	1x24.30
Kocabas-2Junction	1	30.00	24.80	1	1x30.00
HonazJunction	1	25.00	20.00	1	1x25.00
DSI	1	35.70	24.80	1	1x35.70
DDYoverpass-1	1	20.00	21.40	1	1x20.00
BitlisCreek-1 Left&Right	1	18.90	30.00	1	1x18.90
Karasu-9	1	15.70	13.25	1	1x15.70
DDYoverpass-3	1	15.00	13.70	1	1x15.00
YirimCreek	1	22.50	14.06	2	2 x 12.50
Kanlidere	1	23.50	13.25	1	1 x 23.50
Cumayani	1	24.00	13.70	1	1 x 24.00
DSIcanal	1	25.00	28.95	1	1 x 25.00
BoluStreetUnderpass	1	25.00	33.95	1	1 x 25.00
DSIcanal	1	25.00	16.00	1	1 x 25.00
D100Junction	1	26.00	28.40	1	1 x 26.00
Karakaya	1	26.00	13.70	2	2 x 13.30
Beygircioglu	1	26.60	13.25	2	2 x 13.00
Imbat	1	28.48	14.75	2	2 x 14.24
BitlisCreek-12	1	30.00	24.00	1	1 x 30.00
BitlisCreek-18	1	30.00	17.10	1	1 x 30.00
DDYunderpass	1	38.50	35.00	1	1 x 35.00
DCYundercrossing-1	1	35.10	28.95	2	2 x 17.00
ElekCreek	1	40.60	13.70	2	2 x 20.00
Yalakdere	1	43.60	13.25	3	15.00 + 13.60 + 15.00

Table A.1 (Continued). Summarized information of the bridges in the database.

Bridge Name	EQ Region	Total Length (m)	Width (m)	No. of Spans	Span Arrangement
GolyakaJunction Overpass	1	45.10	34.10	2	2 x 22.00
DuzceJunction Overpass	1	45.10	32.50	2	2 x 20.00
KolayliDDY	1	46.20	36.00	3	3 x 15.00
BitlisCreek-13	1	47.00	10.50	2	2 x 23.00
Omerli	1	49.20	12.00	3	3 x 16.00
Yesilirmak	1	49.40	14.00	3	3 x 16.00
DuzceJunction Overpass	1	51.10	23.55	2	2 x 25.00
YeniDalyan	1	57.20	30.50	3	16.00 + 24.00 + 16.00
Koproluunction	1	58.60	35.00	2	2 x 29.30
KarabukJunction	1	60.20	14.00	4	12.20 + 2 x 17.00 + 12.20
BitlisCreek-11	1	61.80	24.00	2	2 x 30.00
GurdukCreek	1	64.60	12.75	4	4 x 15.70
BitlisCreek-3	1	64.80	14.00	3	16.00 + 2 x 23.00
Gokirmak	1	69.80	12.70	4	4 x 17.00
Tersakan	1	72.00	12.75	3	19.70 + 29.40 + 19.70
NehirkentHighway	1	76.50	13.50	3	27.50 + 24.00 + 25.00
Kirazlı	1	76.80	14.00	4	19.05 + 2 x 19.35 + 19.05
Kirazlı -2	1	76.80	9.00	4	19.05 + 2 x 19.35 + 19.05
AlasehirCreek	1	78.40	16.00	3	3 x 25.00
BesgozDDYoverpass	1	89.00	12.00	3	25.00 + 35.00 + 25.00
Elengullu	1	89.40	12.00	6	6 x 14.40
Kuzgece-II	1	102.40	10.20	5	5 x 20.00
AsarCreek	1	103.30	33.20	4	4 x 25.00
KullarCreek	1	110.70	12.75	6	14.30 + 18.00 + 21.55 + 17.85 + 2 x 18.00
KucukMelen	1	113.20	12.00	5	5 x 22.00
Melen	1	113.30	16.00	4	4 x 27.50
GedizCreek	1	128.80	16.00	5	5 x 25.00
Goy nuk	1	129.80	14.00	8	8 x 15.70
Uluabat-II	1	153.40	12.00	7	7 x 21.40
Duzce Cevreyolu Overpass	1	41.10	23.20	2	2 x 20.00
Golmarmara Evacuation Ch	1	15.60	25.00	1	1x15.60

Table A.1 (Continued). Summarized information of the bridges in the database.

Bridge Name	EQ Region	Total Length (m)	Width (m)	No. of Spans	Span Arrangement
AksuCreek	1	212.80	31.20	6	34.40 + 4 x 36.00 + 34.40
CuruksuCreek	1	266.80	38.50	7	37.40 + 5 x 38.40 + 37.40
Karahanlar	1	20.50	20.00	1	1x20.50
DDYoverpass-2	1	25.00	24.00	1	1x25.00
DDYunderpass	1	23.00	16.00	1	1x23.00
DBYoverpass-1	1	46.00	15.00	2	2x23.00
DCYoverpass-2	1	56.00	24.80	2	2x28.00
DCYoverpass-3	1	48.00	15.35	2	2x24.00
DCYoverpass-4	1	34.00	14.00	2	2x17.00
DCYoverpass-5	1	60.00	18.00	2	2x30.00
DSLcanal-1	1	35.00	13.25	1	1x35.00
DBY Overpass-2	1	30.00	14.00	2	2x15.00
DOBY Overpass-1	1	46.00	23.00	2	2x23.00
HorasanOutlet	2	154.50	13.25	8	16.60 + 6 x 18.70 + 16.60
Uzulmez	2	24.00	14.25	1	1 x 24
Batkin	2	25.00	13.00	2	2 x 12.50
Ecekler(Cam)	2	28.00	13.25	1	1 x 28
KokaksuDDYoverpass	2	29.40	13.25	1	1 x 29.40
DDYoverpass	2	30.00	13.25	1	1 x 30.00
Milic-2	2	39.00	12.40	3	3 x 12.40
RailwayOvercrossing	2	49.20	12.00	3	3 x 16.00
Milic-1	2	51.40	14.00	4	4 x 12.40
Terme	2	51.40	14.00	4	4 x 12.40
DDYoverpass	2	53.00	13.25	3	14.50 + 24.00 + 14.50
Kerimbey	2	64.80	56.00	2	2 x 31.50
Kurtun	2	77.80	12.00	5	15.00 + 3 x 15.00 + 15.00
Karpuzcay	2	131.40	13.70	6	6 x 21.40
Godiren	2	30.00	13.50	1	1x30.00
Banaz	2	25.00	12.40	1	1x25.00
DBYovercrossing-1	1	41.10	12.50	2	2 x 20.00
DCYoverpass-1	1	41.10	26.00	2	2 x 20.00
DilsizCreek	1	41.20	13.10	2	24.45 + 15.25

Table A.2. Summarized information of abutments in the database.

Bridge Name	Bridge Width (m)	Height (m)	Wall Length (m)	Wall Width (cm)	Footing Width (m)	Cost (US\$)
Bitlis Creek-9	24.00	7.25	4.65	115.00	5.00	185,813
Bitlis Creek-9	24.00	4.13	1.65	115.00	5.00	119,279
Bitlis Creek-21	24.80	4.04	1.75	115.00	5.00	116,600
Bitlis Creek-21	24.80	6.03	4.75	115.00	5.00	165,198
Kerimbey	29.60	5.75	1.65	115.00	6.40	138,254
Dagdelen	13.70	6.24	4.45	120.00	5.00	87,241
Dagdelen	13.70	6.55	4.45	120.00	5.00	89,763
Delice-1	32.00	4.35	1.75	115.00	5.00	127,659
Delice-1	32.00	4.92	1.75	115.00	5.00	135,840
Cumayani	13.70	4.18	2.60	120.00	1.20	40,197
Cumayani	13.70	4.64	2.60	120.00	1.20	43,166
DSlcanal	29.00	2.58	1.70	120.00	5.00	95,523
DSlcanal	29.00	2.07	1.80	120.00	5.00	91,242
Bolu Street Underpass	35.35	5.94	4.75	115.00	5.00	194,811
Bolu Street Underpass	35.35	5.39	4.75	115.00	5.00	188,968
Ibrahimaga	31.50	5.11	5.25	115.00	4.50	206,632
Ibrahimaga	31.50	5.30	5.25	115.00	4.50	207,029
Bitlis Creek-4	26.12	7.41	8.10	120.00	6.00	302,532
Bitlis Creek-4	26.12	6.90	6.62	120.00	6.00	297,534
Bitlis Creek-5	24.00	8.36	4.75	115.00	5.00	171,835
Bitlis Creek-5	24.00	7.95	4.75	115.00	5.00	171,037
Demircik	13.00	6.60	4.25	115.00	7.00	94,480
Karasu-9	13.25	7.10	3.70	115.00	6.50	110,954
Karasu-6	13.25	4.50	2.50	115.00	4.60	93,458
Karasu-6	13.25	4.30	2.50	115.00	4.60	91,785
Horasan Outlet	13.25	7.40	3.90	120.00	6.80	113,985
BitlisCreek-10	24.00	6.42	1.65	115.00	5.00	156,091
BitlisCreek-10	24.00	5.15	1.65	115.00	5.00	120,044
Beygircioglu	13.25	3.65	1.40	115.00	4.40	85,458
Beygircioglu	13.25	2.80	1.40	115.00	4.40	78,589
Karasu-9	13.25	6.80	3.70	115.00	6.50	105,891

Table A.2 (Continued). Summarized information of abutments in the database.

Bridge Name	Bridge Width (m)	Height (m)	Wall Length (m)	Wall Width (cm)	Footing Width (m)	Cost (US\$)
Bitlis Creek-8	14.00	4.87	1.65	115.00	5.00	94,918
Bitlis Creek-8	14.00	5.56	1.65	115.00	5.00	144,516
Bitlis Creek-12	24.00	7.51	4.70	110.00	5.00	222,019
Bitlis Creek-12	24.00	6.87	6.83	110.00	5.00	173,678
Bitlis Creek-22	13.20	9.95	4.70	115.00	5.00	112,689
Bitlis Creek-22	13.20	6.40	4.70	115.00	5.00	112,689
Bitlis Creek-22	28.40	8.18	4.70	115.00	5.00	187,264
Bitlis Creek-22	28.40	7.73	4.70	115.00	5.00	180,192
Bitlis Creek-19	28.40	6.39	4.70	115.00	5.00	168,693
Bitlis Creek-19	28.40	6.12	4.70	115.00	5.00	165,873
MelenCreek	16.00	4.37	1.75	115.00	5.00	69,190
MelenCreek	16.00	4.67	3.75	115.00	5.00	85,665
GOP university Junction	16.00	6.37	4.05	130.00	7.00	147,443
GOP university Junction	16.00	8.82	4.05	130.00	7.00	179,385
DDYoverpass-3	13.70	8.62	4.25	120.00	5.00	129,659
CumayeriJunction Overpass	23.20	7.64	9.50	115.00	5.00	210,710
CumayeriJunction Overpass	23.20	7.24	9.50	115.00	5.00	205,765
Carsak	13.70	3.98	2.15	120.00	4.50	57,929
Bitlis Creek-14L	10.50	6.14	5.94	120.00	5.00	58,365
Bitlis Creek-14L	10.50	8.29	5.94	120.00	5.00	63,725
Bitlis Creek-16	24.00	8.19	7.62	120.00	7.00	125,895
Bitlis Creek-16	24.00	7.89	7.62	120.00	7.00	123,589
Bitlis Creek-7	11.00	5.05	1.70	115.00	5.00	55,362
Bitlis Creek-20	28.40	6.18	3.65	115.00	5.00	118,897
Bitlis Creek-20	28.40	3.68	3.65	115.00	5.00	85,567
DDYoverpass-3	13.70	7.64	4.25	120.00	5.00	118,261

Table A.3. Summarized information of piers in the database.

Bridge Name	Bridge Width (m)	Height (m)	Pier Width (cm)	Pier Length (cm)	Footing Width (m)	Cost (US\$)
Bitlis Creek-9	24.00	9.77	100.00	200.00	5.00	162,930
Bitlis Creek-9	24.00	9.54	100.00	200.00	5.00	161,705
Bitlis Creek-21	13.00	8.32	100.00	100.00	5.00	56,073
Bitlis Creek-21	13.00	9.05	100.00	100.00	5.00	58,825
Kerimbey	28.40	14.32	200.00	200.00	10.00	255,433
Dagdelen	28.40	30.39	200.00	200.00	10.00	379,063
Dagdelen	28.40	30.05	200.00	200.00	10.00	376,092
Delice-1	13.25	2.10	100.00	150.00	4.00	38,589
Delice-1	13.25	8.40	100.00	200.00	5.50	63,856
Cumayani	13.25	8.25	100.00	200.00	5.50	61,879
Cumayani	13.25	6.70	100.00	150.00	5.00	55,789
DSlcanal	13.25	7.40	100.00	150.00	5.00	58,785
DSlcanal	24.00	13.27	200.00	200.00	8.00	242,739
BoluStreet Underpass	24.00	14.98	200.00	200.00	8.00	255,273
BoluStreet Underpass	24.00	14.69	200.00	200.00	8.00	253,256
Ibrahimaga	23.20	6.71	100.00	160.00	5.00	104,971
Ibrahimaga	28.40	16.66	200.00	200.00	10.00	308,748
Bitlis Creek-4	13.20	18.17	200.00	200.00	10.00	157,130
Bitlis Creek-4	13.20	15.15	200.00	200.00	10.00	151,784
Bitlis Creek-5	28.40	27.23	200.00	200.00	10.00	389,846
Bitlis Creek-5	28.40	26.31	200.00	200.00	10.00	382,244
Demircik	28.40	19.38	200.00	200.00	10.00	330,991
Bitlis Creek-8	28.40	36.78	200.00	200.00	10.00	482,726
Karasu-6	28.40	30.73	200.00	200.00	10.00	400,036
HorasanOutlet	28.40	30.39	200.00	200.00	10.00	396,526
BitlisCreek-10	13.20	15.97	200.00	200.00	10.00	141,535
BitlisCreek-10	13.20	30.88	200.00	200.00	10.00	200,728
DDYoverpass-3	13.20	30.54	200.00	200.00	10.00	198,684
Karasu-9	11.00	10.23	100.00	150.00	5.00	96,249
Karasu-9	11.00	9.70	100.00	150.00	5.00	94,337
Karasu-6	28.40	16.13	200.00	200.00	10.00	284,136

Table A.3 (Continued). Summarized information of piers in the database.

Bridge Name	Bridge Width (m)	Height (m)	Pier Width (cm)	Pier Length (cm)	Footing Width (m)	Cost (US\$)
Bitlis Creek-8	28.40	35.68	200.00	200.00	10.00	471,853
Bitlis Creek-12	28.40	23.58	200.00	200.00	10.00	363,118
Bitlis Creek-12	28.40	13.50	200.00	200.00	10.00	290,265
Bitlis Creek-22	16.00	11.52	100.00	100.00	6.00	87,642
Bitlis Creek-22	16.00	12.02	100.00	100.00	6.00	89,394
Bitlis Creek-22	16.00	13.27	100.00	100.00	6.00	93,899
Bitlis Creek-22	13.70	2.60	100.00	200.00	4.00	32,571
Bitlis Creek-19	10.50	10.20	100.00	100.00	5.00	53,720
Bitlis Creek-19	10.50	9.82	100.00	100.00	5.00	50,177
MelenCreek	13.00	6.06	100.00	150.00	6.00	63,518
MelenCreek	13.00	6.39	100.00	150.00	6.00	66,666
GOPuniversity Junction	24.00	7.79	100.00	150.00	6.00	160,812
GOPuniversity Junction	14.00	11.33	100.00	150.00	5.00	96,733
Beygircioglu	14.00	11.93	100.00	150.00	5.00	105,466
Beygircioglu	11.00	10.78	100.00	150.00	5.00	98,015

Table A.4. Summarized information of superstructures in the database.

Bridge Name	Slab Width (m)	Span Length (m)	Girder Depth (cm)	Girder Spacing (m)	Cost (US\$)
Bitlis Creek-9	24.00	16.00	90.00	81.50	127,741
Bitlis Creek-9	24.00	23.00	90.00	81.50	181,872
Taşköprü Bridge	13.00	17.00	127.50	160.00	55,546
Bitlis Creek-21	28.40	22.80	120.00	130.00	227,127
Bitlis Creek-21	28.40	30.00	120.00	130.00	296,775
Yildizeli Creek	12.75	13.00	90.00	81.50	57,443
Dagdelen	13.70	20.00	140.00	170.00	73,432
Delice-1	32.00	20.00	90.00	81.50	203,842
Cumayani	13.70	24.00	90.00	81.50	111,170
DSI Canal	29.00	25.00	120.00	130.00	243,392
Bolu Street Underpass	35.35	25.00	120.00	130.00	295,052
DSI Canal	16.00	25.00	120.00	130.00	147,494
D100 Junction Bridge	28.40	26.00	120.00	130.00	256,143
Karayaka	14.00	13.00	75.00	170.00	44,836
Ibrahimaga	31.50	27.50	120.00	130.00	291,456
Bitlis Creek-4	26.12	27.80	120.00	130.00	242,123
Imbat	14.75	14.24	75.00	120.00	59,190
BitlisCreek-8	14.00	30.00	120.00	130.00	154,129
BitlisCreek-12	24.00	30.00	120.00	130.00	249,016
BitlisCreek-18	17.10	30.00	120.00	130.00	191,740
DDY Overpass	13.25	30.00	120.00	130.00	148,578
Catak	13.00	17.00	127.50	160.00	53,872
Kemalli	28.50	17.00	90.00	81.50	176,221
AyasRoad	20.00	22.50	90.00	82.50	163,628
SuperHighway	38.50	14.50	150.00	150.00	150,735
SuperHighway	38.50	26.80	150.00	150.00	270,404
KirazliHES downstream	14.00	19.00	90.00	82.50	88,515
IrrigationCanal Underpass	38.50	26.00	160.00	135.50	365,440
DuzceJunction Overpass	32.50	22.00	90.00	81.50	225,265

Table A.4 (Continued). Summarized information of superstructures in the database.

Bridge Name	Slab Width (m)	Span Length (m)	Girder Depth (cm)	Girder Spacing (m)	Cost (US\$)
DDY Underpass	44.00	38.50	200.00	135.50	615,479
DCY Underpass-1	29.00	17.00	90.00	81.50	160,347
ElekCreek	13.70	20.00	140.00	170.00	68,370
Sariz	13.00	20.00	140.00	160.00	69,588
CumayeriJunction Overpass	23.20	20.00	90.00	82.50	147,289
DCYoverpass	23.20	20.00	90.00	82.50	148,030
DBYovercrossing-1	12.50	20.00	90.00	81.50	89,503
DCYoverpass-1	12.50	20.00	90.00	81.50	89,503
DDYoverpass	12.75	12.50	90.00	81.50	57,058
DDYoverpass	12.75	17.00	90.00	81.50	63,151
Kefenin	13.00	13.00	127.50	160.00	41,500
Kefenin	13.00	17.00	127.50	160.00	54,272
Ulusal	13.00	13.00	127.50	160.00	42,380
Ulusal	13.00	17.00	127.50	160.00	54,845
GolyakaJunction Overpass	24.85	22.00	90.00	82.50	172,430
Saricay	13.25	13.00	75.00	77.00	68,235
Beygircioglu	13.25	15.00	75.00	77.00	73,568
Karasu-9	13.25	15.70	90.00	145.00	75,589
Karasu-6	13.25	20.00	90.00	82.00	80,523
KerimBey	29.60	31.50	170.00	150.00	250,742
Tekgsoz	12.00	18.70	150.00	170.00	85,965
Tekgsoz	12.00	24.40	150.00	170.00	105,852
Kocabas-1 Junction	41.25	38.50	200.00	135.50	635,015
Kocabas-2 Junction	38.50	40.00	200.00	135.50	616,180
HonazJunction	31.00	38.50	200.00	139.00	470,123
BitlisCreek-22	28.40	30.00	120.00	130.00	298,420
BitlisCreek-19	28.40	30.00	120.00	130.00	292,583
BitlisCreek-19	28.40	22.80	120.00	130.00	222,763
GOPuniversity Junction	16.00	17.00	75.00	77.50	92,276
MelenCreek	16.00	27.50	120.00	130.00	159,897

Table A.4 (Continued). Summarized information of superstructures in the database.

Bridge Name	Slab Width (m)	Span Length (m)	Girder Depth (cm)	Girder Spacing (m)	Cost (US\$)
KirazliHES downstream	9.00	19.00	90.00	82.50	59,834
AlasehirCreek	16.00	25.00	120.00	130.00	150,007
BitlisCreek-17	14.00	27.80	120.00	130.00	143,028
Gomleksiz	13.50	35.00	150.00	122.50	201,034
KopruluJunction	35.00	28.95	120.00	130.00	349,462
BitlisCreek-3	14.00	16.00	90.00	82.50	79,025
BitlisCreek-3	14.00	23.00	90.00	82.50	106,683
HorasanOutlet	13.25	16.60	127.50	145.00	76,235
HorasanOutlet	13.25	18.70	127.50	145.00	81,562
BitlisCreek-10	24.00	22.80	120.00	130.00	189,371
BitlisCreek-11	24.00	27.80	120.00	130.00	231,234
DDYoverpass-3	13.70	15.00	90.00	150.00	50,707
Carsak	13.70	17.00	127.50	170.00	53,511
KarasuCreek	13.00	17.00	127.50	160.00	61,482
Bitlis Creek-14L	10.50	22.80	120.00	130.00	85,090
Bitlis Creek-14L	10.50	27.80	120.00	130.00	104,245
BitlisCreek-16	24.00	27.80	120.00	130.00	232,706
BitlisCreek-7	11.00	23.00	90.00	81.50	81,491
BitlisCreek-7	11.00	16.00	90.00	81.50	69,285

APPENDIX B

SAMPLE COST CALCULATIONS

Table B.1. Sample input table for cost calculation of abutments.

Abutment Cost Calculation Input Table		
Bridge Project: Bitlis Creek-9		
Definition	Value	Unit
Number of superstructure slabs on the abutment ceiling	1	
Piles Exist ?	y	
Number of piles	22	
Diameter of piles	100.00	cm
Length of 1 pile	9.00	m
Abutment Approach Plate Dimensions		
Approach plate plain concrete height	0.10	m
Approach plate plain concrete width	2.80	m
Approach plate plain concrete length	27.92	m
Approach plate height	0.25	m
Approach plate width	3.00	m
Approach plate length	27.42	m
Abutment Foundation Dimensions		
Basement plain concrete height	0.25	m
Basement plain concrete width	5.50	m
Basement plain concrete extension width (<i>if exists</i>)	3.00	m

Table B.1 (Continued). Sample input table for cost calculation of abutments.

Abutment Cost Calculation Input Table		
Bridge Project: Bitlis Creek-9		
Definition	Value	Unit
Basement extension width (if exists)	3.00	m
Basement length	33.00	m
Basement extension length (if exists)	6.35	m
Abutment inner length (plan view)	19.38	m
Abutment side wall inner width (plan view)	3.81	m
Abutment side wall width (plan view)	10.15	m
Abutment Wall Dimensions		
Abutment thickness (Cross-section)	1.15	m
Abutment height	7.25	m
Abutment length	30.46	m
Abutment height (superstructure part)	1.62	m
Abutment width (Cross-section / superstructure part)	0.35	m
Abutment trapezoidal part average height (Cross-section / superstructure part)	0.45	m
Abutment trapezoidal part width (Cross-section / superstructure part)	0.30	m
Abutment trapezoidal average height (Cross-section / transverse part)	2.50	m
Abutment trapezoidal projected width (Cross-section / transverse part)	2.36	m
Abutment trapezoidal part length (plan view / transverse part)	0.70	m
Abutment transverse wall height	8.96	m
Abutment transverse wall length (plan view)	5.90	m
Abutment transverse wall extension length (plan view)	3.00	m
Abutment transverse wall width (plan view)	1.14	m
Abutment transverse wall projected length	4.65	m
Abutment Steel Amounts		
8-12mm steel amount (foundation and walls)	0.91	tons

Table B.1 (Continued). Sample input table for cost calculation of abutments.

Abutment Cost Calculation Input Table		
Bridge Project: Bitlis Creek-9		
Definition	Value	Unit
14-28mm steel amount (foundation and walls)	57.69	tons
Basement plain concrete length	33.64	m
Basement plain concrete extension length (<i>if exists</i>)	6.98	m
Basement height	1.50	m
Basement width	5.00	m
Abutment Elastomeric Steel Supports		
Number of elastomeric steel support on the abutment	29	
Construction of Piles having inner diameter of 100cm (0-32 m)	218.68	/m
16.101/K: "Plain Concrete (Foundations)"	54.58	/m ³
16.132/K: "Reinforced Concrete"	142.80	/m ³
21.011: "Concrete & Reinf. Concrete Formwork (Plain Surface)"	9.73	/m ²
21.013: "Concrete & Reinf. Concrete Formwork (Grater Surface)"	11.89	/m ²
21.057: "Scaffolding for Wood Formworks (4 - 6m)"	3.54	/m ³
23.014: "8-12mm Steel"	895.13	/tons
23.015: "14-28mm Steel"	837.81	/tons
23.250: "Bridge Steel Support"	6.24	/kgs
23.252: "Copper Plate"	9.62	/kgs
23.254: "Lead Plate"	3.74	/kgs

Table B.2. Sample details table for cost calculation of abutments.

Abutment Cost Calculation Details								
Bridge Project: Bitlis Creek-9								
Work Type	Work No	quantity	Length	Width	Height	Amount	Unit	Sum
-	-	-	(m)	(m)	(m)	-	-	-
Construction of Piles having inner diameter of 100cm (0-32 m)	16.074/K-2							
Abutment foundation		22	9.00			198.00	m	
							m	198.00
Plain Concrete (Foundations)	16.101/K							
Abutment foundation basement		1	33.64	5.50	0.25	46.255	m ³	
Abutment foundation basement (side extensions if exists)		2	6.98	3.00	3.00	125.658	m ³	
Abutment approach plate		1	27.92	2.80	0.10	7.817	m ³	
							m ³	179.730
Reinforced Concrete	16.132/K							
Abutment foundation basement (main)		1	33.00	5.00	1.50	247.500	m ³	
Abutment foundation basement (side extensions if exists)		2	6.35	3.00	1.50	57.123	m ³	
Abutment approach plate		1	27.42	3.00	0.25	20.564	m ³	
Abutment walls		1	30.46	1.15	7.25	254.100	m ³	

Table B.2 (Continued). Sample details table for cost calculation of abutments.

Abutment Cost Calculation Details								
Bridge Project: Bitlis Creek-9								
Work Type	Work No	quantity	Length	Width	Height	Amount	Unit	Sum
-	-	-	(m)	(m)	(m)	-	-	-
		1	30.46	0.35	1.62	17.313	m ³	
		1	30.46	0.45	0.30	4.112	m ³	
		2	4.65	1.14	8.96	94.858	m ³	
		2	2.50	0.70	2.36	8.274	m ³	
							m ³	703.844
Concrete & Reinf. Concrete Formwork (Plain Surface)	21.011							
Abutment foundation basement (main)		1	33.00		1.50	49.50	m ²	
		2	10.15		1.50	30.45	m ²	
		2	6.35		1.50	19.04	m ²	
		2	3.81		1.50	11.43	m ²	
		1	19.38		1.50	29.07	m ²	
							m ²	139.49
Concrete & Reinf. Concrete Formwork (Grater Surface)	21.013							
Abutment transverse walls		2	30.46		7.25	441.91	m ²	
		2	30.46		1.62	98.93	m ²	
		2	30.46		0.30	18.28	m ²	
		4	5.90		8.96	211.41	m ²	
		4	2.50		3.00	30.00	m ²	

Table B.2 (Continued). Sample details table for cost calculation of abutments.

Abutment Cost Calculation Details								
Bridge Project: Bitlis Creek-9								
		2	0.44		8.96	7.86	m ²	
		2	0.70		8.96	12.54	m ²	
		2	0.70		3.00	4.20	m ²	
							m ²	825.13
Scaffolding for Wood Formworks (4 - 6m)	21.057							
Abutment foundation basement		1	33.00	0.75	1.50	18.563	m ³	
		2	10.15	0.75	1.50	11.419	m ³	
		2	6.35	0.75	1.50	7.140	m ³	
		2	3.81	0.75	1.50	4.286	m ³	
		1	19.38	0.75	1.50	10.901	m ³	
Abutment transverse walls		2	30.46	4.44	8.88	1,200.41 2	m ³	
		2	0.70	4.44	8.88	27.587	m ³	
		2	0.44	4.44	8.88	17.301	m ³	
		2	5.90	4.44	8.88	232.595	m ³	
		2	3.00	4.44	8.88	118.228	m ³	
		2	7.40	4.44	8.88	291.709	m ³	
							m ³	1,940.140
8-12mm Steel	23.014							
Abutment (foundation and walls)		1			0.914	0.914	tons	
							tons	0.914

Table B.2 (Continued). Sample details table for cost calculation of abutments.

Abutment Cost Calculation Details								
Bridge Project: Bitlis Creek-9								
14-28mm Steel	23.015							
Abutment (foundation and walls)		1			57.690	57.690	tons	
							tons	57.690
Abutment Elastomeric Steel Support	23.250							
		29	0.45	0.65	0.05	331.242	kgs	
							kgs	331.242
Abutment Elastomeric Support Copper Plate	23.252							
		29	0.35	0.50	0.08	462.109	kgs	
							kgs	462.109
Abutment Elastomeric Support Lead Plate	23.254							
		29	0.35	0.50	0.08	482.145	kgs	
							kgs	482.145

Table B.3. Sample results table for cost calculation of abutments.

Tabular Results for Cost Calculation of Abutments						
Bridge Project: Bitlis Creek-9						
Work No	Construction Type	Unit	Amount	Unit Cost	Cost	Cost %
A - CONSTRUCTION WORKS						
16.074/K-2	Construction of Piles having inner diameter of 100cm (0-32 m)	m	0.000	218.68	0.00	0.00
16.101/K	Plain Concrete (Foundations)	m ³	179.730	54.58	9,808.99	5.28
16.132/K	Reinforced Concrete	m ³	703.844	142.80	100,510.80	54.09
21.011	Concrete & Reinf. Concrete Formwork (Plain Surface)	m ²	139.49	9.73	1,357.76	0.73
21.013	Concrete & Reinf. Concrete Formwork (Grater Surface)	m ²	825.133	11.89	9,809.69	5.28
21.057	Scaffolding for Wood Formworks (4 - 6m)	m ³	1,940.140	3.54	6,858.60	3.69
23.014	8-12mm Steel	tons	0.914	895.13	818.15	0.44
23.015	14-28mm Steel	tons	57.690	837.81	48,333.18	26.01
23.250	Abutment Elastomeric Steel Support	kgs	331.242	6.24	2,067.25	1.11
23.252	Copper Plate	kgs	462.109	9.62	4,444.86	2.39
23.254	Lead Plate	kgs	482.145	3.74	1,803.67	0.97
	TOTAL COST				185,812.95	100.00

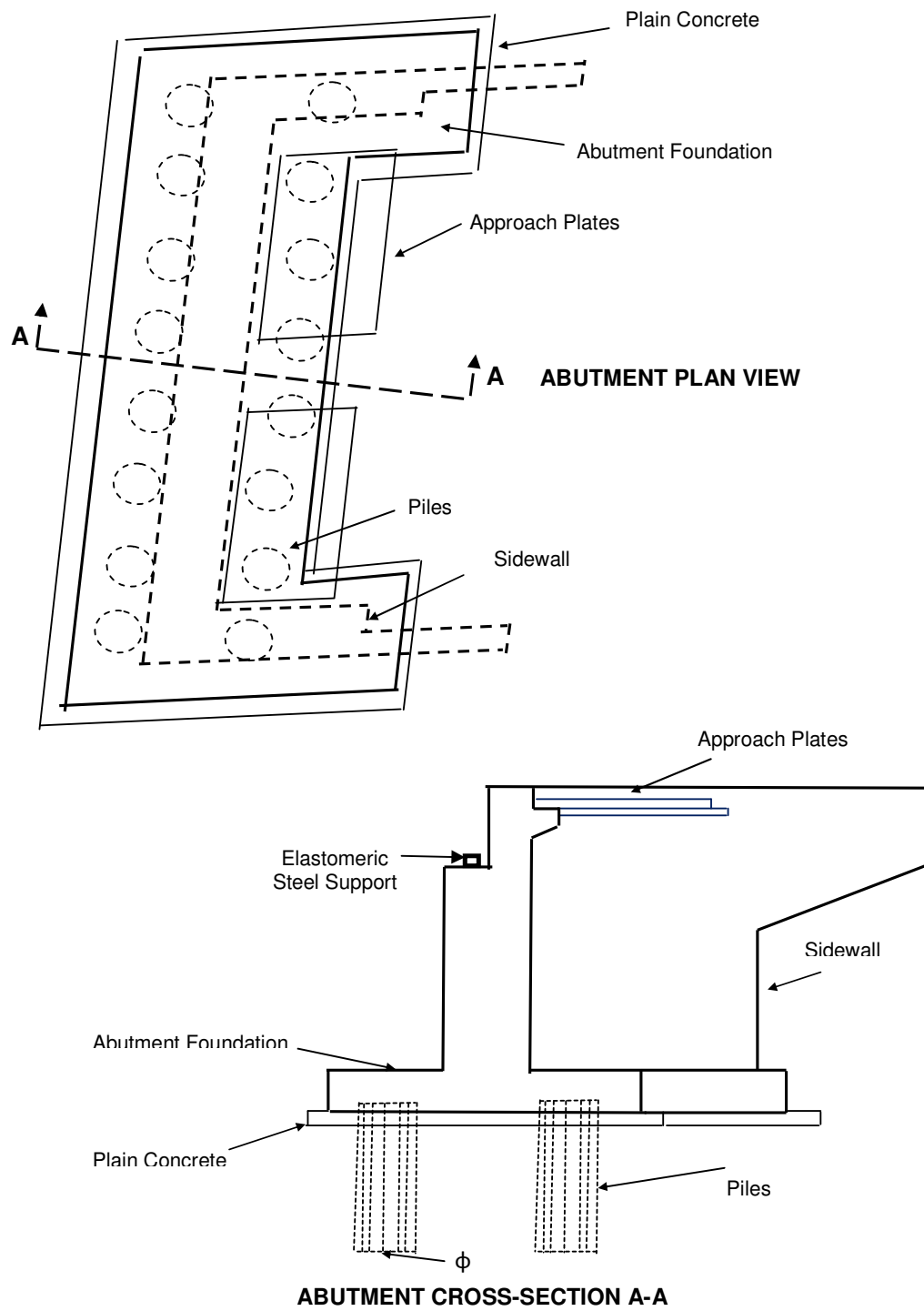


Figure B.1. Schematics for abutments.

Table B.4. Sample input table for cost calculation of piers.

Pier Cost Calculation Input Table		
Bridge Project: Bitlis Creek-9		
Definition	Value	Unit
Number of superstructure slabs on the pier ceiling	1	
Piles Exist ?	N	
Number of piles	0	
Diameter of 1 piles	0.00	cm
Length of 1 pile	0.00	m
Pier Foundation Dimensions		
Basement plain concrete height	0.25	m
Basement plain concrete width	5.50	m
Basement plain concrete length (for 1 slab)	30.50	m
Basement height	2.00	m
Basement width	5.00	m
Basement length	30.00	m
Pier Column Dimensions		
Number of pier columns on each (1) slab	4	
Pier column height	9.77	m
Pier column length (rectangular part)	2.00	m
Pier column width (diameter of curved section)	1.00	m
Pier column heading girder-1 height (transverse direction)	0.75	m
Pier column heading girder-1 width (transverse direction)	2.20	m
Pier column heading girder length (transverse direction)	30.27	m
Pier column heading girder-2 height (transverse direction)	1.07	m
Pier column heading girder-2 width (transverse direction)	0.40	m
Pier Steel Amounts		
8-12mm steel amount (foundation and columns along the all slabs)	1.70	tons
14-28mm steel amount (foundation and columns along the all slabs)	69.82	tons

Table B.4 (Continued). Sample input table for cost calculation of piers.

Pier Cost Calculation Input Table		
Bridge Project: Bitlis Creek-9		
Pier Elastomeric Steel Supports		
Number of elastomeric steel support on the pier	58	
UNIT COSTS		
Construction of Piles having inner diameter of ϕ cm (0 - L m)	218.68	/m
16.101/K: "Plain Concrete (Foundations)"	54.58	/m ³
16.132/K: "Reinforced Concrete"	142.80	/m ³
21.011: "Concrete & Reinf. Concrete Formwork (Plain Surface)"	9.73	/m ²
21.013: "Concrete & Reinf. Concrete Formwork (Grater Surface)"	11.89	/m ²
21.057: "Scaffolding for Wood Formworks (4 - 6m)"	3.54	/m ³
23.014: "8-12mm Steel"	895.13	/tons
23.015: "14-28mm Steel"	837.81	/tons
23.250: "Bridge Steel Support"	6.24	/kgs
23.252: "Copper Plate"	9.62	/kgs
23.254: "Lead Plate"	3.74	/kgs

Table B.5. Sample details table for cost calculation of piers.

Pier Cost Calculation Details Table								
Bridge Project: Bitlis Creek-9								
Work Type	Work No	quantity	Length	Width	Height	Amount	Unit	Sum
-	-	-	(m)	(m)	(m)	-	-	-
Construction of Piles having inner diameter of ϕ cm (0 - L m)	16.074/K-2							
Pier foundation		0	0.00			0.00	m	
							m	0.00
Plain Concrete (Foundations)	16.101/K							
Pier footing basement		1	30.50	5.50	0.25	41.938	m ³	
							m ³	41.938
Reinforced Concrete	16.132/K							
Pier footing basement		1	30.00	5.00	2.00	300.000	m ³	
Pier body		4	2.00	1.00	9.77	78.160	m ³	
		4	0.79	1.00	9.77	30.693	m ³	
		1	30.27	2.20	0.75	49.952	m ³	
		1	30.27	0.40	1.07	12.957	m ³	
							m ³	471.762
Concrete & Reinf. Concrete Formwork (Plain Surface)	21.011							
Pier footing basement		1	70.00		2.00	140.00	m ²	
							m ²	140.00

Table B.5 (Continued). Sample details table for cost calculation of piers.

Pier Cost Calculation Details Table								
Bridge Project: Bitlis Creek-9								
Concrete & Reinf. Concrete Formwork (Grater Surface)	21.013							
Pier column		8	2.00		9.77	156.32	m ²	
		8	1.57		9.77	122.77	m ²	
Pier heading girder		2	30.27		0.75	45.41	m ²	
		2	30.27		1.07	64.79	m ²	
		2	2.20		0.75	3.30	m ²	
		2	0.40		1.07	0.86	m ²	
		1	30.27		1.20	36.33	m ²	
							m ²	429.78
Scaffolding for Wood Formwork (4 - 6m)	21.057							
Pier footing basement		1	70.00	1.00	2.00	70.000	m ³	
Pier columns		8	2.00	4.89	9.77	381.812	m ³	
		8	1.57	4.89	9.77	299.874	m ³	
Pier heading girder		2	30.27	5.80	11.59	2,033.32	m ³	
		2	1.30	5.80	11.59	87.313	m ³	
							m ³	2,872.323
8-12mm Steel	23.014							
Pier support foundation and columns		1			1.699	1.699	ton	
							tons	1.699

Table B.5 (Continued). Sample details table for cost calculation of piers.

Pier Cost Calculation Details Table								
Bridge Project: Bitlis Creek-9								
14-28mm Steel	23.015							
Pier support foundation and columns		1			69.817	69.817	ton	
							tons	69.817
Pier Elastomeric Steel Support	23.250							
		58	0.45	0.65	0.05	662.483	kgs	
							kgs	662.483
Pier Elastomeric Support Copper Plate	23.252							
		58	0.35	0.50	0.08	924.218	kgs	
							kgs	924.218
Pier Elastomeric Support Lead Plate	23.254							
		58	0.35	0.50	0.08	964.291	kgs	
							kgs	964.291

Table B.6. Sample results table for cost calculation of piers.

Tabular Results for Cost Calculation of Piers						
Bridge Project: Bitlis Creek-9						
Work No	Construction Type	Unit	Amount	Unit Cost	Cost	Cost %
A - CONSTRUCTION WORKS						
16.074/K-2	Construction of Piles having inner diameter of φ cm (0 - L m)	m	0.000	218.68	0.00	0.00
16.101/K	Plain Concrete (Foundations)	m ³	41.938	54.58	2,288.82	1.40
16.132/K	Reinforced Concrete	m ³	471.762	142.80	67,368.87	41.35
21.011	Concrete & Reinf. Concrete Formwork (Plain Surface)	m ²	140.00	9.73	1,362.71	0.84
21.013	Concrete & Reinf. Concrete Formwork (Grater Surface)	m ²	429.776	11.89	5,109.44	3.14
21.057	Scaffolding for wood formworks (4 - 6m)	m ³	2,872.323	3.54	10,153.98	6.23
23.014	8-12mm Steel	tons	1.699	895.13	1,520.82	0.93
23.015	14-28mm Steel	tons	69.817	837.81	58,493.29	35.90
23.250	Pier Elastomeric Steel Support	kgs	662.483	6.24	4,134.51	2.54
23.252	Copper Plate	kgs	924.218	9.62	8,889.73	5.46
23.254	Lead Plate	kgs	964.291	3.74	3,607.33	2.21
	TOTAL COST				162,929.50	100.00

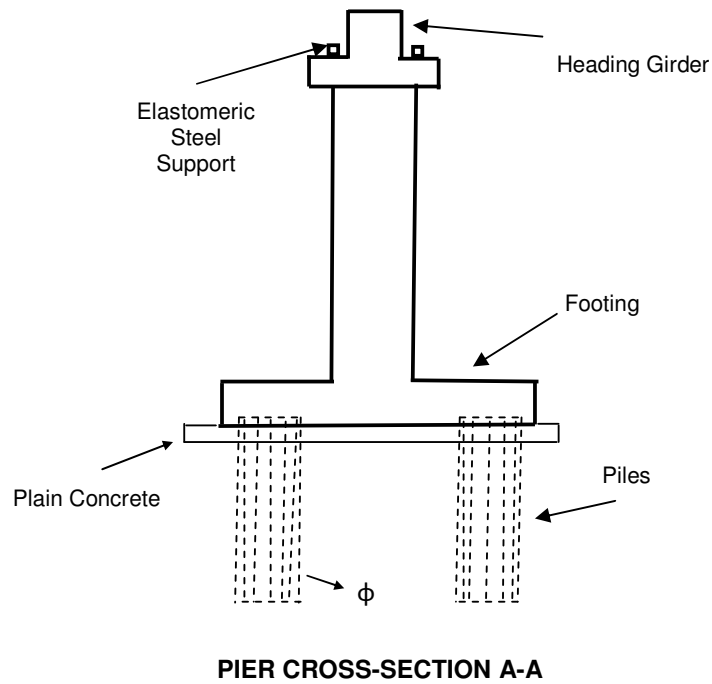
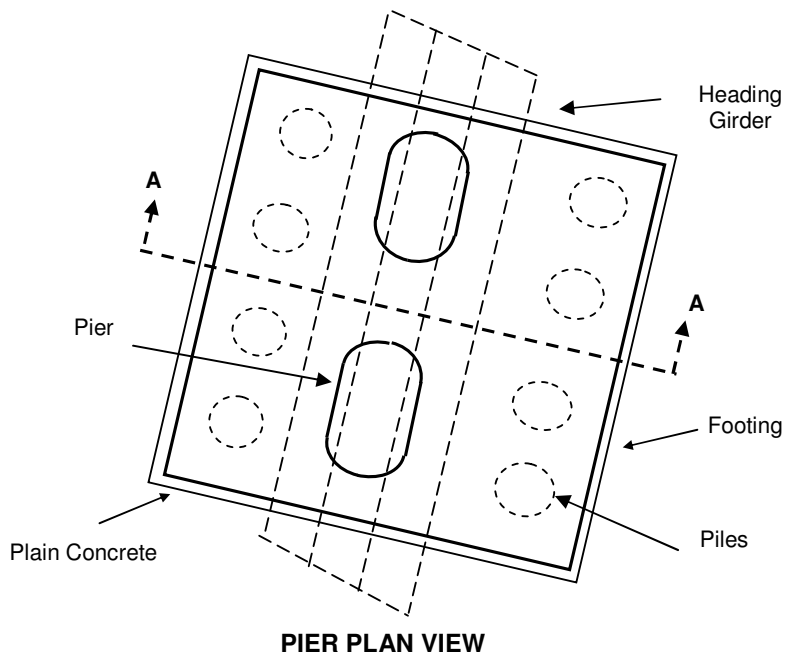


Figure B.2. Schematics for piers.

Table B.7. Sample input table for cost calculation of superstructure.

Superstructure Cost Calculation Input Table		
Bridge Project: Bitlis Creek-9		
Definition	Value	Unit
Span Length	16.00	m
Slab width	24.00	m
Number of Slabs	1	
Slab height	0.25	m
Pedestrian road height	0.25	m
Pedestrian road width-1	1.43	m
Pedestrian road width-2	1.43	m
Number of prestressed-concrete girders per total bridge width/slabs	29	
Prestressed-concrete girder dimensions		
Top flange top-width	0.80	m
Top flange height	0.10	m
Top flange bottom-width	0.15	m
Top flange height-1	0.08	m
Web thickness	0.15	m
Top flange height-2	0.00	m
Web height	0.50	m
Bottom flange top-width	0.50	m
Bottom flange height-1	0.08	m
Bottom flange height	0.15	m
Bottom flange bottom-width	0.50	m
Prefabricated front-members		
Number of prefabricated front-members Pc1	21	

Table B.7 (Continued). Sample input table for cost calculation of superstructure.

Superstructure Cost Calculation Input Table		
Bridge Project: Bitlis Creek-9		
Number of prefabricated front-members Pc2	0	
Prefabricated front-members Pc width	0.07	m
Prefabricated front-members Pc height	0.60	m
Prefabricated front-members Pc1 length	1.49	m
Prefabricated front-members Pc2 length	1.39	m
8-12mm steel weight		
Girder (for 1-girder)	1.02	tons
Slab (for 1-span)	10.89	tons
14-28mm steel weight		
Girder (for 1-girder)	0.28	tons
Prefabricated front-members (Total: Pc1+Pc2)	0.41	tons
Superstructure Barriers		
Number of vertical members per 1m length (for 1 side)	5	
Length of 1 vertical member	0.95	m
Number of horizontal members per 1m length (for 1 side)	2	
UNIT COSTS		
16.132/K: "Reinf.Conc"	142.80	/m ³
16.132/K-1: "Reinf.Conc (Slabs of I-girders)"	190.35	/m ³
16.136/K-1: "Placement of Precast Girders"	39.26	/tons
16.137/K-1-A: "Reinf.Conc (I-girders)"	321.54	/m ³
21.013: "Concrete Formwork (Grater Surface)"	11.89	/m ²
23.014: "8-12mm Steel"	895.13	/tons
23.015: "14-28mm Steel"	837.81	/tons
23.176/K: "Profiled Steel Barrier Workmanship (painting excluded)"	2,078.05	/tons
25.016: "Painting of Steel Members"	9.47	/m ²

Table B.8. Sample details table for cost calculation of superstructure.

Superstructure Cost Calculation Details Table								
Bridge Project: Bitlis Creek-9								
Work Type	Work No	quantity	Length	Width	Height	Amount	Unit	Sum
-	-	-	(m)	(m)	(m)	-	-	-
Reinforced Concrete	16.132/K							
Prefabricated front-member Pc1		21	1.49	0.60	0.07	1.314	m ³	
Prefabricated front-member Pc2		0	1.39	0.60	0.07	0.000	m ³	
							m ³	1.31
Reinf.Conc (Slabs of I-girders)	16.132/K-1							
Superstructure slab		1	16.00	24.00	0.25	96.000	m ³	
Superstructure pedestrian road		1	16.00	1.43	0.25	5.700	m ³	
Superstructure pedestrian road		1	16.00	1.43	0.25	5.700	m ³	
							m ³	107.400
Placement of Precast Girders	16.136/K-1							
						322.944	tons	
							tons	322.944
Reinf.Conc (I-girders)	16.137/K-1-A							
The prestressed-concrete girders		29	16.00	0.80	0.10	37.120	m ³	
		29	16.00	0.48	0.08	16.530	m ³	
		29	16.00	0.15	0.00	0.000	m ³	
		29	16.00	0.15	0.50	34.800	m ³	

Table B.8 (Continued). Sample details table for cost calculation of superstructure.

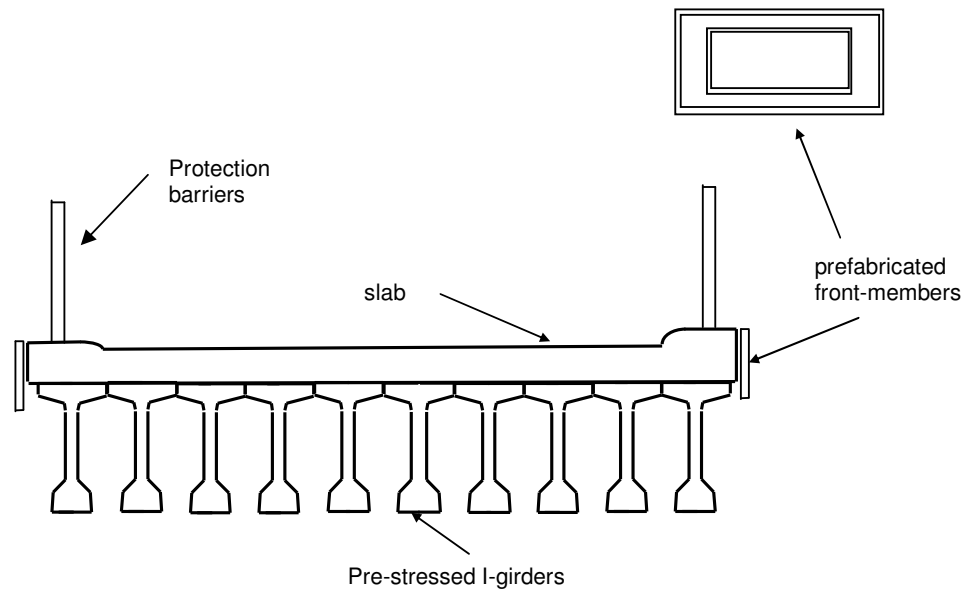
Superstructure Cost Calculation Details Table								
Bridge Project: Bitlis Creek-9								
		29	16.00	0.33	0.08	11.310	m ³	
		29	16.00	0.50	0.15	34.800	m ³	
							m ³	134.56
Concrete Formwork (Grater Surface)	21.013							
Prefabricated front-member Pc1		21	4.18		0.07	6.14	m ²	
Prefabricated front-member Pc2		0	3.98		0.07	0.00	m ²	
Pedestrian road		2	16.00		0.25	8.000	m ²	
							m ²	14.14
8-12mm Steel	23.014							
Girders		29			1.019	29.551	tons	
Slab		1			10.890	10.890	tons	
							tons	40.441
14-28mm Steel	23.015							
Girders		29			0.284	8.236	tons	
Prefabricated front-members (Total: Pc1+Pc2)		1			0.410	0.410	tons	
							tons	8.646
Profiled Steel Barrier Workmanship (painting excluded)	23.176/K							

Table B.8 (Continued). Sample details table for cost calculation of superstructure.

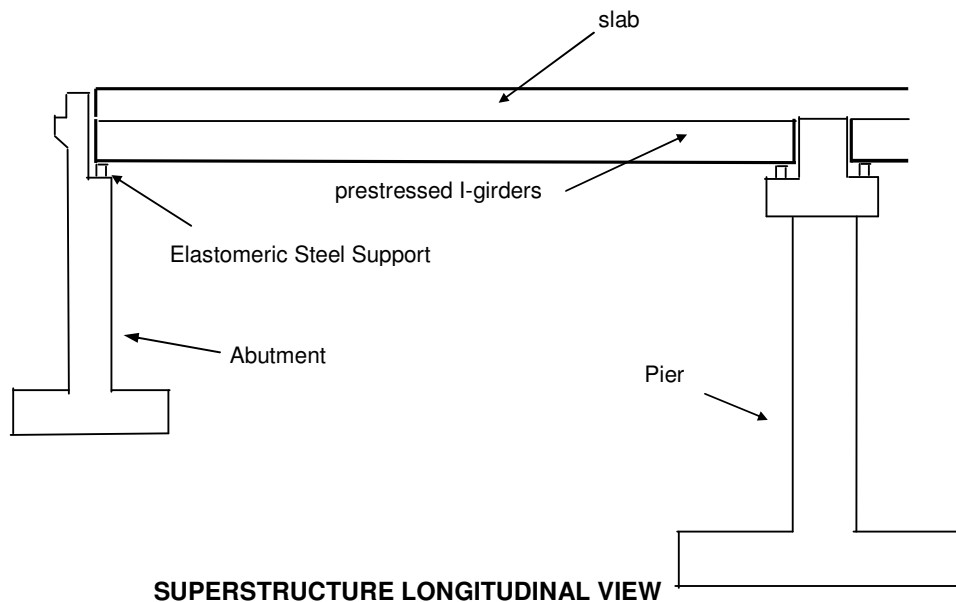
Superstructure Cost Calculation Details Table								
Bridge Project: Bitlis Creek-9								
Vertical members L 100 x 100 x 10		160	0.95		0.02	2.280	tons	
Longitudinal members L 100 x 100 x 10		4	16.00		0.02	0.960	tons	
							tons	3.240
Painting of Steel Members	25.016							
Vertical members L 100 x 100 x 10		160	0.95	0.10	0.10	60.80	m ²	
Longitudinal members L 100 x 100 x 10		4	16.00	0.10	0.10	25.60	m ²	
							m ²	86.40

Table B.9. Sample resultstable for cost calculation of superstructure.

Tabular Results for Cost Calculation of Superstructure						
Bridge Project: Bitlis Creek-9						
Work No	Construction Type	Unit	Amount	Unit Cost	Cost	Cost %
A - CONSTRUCTION WORKS						
16.132/K	Reinforced Concrete	m ³	1.314	142.80	187.64	0.15
16.132/K-1	Reinf.Conc (Slabs of I-girders)	m ³	107.400	190.35	20,443.71	16.00
16.136/K-1	Placement of Precast Girders	tons	322.944	39.26	12,679.27	9.93
16.137/K-1-A	Reinf.Conc (I-girders)	m ³	134.560	321.54	43,266.90	33.87
21.013	Concrete Formwork (Grater Surface)	m ²	14.14	11.89	168.16	0.13
23.014	8-12mm Steel	tons	40.441	895.13	36,199.84	28.34
23.015	14-28mm Steel	tons	8.646	837.81	7,243.69	5.67
23.176/K	Profiled Steel Barrier Workmanship (painting excluded)	tons	3.240	2,078.05	6,732.88	5.27
25.016	Painting of Steel Members	m ²	86.400	9.47	818.50	0.64
	TOTAL COST				127,740.59	100.00



SUPERSTRUCTURE CROSS-SECTIONAL VIEW



SUPERSTRUCTURE LONGITUDINAL VIEW

Figure B.3. Schematics for superstructures.

APPENDIX C

COMPARISON OF GENETIC ALGORITHMS AND DYNAMIC PROGRAMMING OPTIMIZATION TECHNIQUES

C.1 General

In this study, two different optimization approaches were considered. These are dynamic programming and Genetic Algorithms as mentioned in Chapter 5. This study utilizes GA as its major optimization approach due a number of reasons. In this context, a comparative study is performed between these two approaches in order to assess their characteristics.

Dynamic programming is based on enumeration of all the possible alternatives in a decision problem such that some of them are eliminated by dividing the whole problem into sub-problems. This yields a considerable amount of reduction in the number of all alternatives; in other words the search space is narrowed by this way. However, there are still a considerable amount of workload, because all of the alternatives in the narrowed search space are straightforwardly evaluated without any guidance. But for some type of problems, the reduction in the search space may be quite useful to find an optimal solution.

As discussed briefly in Chapter 5, dynamic programming is implemented by dividing the whole problem into sub-problems. Therefore, the optimization of the sub-problems in an inter-connected fashion leads to the optimization of the whole problem, resulting elimination of some of the alternatives in a naive approach. However, the formulation of an optimization problem in terms of dynamic

programming approach is not so easy, because it is usually not obvious to see the sub-problems of the whole problem, even it may be impractical to formulate.

On the other hand, GA uses a guidance in order to approach the best solution within the search space. This guidance, which is also called as “heuristics”, is the “Darwinian evolution phenomenon” as discussed in Chapter 4. This mechanism of GA holds an advantage over dynamic programming, because even the size of the search space increases, GA can still converge to an optimum solution in a reasonable efficiency, which is not the case in dynamic programming. The weakness of GA over dynamic programming is generally due to the probabilistic nature of GA. As a probabilistic approach, the effectiveness of GA depends on the related probabilistic parameters. Therefore, a sensitivity analysis is usually required to assess these parameters on the applied problem. However, since dynamic programming is deterministic, there is not such a workload in the implementation of dynamic programming.

In a summarized form, the comparison of two approaches is presented in Table C.1 in the aspect of this study. Due its generic behavior and its ease of extensibility for the inclusion of additional decision variables, GA is selected as the primary optimization technique of AIROB.

Table C.1. Summarized comparison table for GA versus dynamic programming.

Dynamic Programming	GA
Deterministic	Probabilistic
Highly problem dependent	Generic
May be difficult to construct the problem	More straight-forward
May not be suitable to extend the optimization problem for additional decision variables	Highly extensible
Time consuming when number of spans, N_s increases	Can handle large search space with a better performance

C.2 Case Study

Comparison of Dynamic Programming and GA is illustrated on a case study. The case study problem is very similar to the application problem presented in Chapter 6. The cross-sectional geometry at the bridge section is slightly different than the bridge section of the application problem in Chapter 6 (see Figure C.1). All the remaining input data are exactly the same with the problem in Chapter 6. This problem is only solved for deterministic constraints case with three number of spans, as it is expected to be the overall optimized solution according to the results of the problem in Chapter 6. Besides, the computational efficiency for the dynamic programming approach is most convenient for number of span, $N_s=3$. When the number of spans increases, the computational overload increases abruptly, causing to an impractical test problem for dynamic programming.

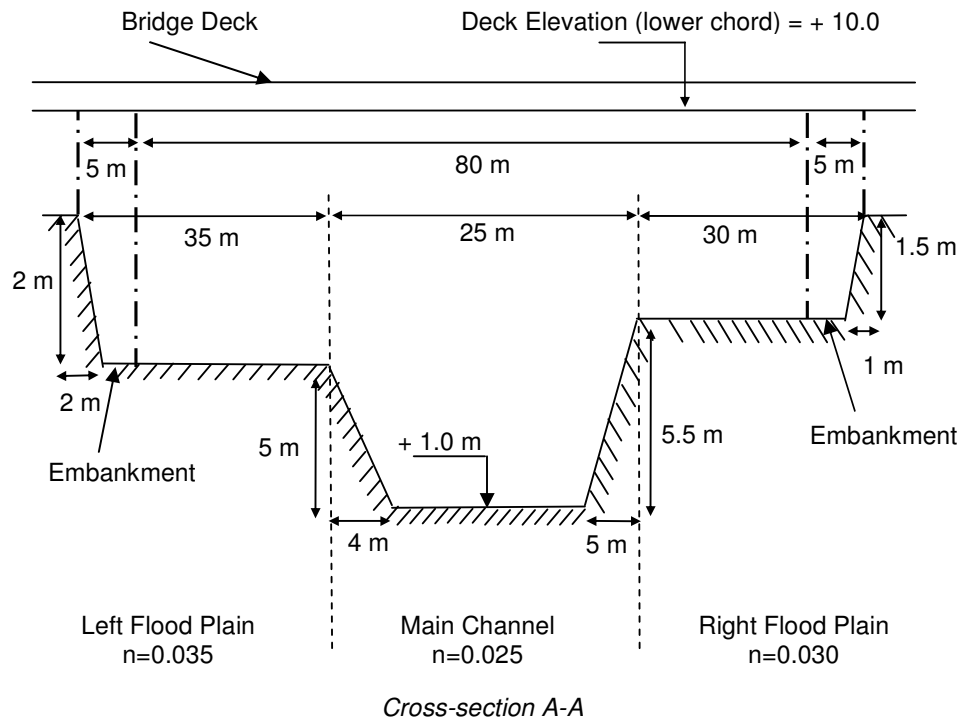


Figure C.1. River cross-section details at bridge opening for the case study (Not to scale).

In addition to the aforementioned information regarding the problem, this problem does not impose the span arrangements to be symmetrical. It is because that the formulation of dynamic programming for a symmetrical span arrangement requires more comprehensive and generic implementation of dynamic programming, which AIROB does not involve such consideration. Furthermore, since the computational details about the solution of the problem by GA is discussed and explained in Chapter 6, in this section the focus is to be on the dynamic programming in terms of the computational tasks.

In the light of the above clarifications about the case study, the problem defined above is solved by both GA and dynamic programming approach. It is found that the results given by both techniques are very similar to each other (see Table C.2). This verifies that both techniques runs in a well established implementation.

Table C.2. Comparison table for the results of GA and dynamic programming approach for the case study.

$N_s=3$ (Deterministic Constraints)	GA Results	Dynamic Programming Results
Span Arrangements (m)	28– 34 - 16	29 – 33.5 – 15.5
Depth of Footings, D_f (m)	2.50 – 3.07 – 2.96 – 1.17	2.63 – 3.0 – 3.0 - 1.13
Total Cost (US\$)	1,234,990	1,236,231

Dynamic programming strategy is implemented base on the recursive equation of the optimization problem of this study as given in Equation (5.10). Starting from one of the abutments, which is abutment-1 in this application, each span of the bridge is evaluated in series up to the other abutment. Therefore, each span of the bridge holds as the stage of the dynamic programming at which a decision is required to be given for the selection of the optimal span length. In this context, since this case study problem is for $N_s=3$, the dynamic programming formulation of this problem has three stages. The tabular results representing the minimum states for each of these stages are presented in Tables C.3 to C.6.

Table C.3. The tabular results of stage-0 for the case study in dynamic programming approach.

Stage - 0			
S_{p_tot}	X_{d_min}	d_{f_min}	Cost_{min}
12.50	12.50	1.13	757,434
13.42	13.42	1.13	259,799
14.33	14.33	1.13	265,368
15.25	15.25	1.13	270,880
16.17	16.17	1.13	307,704
17.08	17.08	1.13	312,132
18.00	18.00	1.13	320,459
18.92	18.92	1.13	328,127
19.83	19.83	1.13	335,250
20.75	20.75	1.13	343,186
21.67	21.67	1.13	352,219
22.58	22.58	1.13	361,967
23.50	23.50	1.13	371,918
24.42	24.42	1.13	381,678
25.33	25.33	1.13	390,999
26.25	26.25	1.13	399,829
27.17	27.17	1.13	408,128
28.08	28.08	1.13	415,825
29.00	29.00	1.13	422,638
29.92	29.92	1.13	428,223
30.83	30.83	1.13	433,359
31.75	31.75	1.13	440,193
32.67	32.67	1.13	448,592
33.58	33.58	1.13	457,648
34.50	34.50	1.13	467,291
35.42	35.42	1.13	477,703
36.33	36.33	1.13	489,170
37.25	37.25	1.13	502,081
38.17	38.17	1.13	516,942
39.08	39.08	1.13	534,366

Table C.4. The tabular results of stage-1 for the case study in dynamic programming approach.

Stage -1				Stage - 0			
S _{p_tot}	X _{d_min}	d _{f_min}	Cost _{min}	S _{p_tot}	X _{d_min}	d _{f_min}	Cost _{min}
25.00	12.50	3.00	985,593	12.50	12.50	1.13	757,434
25.92	12.50	3.00	487,959	13.42	13.42	1.13	259,799
26.83	12.50	3.00	493,528	14.33	14.33	1.13	265,368
27.75	12.50	3.00	499,039	15.25	15.25	1.13	270,880
28.67	15.25	3.00	504,611	13.42	13.42	1.13	259,799
29.58	16.17	3.00	510,162	13.42	13.42	1.13	259,799
30.50	15.25	3.00	515,691	15.25	15.25	1.13	270,880
31.42	16.17	3.00	521,243	15.25	15.25	1.13	270,880
32.33	17.08	3.00	526,963	15.25	15.25	1.13	270,880
33.25	18.00	3.00	533,009	15.25	15.25	1.13	270,880
34.17	18.92	3.00	539,548	15.25	15.25	1.13	270,880
35.08	20.75	3.00	544,694	13.42	13.42	1.13	259,799
36.00	19.83	3.00	546,885	15.25	15.25	1.13	270,880
36.92	20.75	3.00	555,775	15.25	15.25	1.13	270,880
37.83	21.67	3.00	564,404	15.25	15.25	1.13	270,880
38.75	22.58	3.00	573,070	15.25	15.25	1.13	270,880
39.67	23.50	3.00	581,986	15.25	15.25	1.13	270,880
40.58	24.42	3.00	590,952	15.25	15.25	1.13	270,880
41.50	25.33	3.00	599,763	15.25	15.25	1.13	270,880
42.42	26.25	3.00	608,310	15.25	15.25	1.13	270,880
43.33	27.17	3.00	616,606	15.25	15.25	1.13	270,880
44.25	28.08	3.00	624,727	15.25	15.25	1.13	270,880
45.17	29.00	3.00	632,775	15.25	15.25	1.13	270,880
46.08	29.92	3.00	640,845	15.25	15.25	1.13	270,880
47.00	30.83	3.00	649,031	15.25	15.25	1.13	270,880
47.92	31.75	3.00	657,419	15.25	15.25	1.13	270,880
48.83	32.67	3.00	666,103	15.25	15.25	1.13	270,880
49.75	33.58	3.00	675,196	15.25	15.25	1.13	270,880
50.67	34.50	3.00	684,848	15.25	15.25	1.13	270,880
51.58	35.42	3.00	695,266	15.25	15.25	1.13	270,880

Table C.4 (Continued). The tabular results of stage-1 for the case study in dynamic programming approach.

Stage -1				Stage - 0			
S _{p_tot}	X _{d_min}	d _{f_min}	Cost _{min}	S _{p_tot}	X _{d_min}	d _{f_min}	Cost _{min}
52.50	36.33	3.00	706,737	15.25	15.25	1.13	270,880
53.42	37.25	3.00	719,652	15.25	15.25	1.13	270,880
54.33	38.17	3.00	734,517	15.25	15.25	1.13	270,880
55.25	32.67	3.00	745,830	21.67	21.67	1.13	352,219
56.17	33.58	3.00	754,918	21.67	21.67	1.13	352,219
57.08	33.58	3.00	764,243	22.58	22.58	1.13	361,967
58.00	34.50	3.00	773,891	22.58	22.58	1.13	361,967
58.92	34.50	3.00	783,626	23.50	23.50	1.13	371,918
59.83	35.42	3.00	794,039	23.50	23.50	1.13	371,918
60.75	36.33	3.00	805,507	23.50	23.50	1.13	371,918
61.67	37.25	3.00	818,419	23.50	23.50	1.13	371,918
62.58	38.17	3.00	833,280	23.50	23.50	1.13	371,918
63.50	39.08	3.00	850,705	23.50	23.50	1.13	371,918
64.42	39.08	3.00	876,411	24.42	24.42	1.13	381,678
65.33	39.08	3.00	901,367	25.33	25.33	1.13	390,999
66.25	39.08	3.00	924,716	26.25	26.25	1.13	399,829
67.17	32.67	5.78	1,010,751	33.58	33.58	1.13	457,648
68.08	33.58	5.78	1,019,989	33.58	33.58	1.13	457,648
69.00	34.50	5.78	1,029,762	33.58	33.58	1.13	457,648
69.92	35.42	5.78	1,040,283	33.58	33.58	1.13	457,648
70.83	36.33	5.78	1,051,840	33.58	33.58	1.13	457,648
71.75	37.25	5.78	1,064,827	33.58	33.58	1.13	457,648
72.67	38.17	5.78	1,079,751	33.58	33.58	1.13	457,648
73.58	36.33	5.78	1,096,541	36.33	36.33	1.13	489,170
74.50	36.33	5.78	1,109,452	37.25	37.25	1.13	502,081
75.42	37.25	5.78	1,122,461	37.25	37.25	1.13	502,081
76.33	37.25	5.78	1,137,322	38.17	38.17	1.13	516,942
77.25	38.17	5.78	1,152,265	38.17	38.17	1.13	516,942
78.17	39.08	5.78	1,169,760	38.17	38.17	1.13	516,942

Table C.5. The tabular results of stage-2 for the case study in dynamic programming approach.

Stage - 2				Stage - 1			
S _{p_tot}	X _{d_min}	d _{f_min}	Cost _{min}	S _{p_tot}	X _{d_min}	d _{f_min}	Cost _{min}
37.50	12.50	3.00	1,222,264	25.00	12.50	3.00	985,593
38.42	13.42	3.00	1,227,872	25.00	12.50	3.00	985,593
39.33	12.50	3.00	755,157	25.92	12.50	3.00	487,959
40.25	13.42	3.00	760,765	25.92	12.50	3.00	487,959
41.17	14.33	3.00	766,304	25.92	12.50	3.00	487,959
42.08	15.25	3.00	771,809	25.92	12.50	3.00	487,959
43.00	16.17	3.00	777,361	25.92	12.50	3.00	487,959
43.92	17.08	3.00	783,081	25.92	12.50	3.00	487,959
44.83	18.00	3.00	789,127	25.92	12.50	3.00	487,959
45.75	18.92	3.00	795,669	25.92	12.50	3.00	487,959
46.67	19.83	3.00	803,059	25.92	12.50	3.00	487,959
47.58	20.75	3.00	812,156	25.92	12.50	3.00	487,959
48.50	21.67	3.00	821,122	25.92	12.50	3.00	487,959
49.42	22.58	3.00	829,006	25.92	12.50	3.00	487,959
50.33	23.50	3.00	837,537	25.92	12.50	3.00	487,959
51.25	24.42	3.00	846,553	25.92	12.50	3.00	487,959
52.17	25.33	3.00	855,378	25.92	12.50	3.00	487,959
53.08	26.25	3.00	863,923	25.92	12.50	3.00	487,959
54.00	27.17	3.00	872,214	25.92	12.50	3.00	487,959
54.92	28.08	3.00	880,332	25.92	12.50	3.00	487,959
55.83	29.00	3.00	888,373	25.92	12.50	3.00	487,959
56.75	29.92	3.00	896,441	25.92	12.50	3.00	487,959
57.67	30.83	3.00	904,622	25.92	12.50	3.00	487,959
58.58	31.75	3.00	913,007	25.92	12.50	3.00	487,959
59.50	12.50	3.00	918,774	46.08	29.92	3.00	640,845
60.42	12.50	3.00	911,562	47.00	30.83	3.00	649,031
61.33	12.50	3.00	902,637	47.92	31.75	3.00	657,419
62.25	12.50	3.00	900,183	48.83	32.67	3.00	666,103
63.17	13.42	3.00	905,791	48.83	32.67	3.00	666,103
64.08	14.33	3.00	911,330	48.83	32.67	3.00	666,103

Table C.5 (Continued). The tabular results of stage-2 for the case study in dynamic programming approach.

Stage - 2				Stage - 1			
S _{p_tot}	X _{d_min}	d _{f_min}	Cost _{min}	S _{p_tot}	X _{d_min}	d _{f_min}	Cost _{min}
65.00	15.25	3.00	916,835	48.83	32.67	3.00	666,103
65.92	16.17	3.00	922,386	48.83	32.67	3.00	666,103
66.83	17.08	3.00	928,107	48.83	32.67	3.00	666,103
67.75	18.00	3.00	934,153	48.83	32.67	3.00	666,103
68.67	18.92	3.00	940,691	48.83	32.67	3.00	666,103
69.58	19.83	3.00	947,901	48.83	32.67	3.00	666,103
70.50	20.75	3.00	964,918	49.75	33.58	3.00	675,196
71.42	21.67	3.00	973,399	49.75	33.58	3.00	675,196
72.33	22.58	3.00	982,353	49.75	33.58	3.00	675,196
73.25	23.50	3.00	991,475	49.75	33.58	3.00	675,196
74.17	24.42	3.00	1,000,526	49.75	33.58	3.00	675,196
75.08	25.33	3.00	1,009,351	49.75	33.58	3.00	675,196
76.00	26.25	3.00	1,017,890	49.75	33.58	3.00	675,196
76.92	27.17	3.00	1,026,175	49.75	33.58	3.00	675,196
77.83	28.08	3.00	1,034,286	49.75	33.58	3.00	675,196
78.75	29.00	3.00	1,042,323	49.75	<u>33.58</u>	3.00	675,196

Table C.6. Completed form of the dynamic programming result.

Completion of Dynamic PProgramming				Stage - 2			
S _{p_tot}	X _{d_min}	d _{f_min}	Cost _{min}	S _{p_tot}	X _{d_min}	d _{f_min}	Cost _{min}
78.81	-	-	1,236,231	78.75	<u>29.00</u>	3.00	1,042,323

If the tabular results are examined, the dynamic programming stops when the total length of the bridge is reached, which is 78.81 meters in this case study problem (see Table C.6.). The corresponding optimum span length decision for the last span length is found to be 29.00 m as the result of the previous sub-problem, Stage-2. This process continues recursively such that the

corresponding optimum span length decision of Stage-1 is 33.58 m, and the final optimum decision of Stage-0 is 15.25 m. Therefore, by assembling the optimum decisions of each stages inter-connected gives the resulting optimum span arrangement of the whole problem as (29.00 – 33.58 – 15.25) as given in Table C.2. For Tables C.4 to C.6, the underlined values indicate the optimal decision of the previous stage of the current stage, whereas the bold values are the remaining information about the corresponding decisions.

APPENDIX D

USER - MANUAL FOR AIROB

D.1 General Graphical User Interface Layout of AIROB

When AIROB is executed by clicking the executable file “AIROB.exe” in Microsoft Windows environment, the program starts with a main graphical user interface (GUI) windows, in which all the remaining GUI components can easily be accessible (see Figure D.1). This main window hold for the major component of user interaction so that closing this window also finishes the execution of software framework, AIROB.

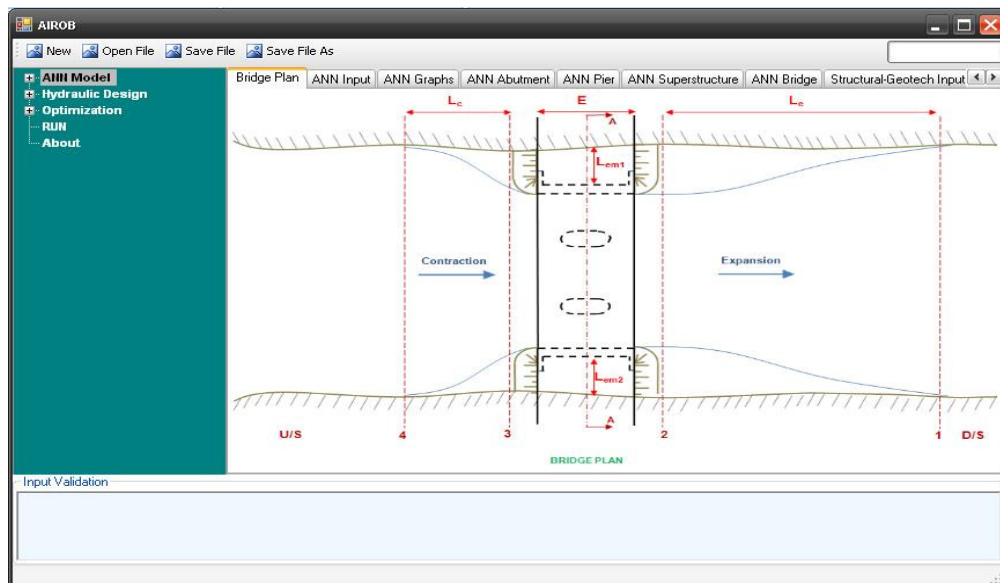


Figure D.1. General layout of AIROB graphical user interface.

The layout of the main window consists of a number of major GUI components, each has a specific function for conveniently directing AIROB. There are basically five components in the context of the main screen as follows:

- **Tab-Pages:** The innermost component of AIROB are composed of tab-pages, which is the major interaction part for the user. Each of these tab-pages holds for specific purpose about accessing and manipulating the numerical libraries of the framework, AIROB such as entering input data and displaying the corresponding output data in different forms.
- **Tree-view:** At the left part of the main windows, a “tree-view” GUI component lays out for quick accessing the tab-pages as a neighbouring GUI component. The listing of the numerical libraries of AIROB can be seen and accessed conveniently from this tree-view component in a hierarchical form.
- **Toolbar:** At the top of the main window, there exists a toolbar, on which there a number of buttons for accessing the general “File” management such as opening or saving the AIROB input data (see Figure D.2). In addition to these, the status of the execution details of AIROB can be followed by the corresponding GUI components on the toolbar such as “Progress Bar”.
- **Input Validation Bar:** The bottom of AIROB displays a enriched textbox for giving appropriate information about the user interaction in order to direct the user to employ the framework properly. The validation of input data is also displayed within the contents of this textbox.
- **Status Bar:** The most bottom of the main window hold the basic information about the name and path of the opened input file and similar file related information as in most of the Windows-based GUI programs.

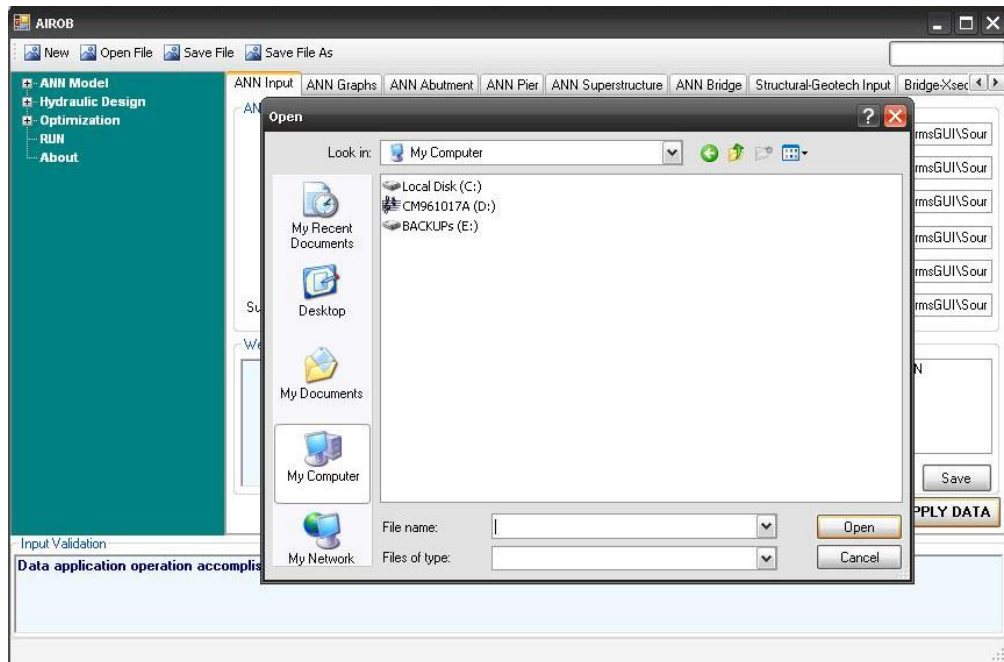


Figure D.2. Opening an AIROB file.

D.2 Tab-pages in AIROB

The main functionalities of the AIROB framework are accessible through the tab-pages. Each of these tab-pages serve for separate task within the content of AIROB. These are either user required input data for a particular library of AIROB or a corresponding output representation of a library such as graphical or tabular representations. In addition to these roles, some settings for the calculations are also accessible by these tab-pages.

AIROB is an extensive software framework, from which different applications regarding bridge hydraulics based applications can be derived. Therefore, the number of tab-pages can be extended regarding to the application requirements of the user. In this manual, the fundamental portions of these tab-pages within the content of this study is presented.

D.2.1 ANN Input

This tab-page is designed for holding the required input data for ANN models in AIROB (see Figure D.3). AIROB entails six ANN models, three of which are for design purposes of bridge structural components, and remaining are for the cost estimation of these components. Therefore, each of the ANN models require a model definition file, which are simple XML-based text documents that define the architecture of the ANN. These ANN model definition files are specified in the context of AIROB framework, and any user that would utilize ANN models in AIROB should construct the related ANN model according to this specification. This study already developed the necessary ANN model files that can be used within the AIROB. Therefore, for the users that do not require to load their personally developed ANN models, this tab-page can be disregarded. For the users to load their own ANN models, only requirement is to load the corresponding ANN files from the buttons “Open” next to the related ANN model as seen in Figure D.3.

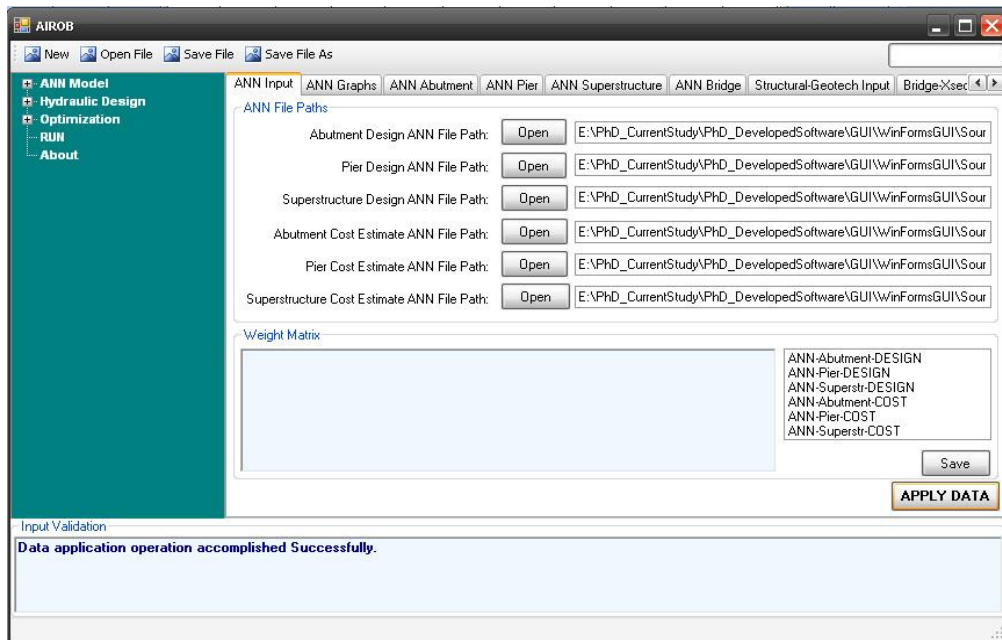


Figure D.3. ANN input tab-page.

The content of each file can be displayed under the textbox, named “Weight Matrix”. For the inputs to be effective, the user must press the button, “APPLY DATA”.

D.2.2 Structural-Geotechnical Input

In this tab-page, the structural and geotechnical related input data is presented to AIROB, such as the number of spans, abutment shape, pier shape, SPTN values, etc (see Figure D.4).

Parameter	Value
Number of Spans [Ns]	3
Symmetrical Span Arrangement	<input checked="" type="checkbox"/>
Abutment Type	[Dropdown]
Pier Type	[Dropdown]
Abutment-0 wall length [Lw] (m)	1.65
Abutment-1 wall length [Lw] (m)	1.65
Length of Embankment-0 [Lem0] (m)	5
Length of Embankment-1 [Lem1] (m)	5
Embankment Width (m)	5.0
Embankment Slope [1:mV]	0.5
Excavation Slope [1:mV]	1.0
SPTN (Abutment-0)	40
SPTN (Abutment-1)	40
SPTN (Piers)	40
Unit cost for 40cm thick Riprap (US\$) (m3)	40.31
Unit cost for Exc/Fill (US\$) (m3)	6.88
Unit cost for Compaction (US\$) (hrs)	0.834

Figure D.4. Structural–geotechnical input tab-page.

Some of the components have default values such as unit cost values, however they may be overridden if desired.

D.2.3 Inputs for the River Cross-sections at Bridge Site

In this section, the cross-sectional geometries for the bridge hydraulics and optimization tasks are introduced to AIROB. AIROB requires at least three cross sections for water surface profile calculations through a bridge opening. These are, cross-section at the exact location of the bridge, downstream cross-section and upstream (approach) cross-section. AIROB uses these cross-sections in order to automatically generate additional two cross-sections, at just downstream and just upstream of the bridge.

For each of the cross-section defined, the user can observe the graphical view of the corresponding cross-section and check his/her input data for verification. Figures D.5 through D.10 shows the sample input data tab-page and corresponding graph view successively for bridge cross-section, downstream cross-section and upstream cross-section, respectively.

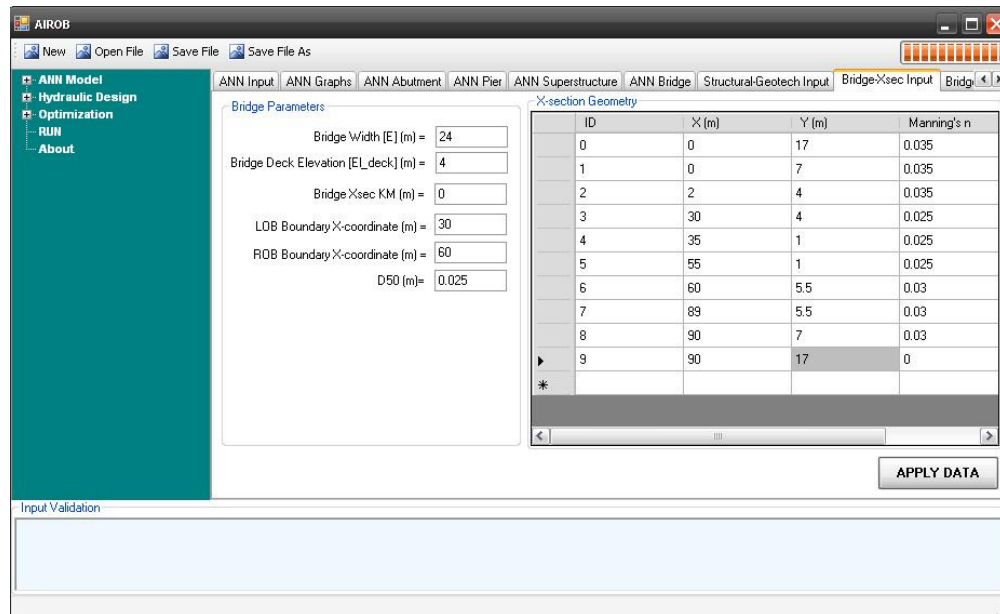


Figure D.5. Input data for bridge cross-section.

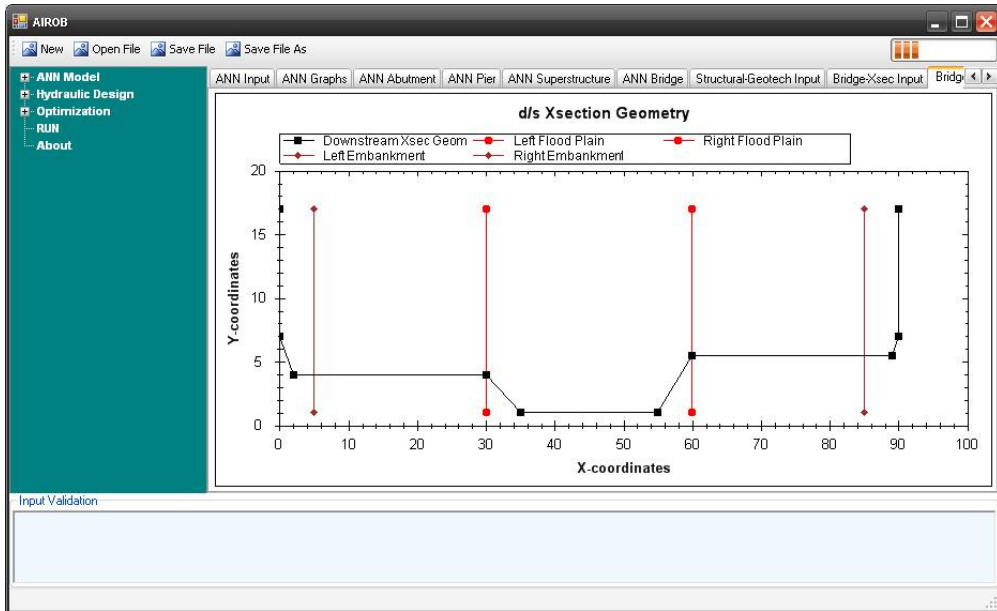


Figure D.6. Graphical view of bridge cross-section.

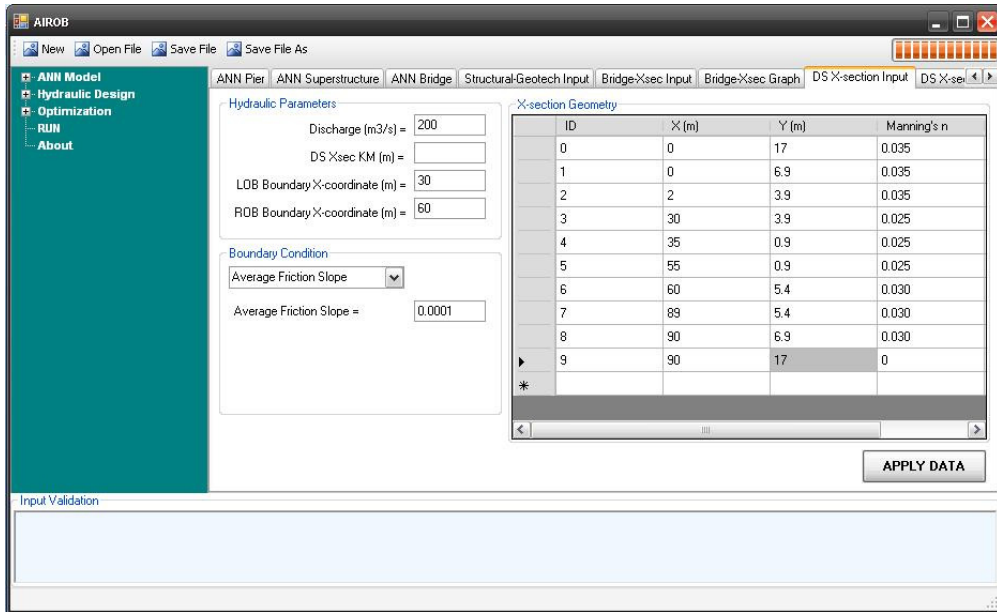


Figure D.7. Input data for the downstream cross-section.

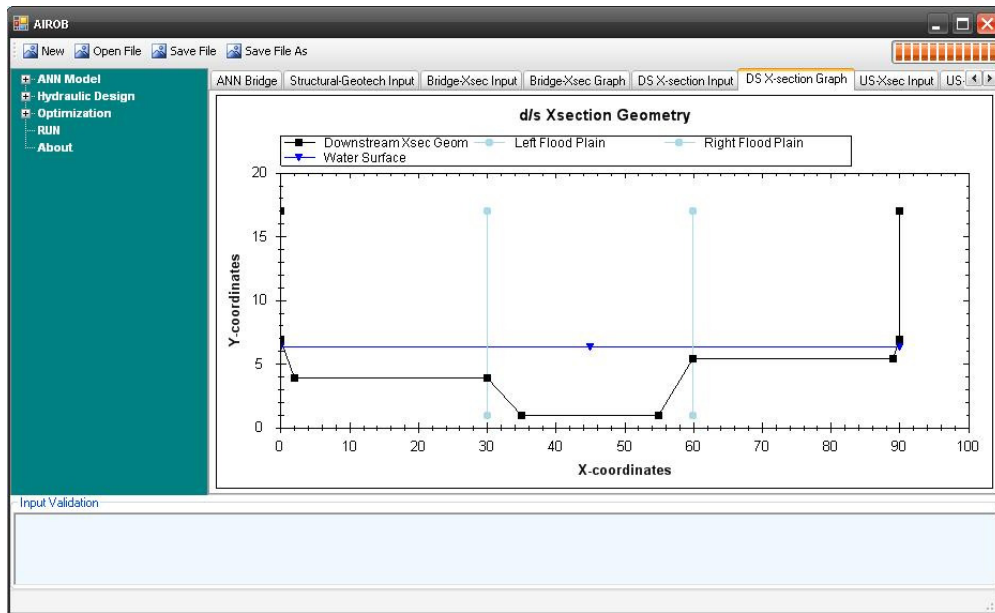


Figure D.8. Graphical view of the downstream cross-section.

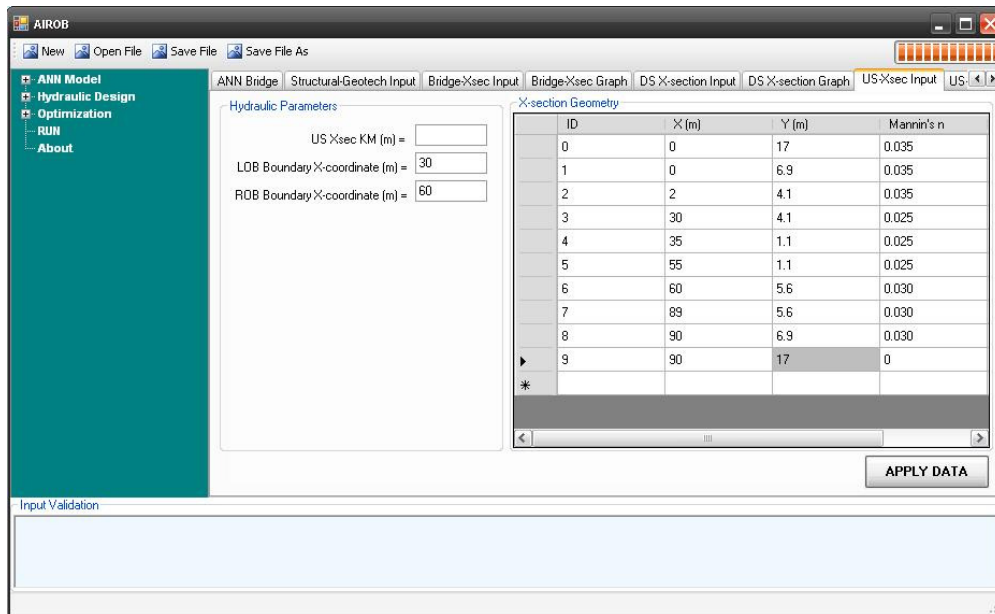


Figure D.9. Input data for the upstream cross-section.

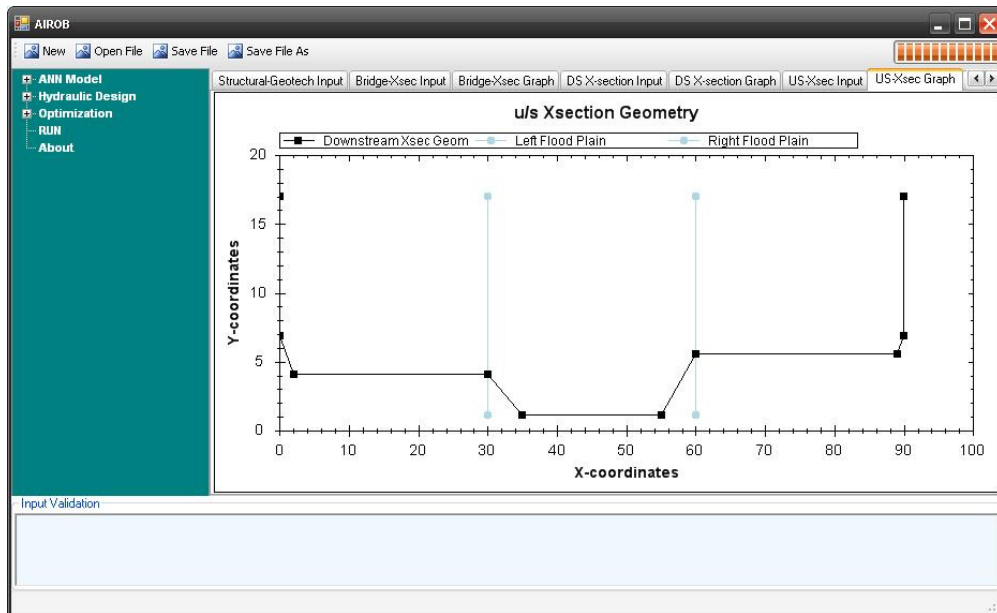


Figure D.10. Graphical view of the upstream cross-section.

The graphical view of the just downstream and just upstream cross-sections generated by AIROB can also be examined by the corresponding tab-pages of AIROB.

The input data requirements form for the cross-sections are very similar to the HEC-RAS (USACE, 1998) style, therefore any familiarities to HEC-RAS software facilitates the usage of AIROB in terms of consistency.

D.2.4 Optimization Engine Related Input Data

The optimization engine implemented by AIROB has also a number of settings to be specified. As the major optimization engine that AIROB utilized is genetic algorithms, the default input data for optimization part is related to GA parameters. Figure D.11 show the corresponding input data tab-page for the optimization data. In addition to GA parameters, some specification related to the

constraints of the optimization problem and the type of the constraints to be handled whether deterministic or reliability-based is also specified in this tab-page (see Figure D.11)

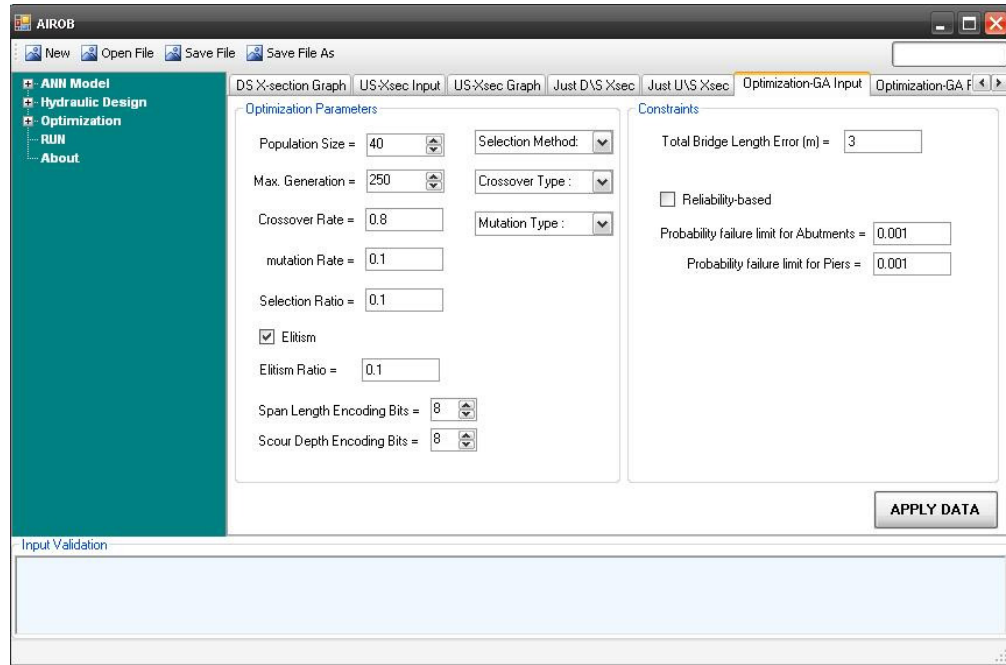


Figure D.11. Optimization engine related Input tab-page.

D.2.5 Calculation Settings

Within AIROB, there are several libraries associated to each other, therefore, various calculation settings also exist and may be specified by the user, even though most of them are defaulted by AIROB. In this tab-page which can be seen in Figure D.12, the required calculation options can be specified and thus AIROB can be directed to be executed in that specified manner. Some of these settings may increase the performance of optimization such as the calculation of water surface profile only once by sacrificing from precision a little. Besides, if the number of flow distribution slices is so high, the calculation performance also degrades, therefore an optimum number should be selected based on the

requirements of the related project. In anyway, AIROB has a wide range of fine-tuning in terms of calculation performance that can be specified.

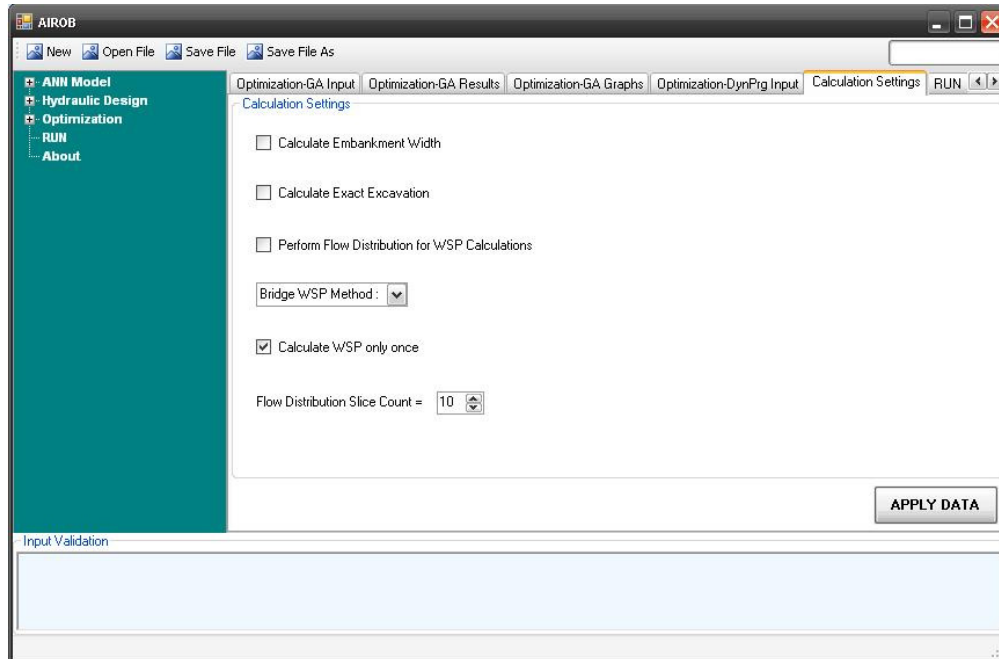


Figure D.12. Calculation settings tab-page.

D.2.6 Computational Process

Computation process is started by the use of this tab-page by clicking the button, "START" (see Figure D.13), after applying all the necessary input data correctly. During the execution, the progress of the calculations can be observed by various tab-pages such as the textual information and dynamically generated charts regarding the optimization tasks (see Figures D.14 and D.15).

According to the optimization process information, user can abort or pause the process and examine the results given by output up to that paused state. It is also possible to resume the computation by any time.

The results of AIROB either can be viewed from the tabular representations in GUI or they may be saved to file in a comma separated value (CSV) format to access the results through other software such as MS Excel, etc (see Figure D.16).

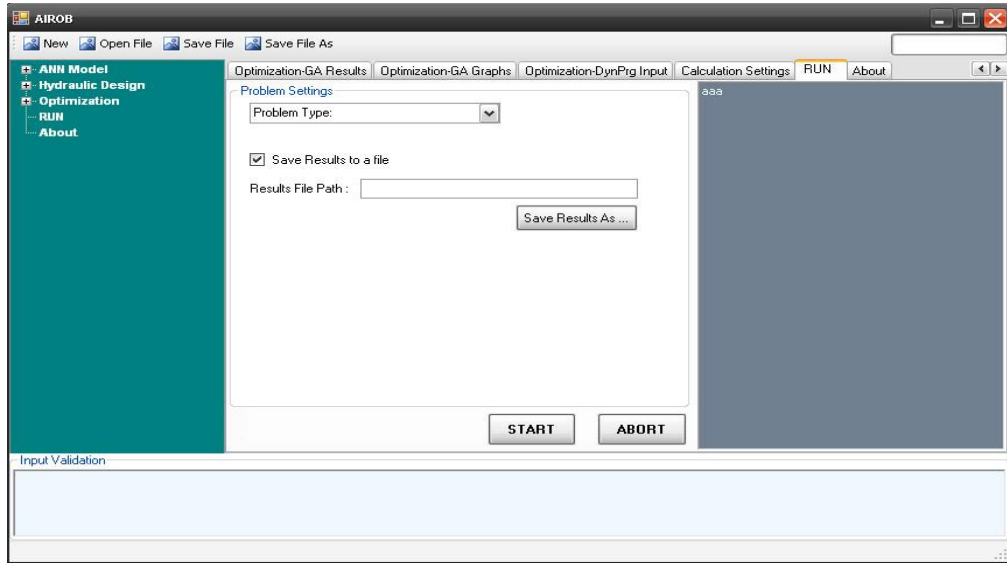


Figure D.13. Computational process related tab-page.

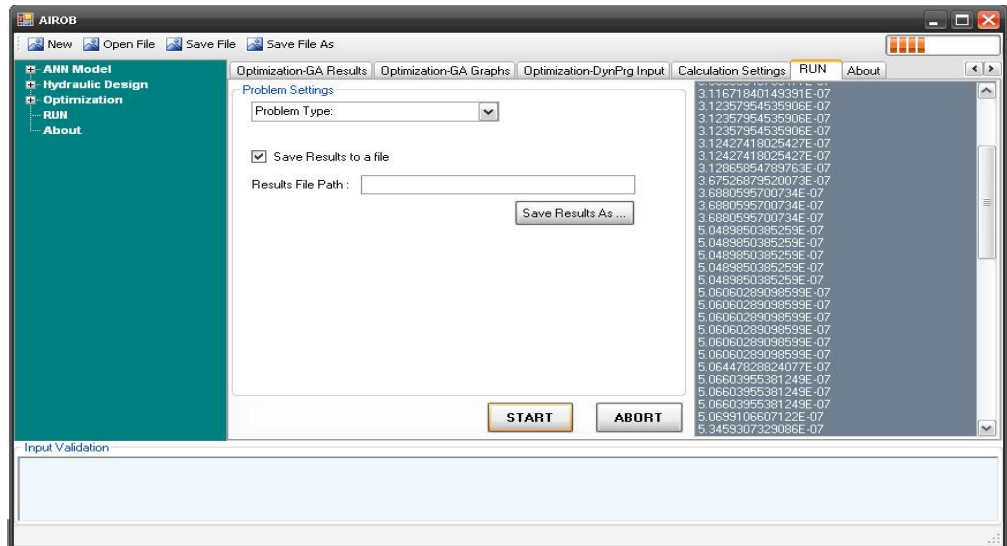


Figure D.14. Computational process information.

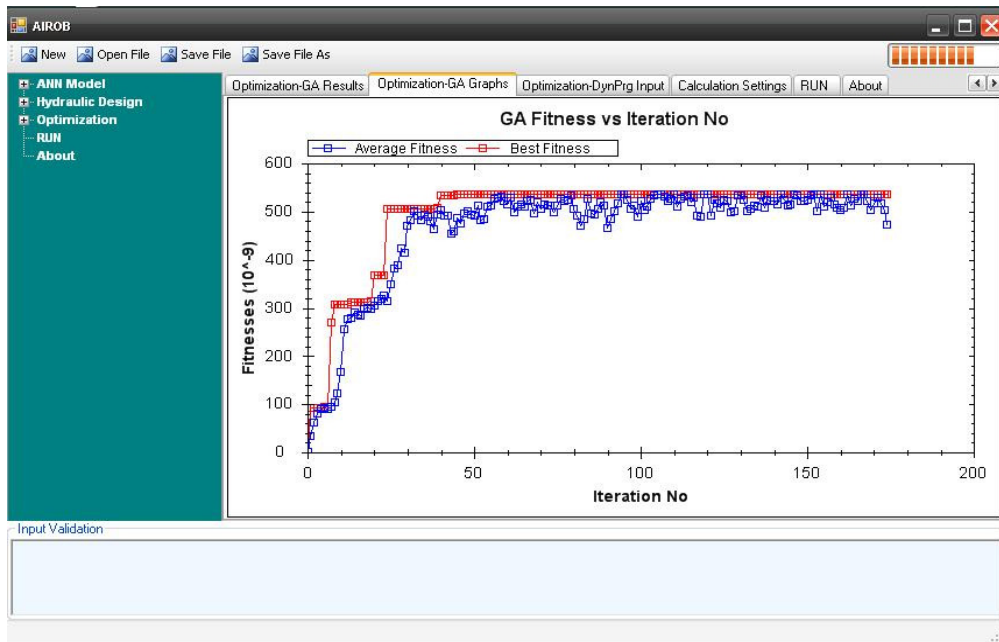


Figure D.15. Dynamic optimization graphs.

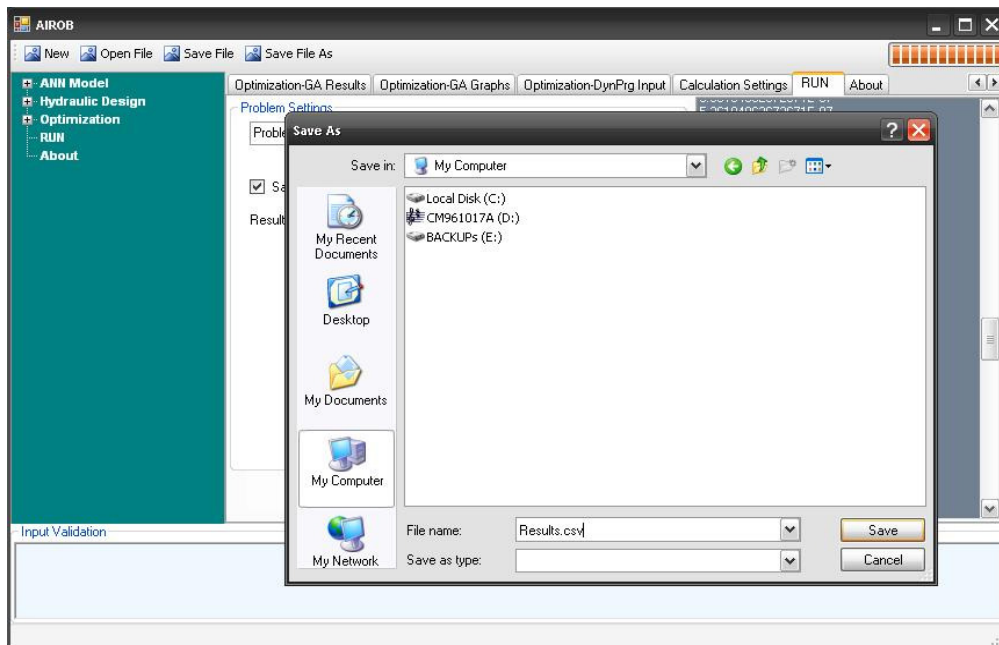


Figure D.16. Saving the results into file.

CIRRICULUM VITAE

PERSONAL INFORMATION

Surname, Name: Turan, Kamil Hakan

Nationality: Turkish (TC)

Date and Place of Birth: 13 February 1978, Ankara

Marital Status: Married

EDUCATION

Degree	Institution	Year of Graduation
MS	METU, Computer Eng. Dept.	2007
MS	METU, Civil Eng. Dept.	2004
BS	METU, Civil Eng. Dept.	2001
High School	Gazi Anatolian High School, Ankara	1996

WORK EXPERIENCE

Year	Place	Enrollment
2001-Present	MIMPAS Muh. A.S.	Project Engineer

FOREIGN LANGUAGES

English (Advanced), German (Beginner)

HOBBIES

Reading, computers, travelling.